First beam-gas events in LHCb using SMOG2

(and a brief update on LHCspin)

L. L. Pappalardo

pappalardo@fe.infn.it

PBC Annual Meeting – CERN – 7-9 November 2022

The SMOG upgrade (SMOG2)

[SMOG2 TDR]

Project approved in Nov. 2019

Main hardware implementations:

- 20 cm **storage cell** for the target gas installed upstream of the VELO
- Brand new, more flexible and sophisticated **Gas Feed System** (GFS)

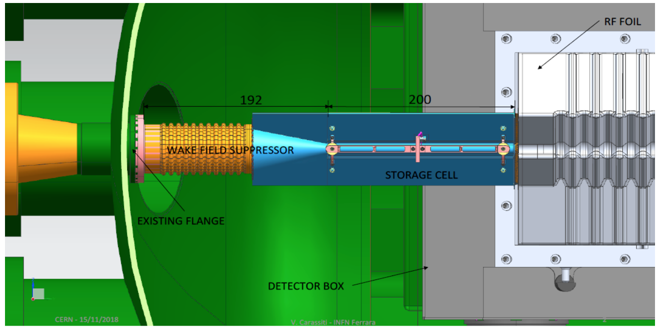

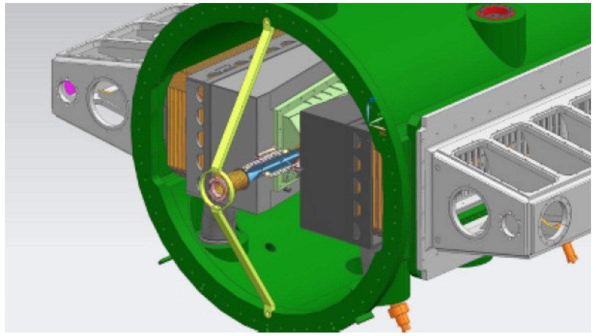

The SMOG upgrade (SMOG2)

[SMOG2 TDR]

Project approved in Nov. 2019

Main hardware implementations:

- 20 cm **storage cell** for the target gas installed upstream of the VELO
- Brand new, more flexible and sophisticated **Gas Feed System** (GFS)

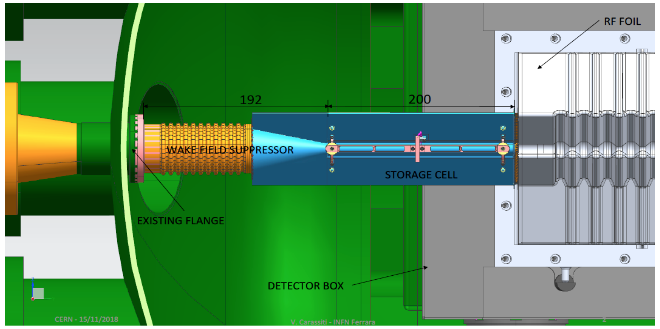

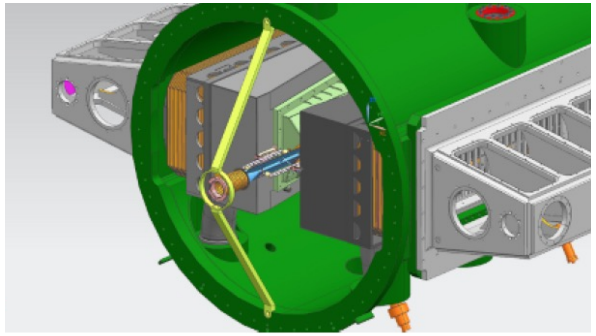

SMOG2 vs. SMOG:

✓ Well **defined interaction region** upstream of the collider IP (limited to cell length/position: $-541 < z < -341$ mm)

✓ **Increase of target density (luminosity)** by factor 8-35 using the same gas load

✓ Possibility to inject **more gas species**: $H_2, D_2, He, N_2, O_2, Ne, Ar, Kr, Xe$

✓ **target density (→ luminosity) with much higher precision** (few % uncert.)

✓ Well displaced int. regions: possibility to **run in parallel with collider mode**

The SMOG upgrade (SMOG2)

[SMOG2 TDR]

Project approved in Nov. 2019

Main hardware implementations:

- 20 cm **storage cell** for the target gas installed upstream of the VELO
- Brand new, more flexible and sophisticated **Gas Feed System** (GFS)

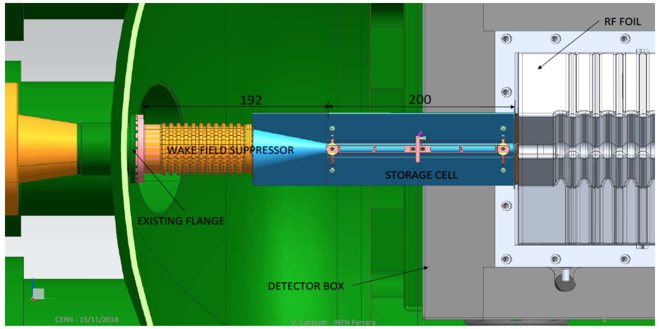

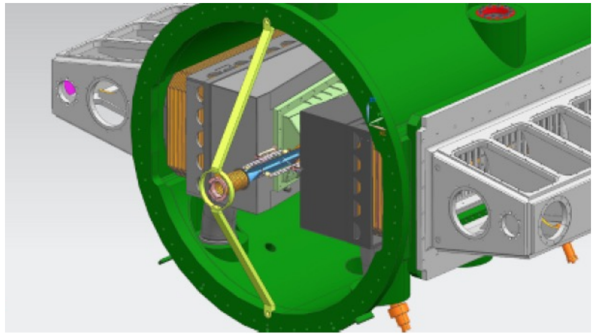

SMOG2 vs. SMOG:

- ✓ Well **defined interaction region** upstream of the collider IP (limited to cell length/position: $-541 < z < -341$ mm)
- ✓ **Increase of target density (luminosity)** by factor 8-35 using the same gas load
- ✓ Possibility to inject **more gas species**: $H_2, D_2, He, N_2, O_2, Ne, Ar, Kr, Xe$
- ✓ **target density (→ luminosity) with much higher precision** (few % uncert.)
- ✓ Well displaced int. regions: possibility to **run in parallel with collider mode**

→ **Very rich and diverse physics program!** (details in backup slides)

SMOG2 performances

- **Beam-beam and beam-gas interaction regions well detached**
- Full reconstruction efficiency (PV + Tracking) retained in beam-gas interaction region despite the distance from the VELO and the different event topology
- **No impact in pp efficiency due to simultaneous p-gas data-taking!**

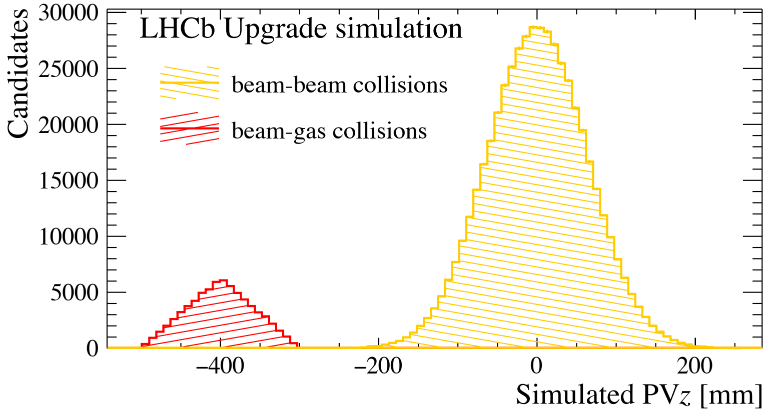

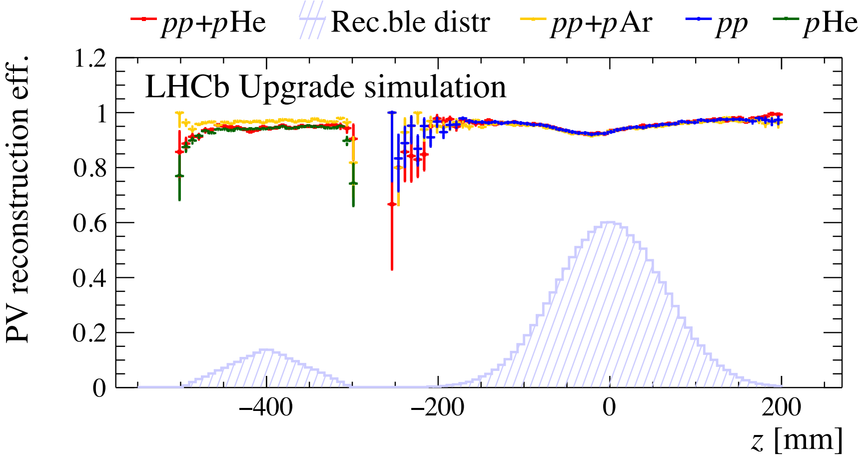

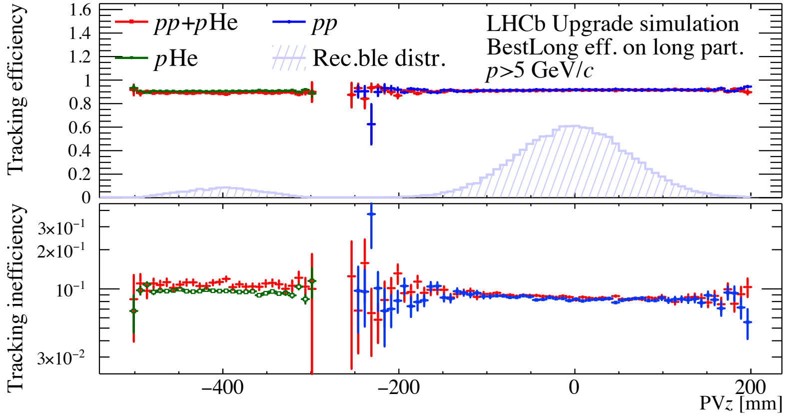

SMOG2 performances

- **Beam-beam and beam-gas interaction regions well detached**
- Full reconstruction efficiency (PV + Tracking) retained in beam-gas interaction region despite the distance from the VELO and the different event topology
- **No impact in pp efficiency due to simultaneous p-gas data-taking!**

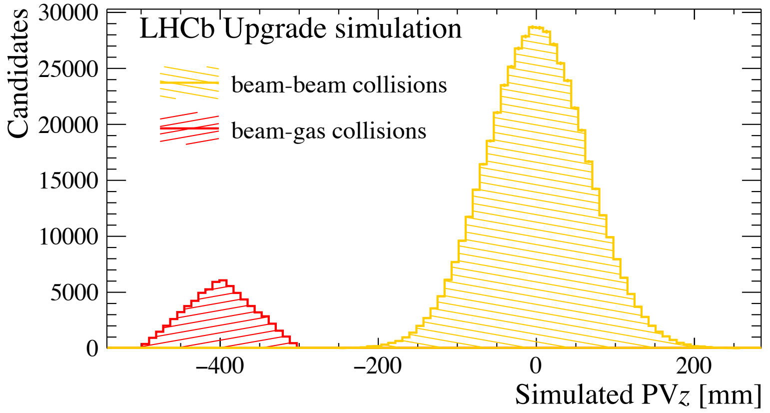

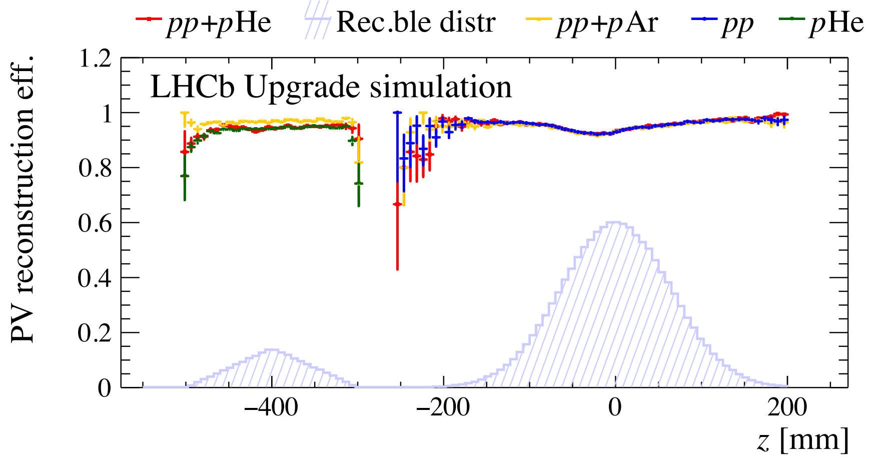

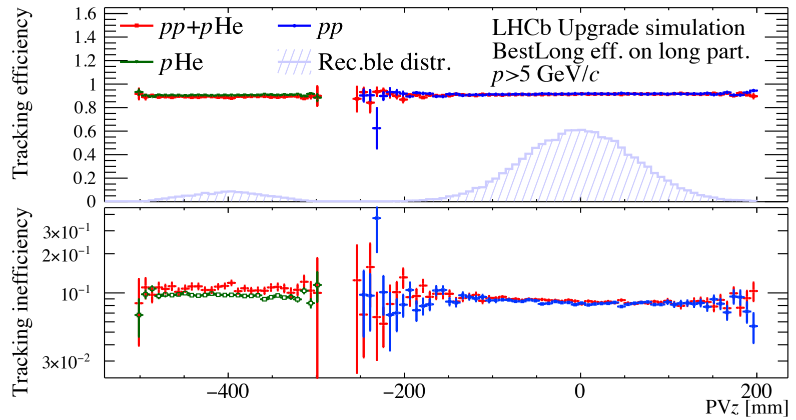

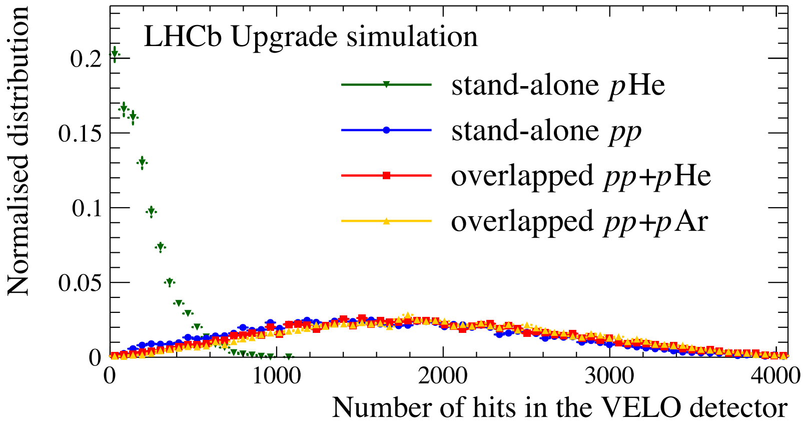

- In case of simultaneous data-taking, beam-gas collisions cause a negligible increase in the detector occupancy
- The gas target provides a negligible impact on beam life-time (e.g. a relative loss of 0.4% is expected for pAr in 10 h [SMOG2 TDR])

SMOG2 implementation

- ✓ **The system is completely installed**: target cell, temperature probes, Gas Feed System, trigger, reconstruction algorithms
- ✓ **Several gas injections performed in the past months with SMOG2 cell and VELO in both OPEN and CLOSED position**
- ✓ **ready for data-taking**!

SMOG2 temperature monitoring system

- **5 temperature probes installed on the cell** (needed for monitoring during operations and gas density estimates)
- Nominal precision: $\Delta T = 0.2\ K$
- Acquisition system is implemented in the LHCb ONLINE monitoring framework and running

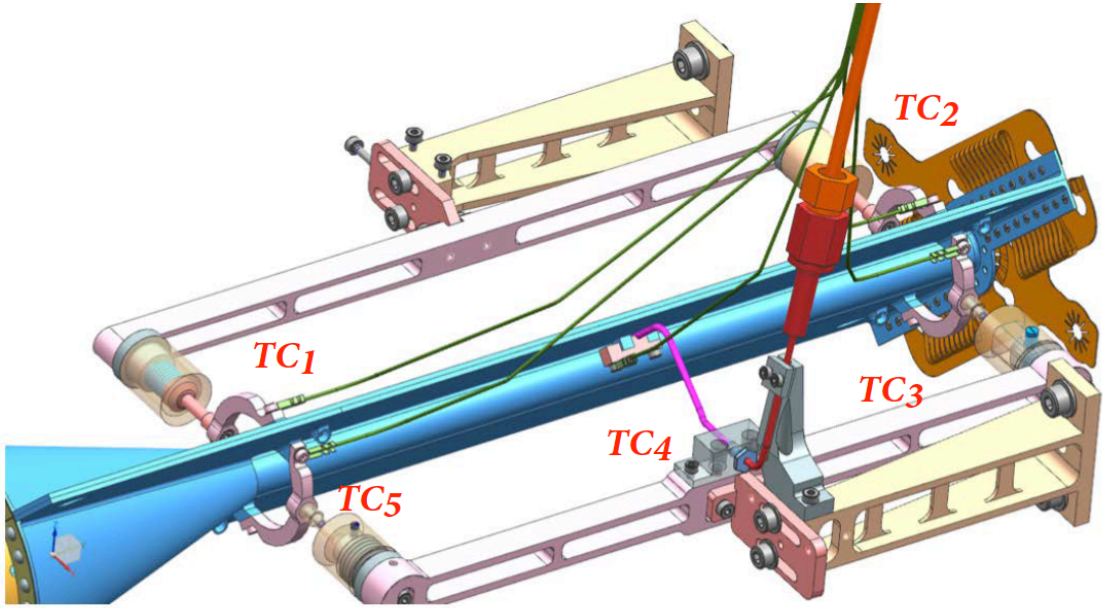

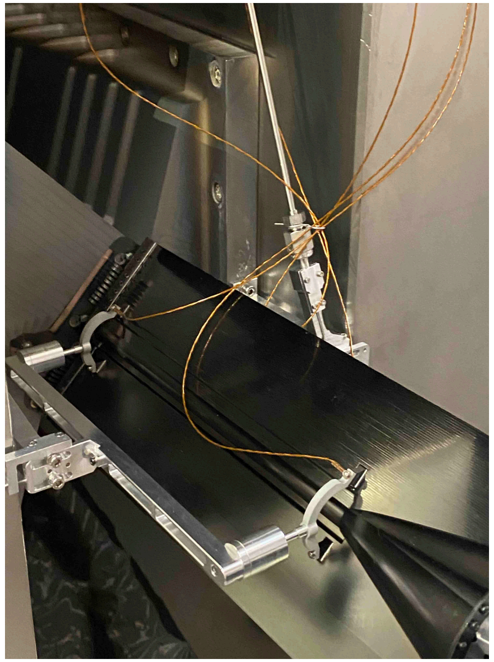

SMOG2 temperature monitoring system

- **5 temperature probes installed on the cell** (needed for monitoring during operations and gas density estimates)
- Nominal precision: $\Delta T = 0.2\ K$
- Acquisition system is implemented in the LHCb ONLINE monitoring framework and running

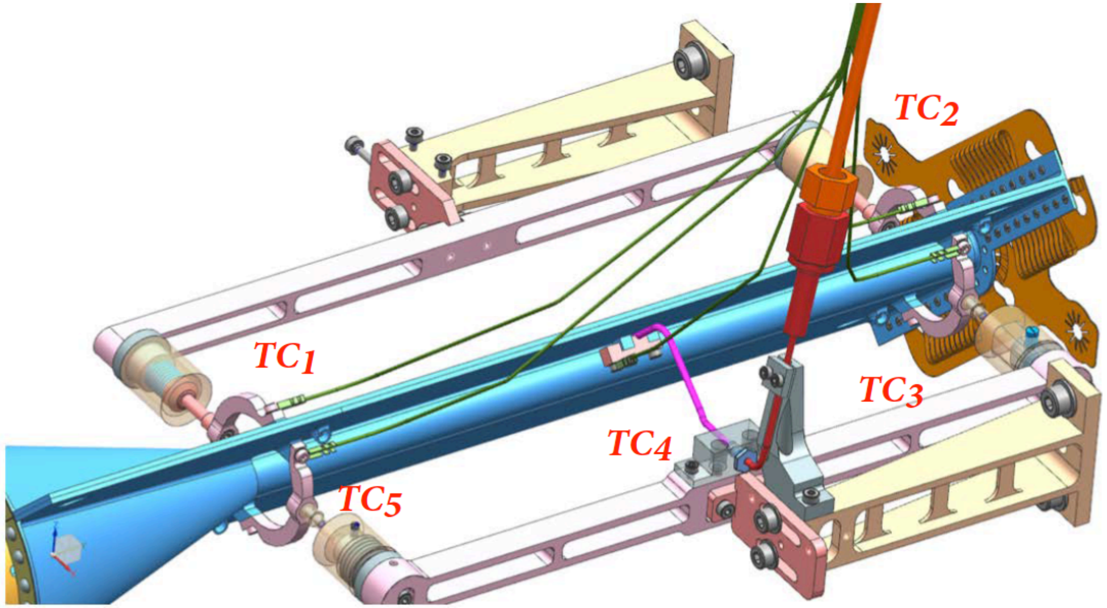

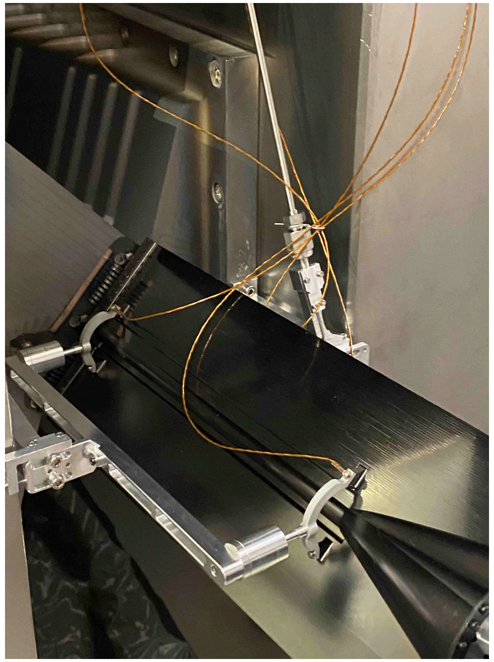

- A temperature increase of the cell with circulating beams is expected due to RF resonant modes of the beams
- Largest effects expected with cell in OPEN position (no resonant heating expected in the closed position according to simulations from the impedance group).

SMOG2 temperature monitoring: cell OPEN, circulating beams

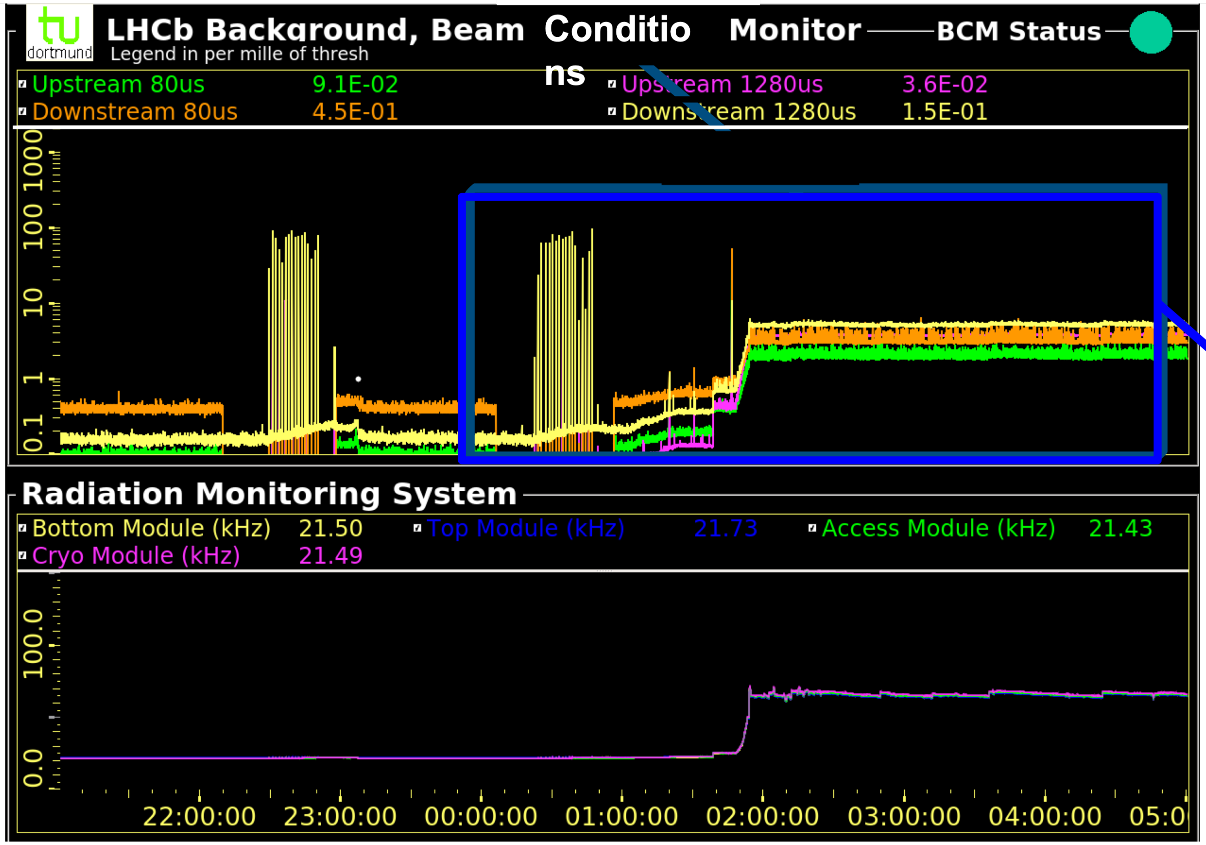

- A ~10 ℃ temperature enhancement (12℃ → 22℃) is observed with ~70 % of LHC circulating bunches
- **Cell prototype tested up to 130 ℃ with no consequences!**

Step-by-step VELO closure with circulating beams

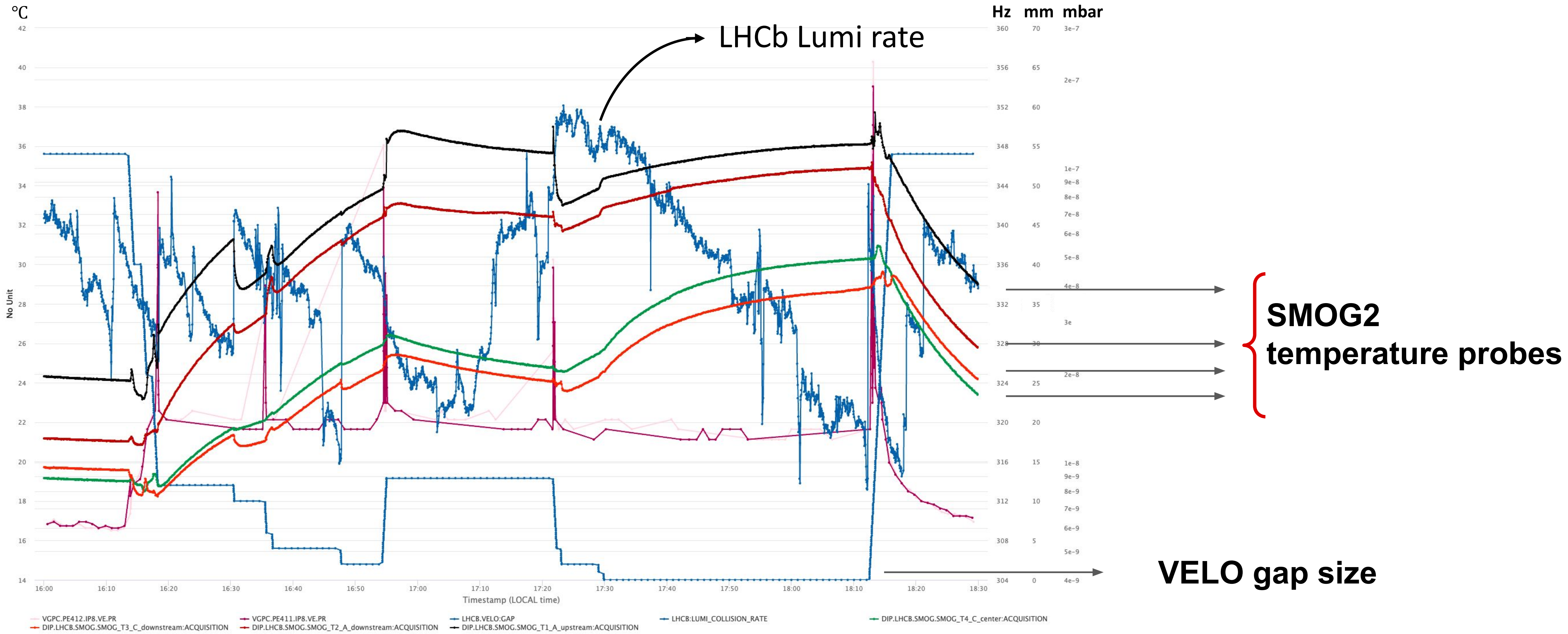

- Temperatures vary during VELO movements, slopes depend on VELO gap, smooth/mild increase observed in closed position
- Temperature always < 38 ℃ (cell tested safely up to 130 ℃)
- Temperatures fully recovered in ~ 20 min after beam dump and VELO opening

First gas injections in RUN3 (June 2022): cell OPEN, circulating beams

Low pressure Ne injection

Pressure increase into the primary vacuum

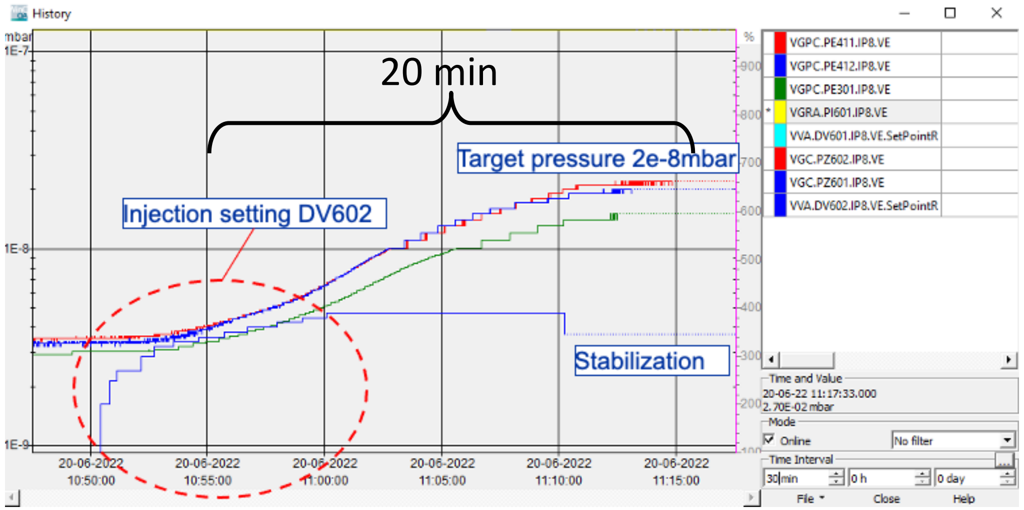

Vacuum recovery after the gas injection stop

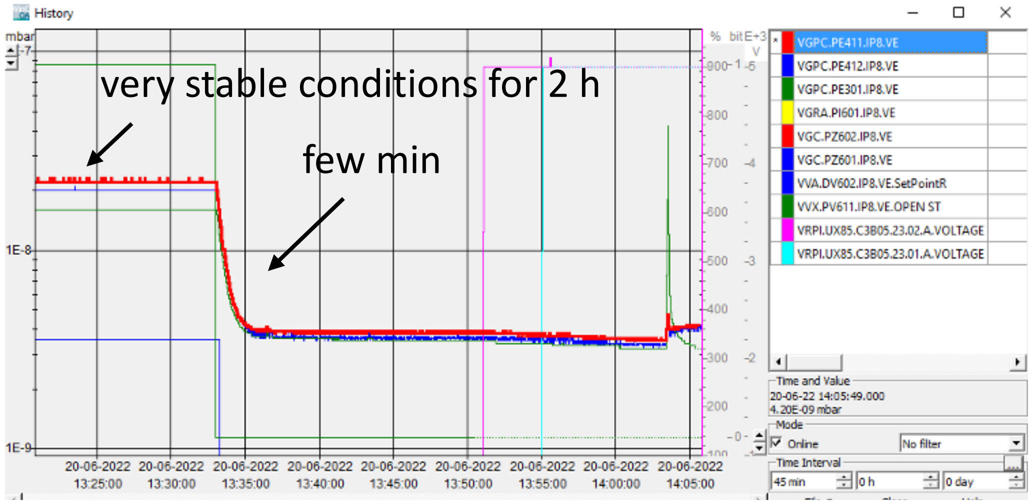

First gas injections in RUN3 (June 2022): <u>cell OPEN, circulating beams</u>

Low pressure Ne injection

Pressure increase into the primary vacuum

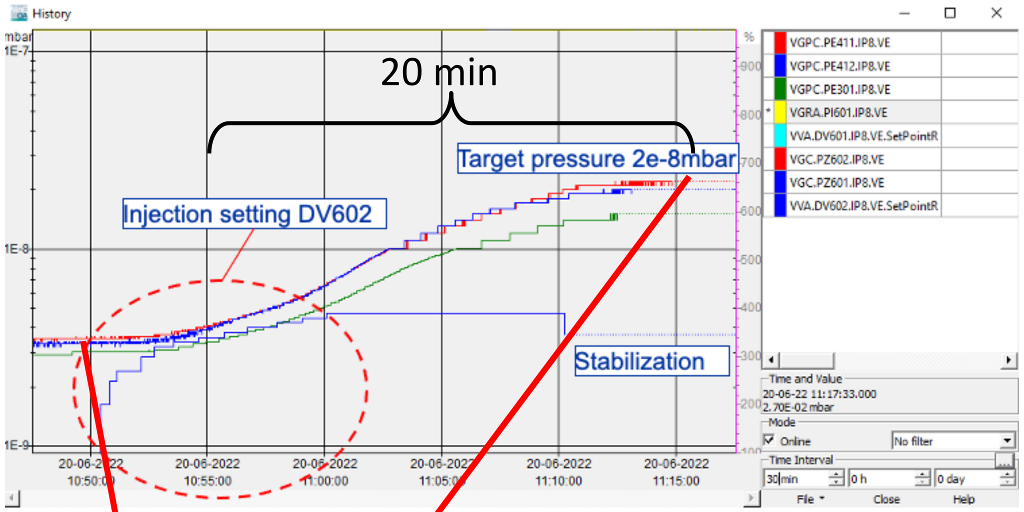

Vacuum recovery after the gas injection stop

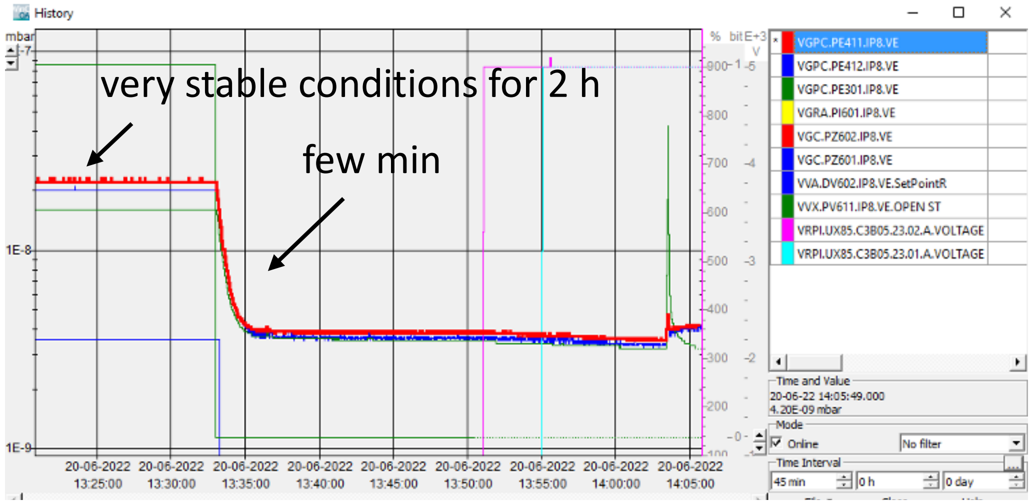

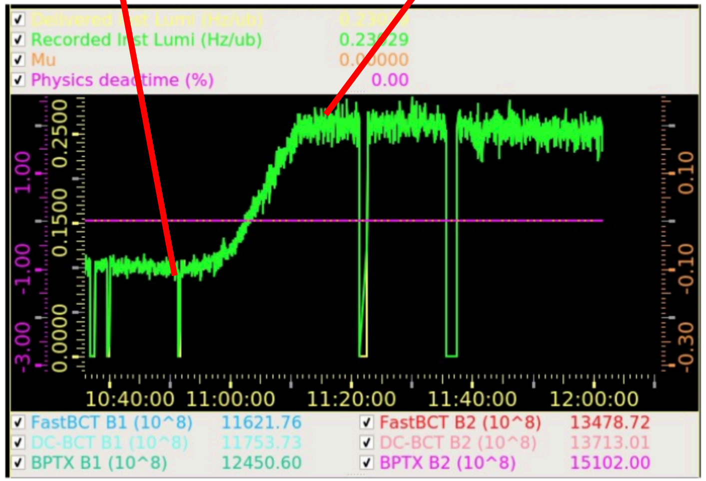

Luminosity increase seen by the LHCb luminometer (Plume)

- ✓ CALO, RICH and Muon systems recorded activity in beam-empty bunch crossing configuration!
- ✓ **Extremely useful not only to test the new Gas Feed System, but also for the commissioning of the upgraded LHCb detector!**

First gas injections in RUN3 (June 2022): cell OPEN, circulating beams

Low pressure Ne injection

Pressure increase into the primary vacuum

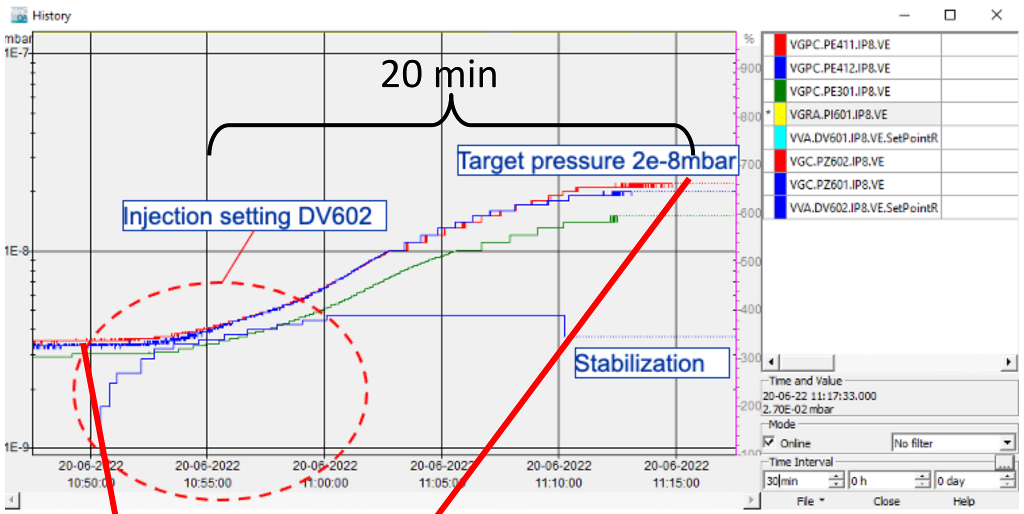

Vacuum recovery after the gas injection stop

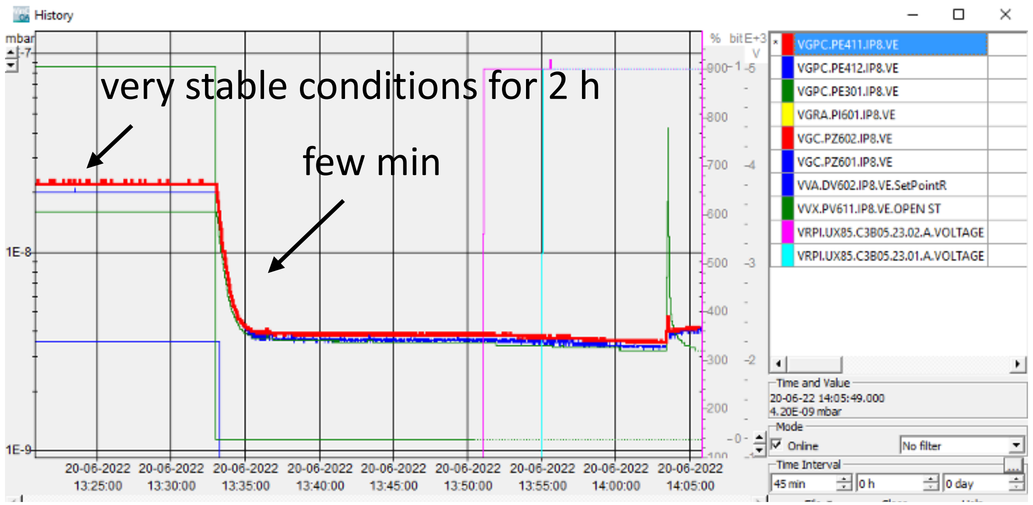

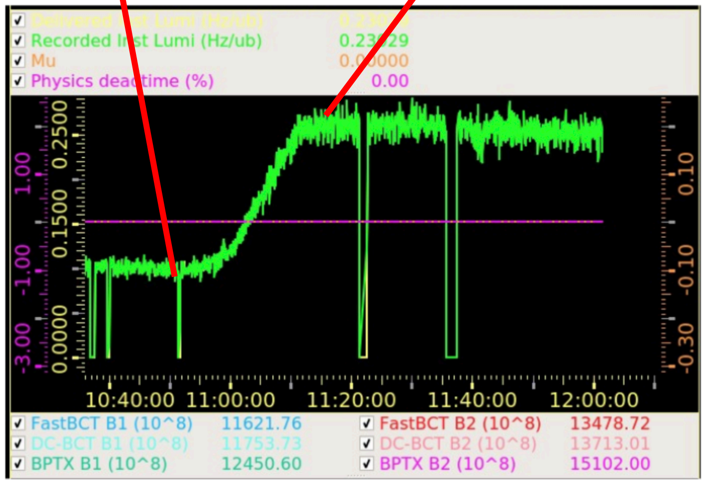

Luminosity increase seen by the LHCb luminometer (Plume)

- ✓ CALO, RICH and Muon systems recorded activity in beam-empty bunch crossing configuration!
- ✓ **Extremely useful not only to test the new Gas Feed System, but also for the commissioning of the upgraded LHCb detector!**
- ✓ **LHC official statement**: no negative feedback during gas injection. Green light to inject when needed.

Towards a full check of the system

- **21/10: first VELO (and cell) closure with 300 circulating bunches (no gas)**

Towards a full check of the system

- **21/10: first VELO (and cell) closure with 300 circulating bunches (no gas)**
- 24/10: VELO (and cell) closed with 600 circulating bunches (no gas)
- 26/10: VELO (and cell) closed with 1200 circulating bunches (no gas)
- 28/10: VELO (and cell) closed with 2400 circulating bunches (no gas)

Towards a full check of the system

- **21/10: first VELO (and cell) closure with 300 circulating bunches (no gas)**
- 24/10: VELO (and cell) closed with 600 circulating bunches (no gas)
- 26/10: VELO (and cell) closed with 1200 circulating bunches (no gas)
- 28/10: VELO (and cell) closed with 2400 circulating bunches (no gas)
- **01/11: VELO (and cell) closed with 2400 circulating bunches, injected gas and full LHCb on and running**

01/11: first VELO (and SMOG2) closure with circulating beams and injected gas

- Beam stable declared at 19:12
- VELO (and cell) fully closed at 19:34
- Gas injection started at 20:30
- Injected **Ar at $\mathbf{1.6 \times 10^{-8}}$ mbar** (a factor 6.5 lower than SMOG, but density x5.5 higher)
- A steep increase of pressure followed by a stable plateau
- **Simultaneous beam-beam and beam-gas data taking with full LHCb detector ON and running**

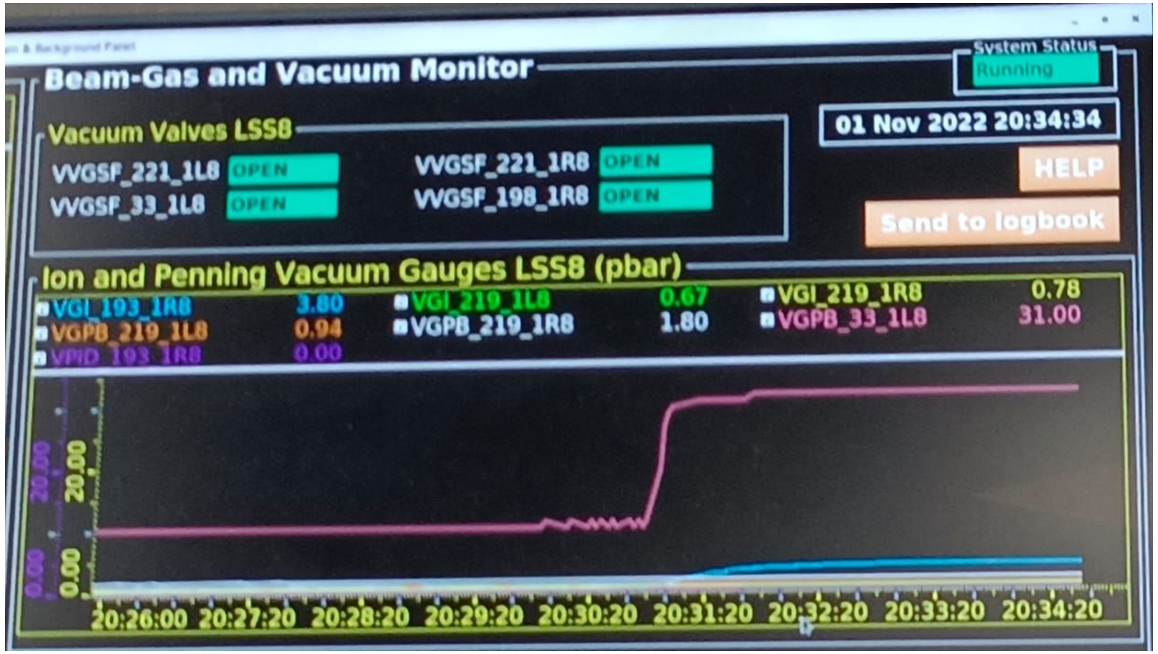

01/11: first VELO (and SMOG2) closure <u>with circulating beams and injected gas</u>

- Beam stable declared at 19:12
- VELO (and cell) fully closed at 19:34
- Gas injection started at 20:30
- Injected **Ar at $\mathbf{1.6{\times}10^{-8}}$ mbar** (a factor 6.5 lower than SMOG, but density x5.5 higher)
- A steep increase of pressure followed by a stable plateau
- **Simultaneous beam-beam and beam-gas data taking with full LHCb detector ON and running**

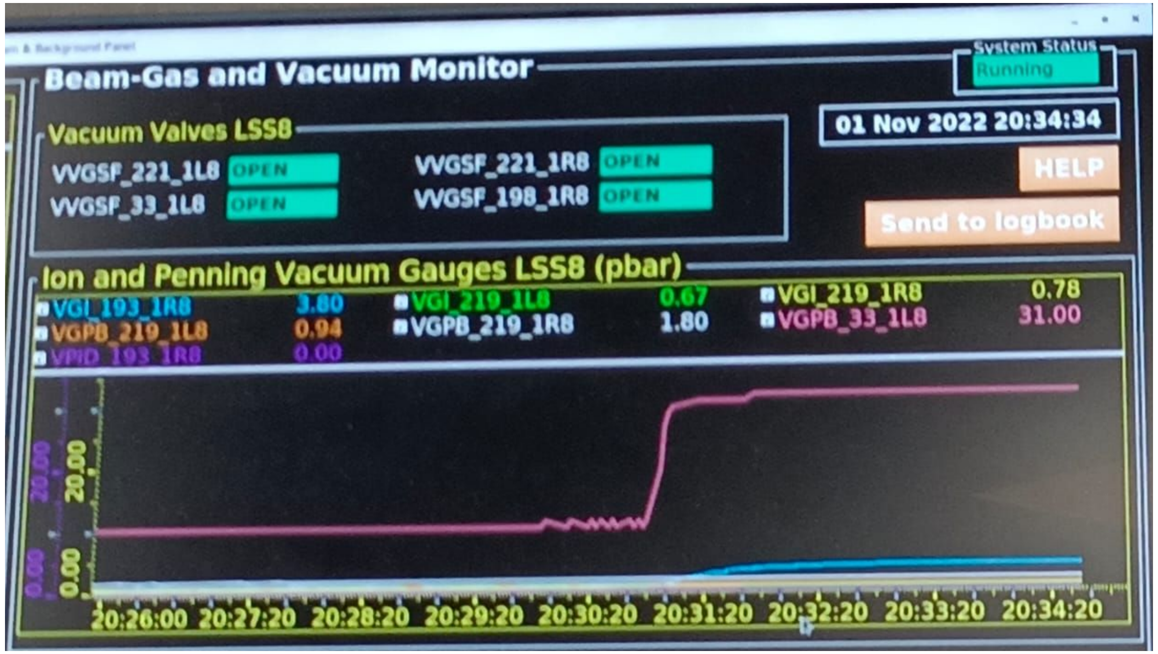

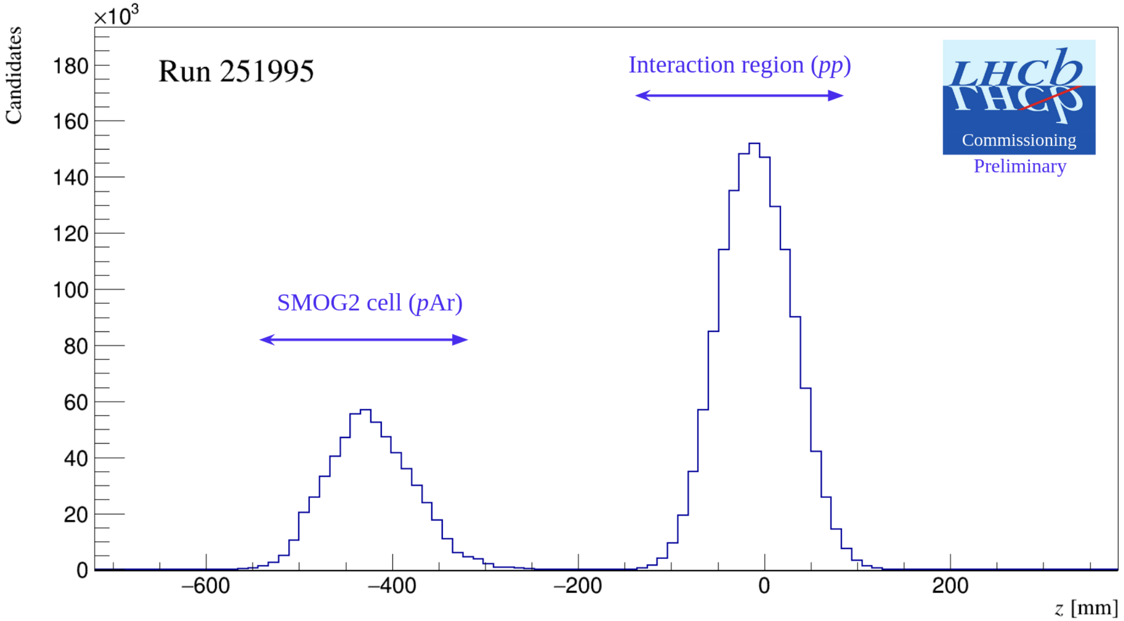

- The two interaction regions are clearly visible and well separated!

01/11: first VELO (and SMOG2) closure with circulating beams and injected gas

- Beam stable declared at 19:12
- VELO (and cell) fully closed at 19:34
- Gas injection started at 20:30
- Injected **Ar at $\mathbf{1.6{\times}10^{-8}}$ mbar** (a factor 6.5 lower than SMOG, but density x5.5 higher)
- A steep increase of pressure followed by a stable plateau
- **Simultaneous beam-beam and beam-gas data taking with full LHCb detector ON and running**

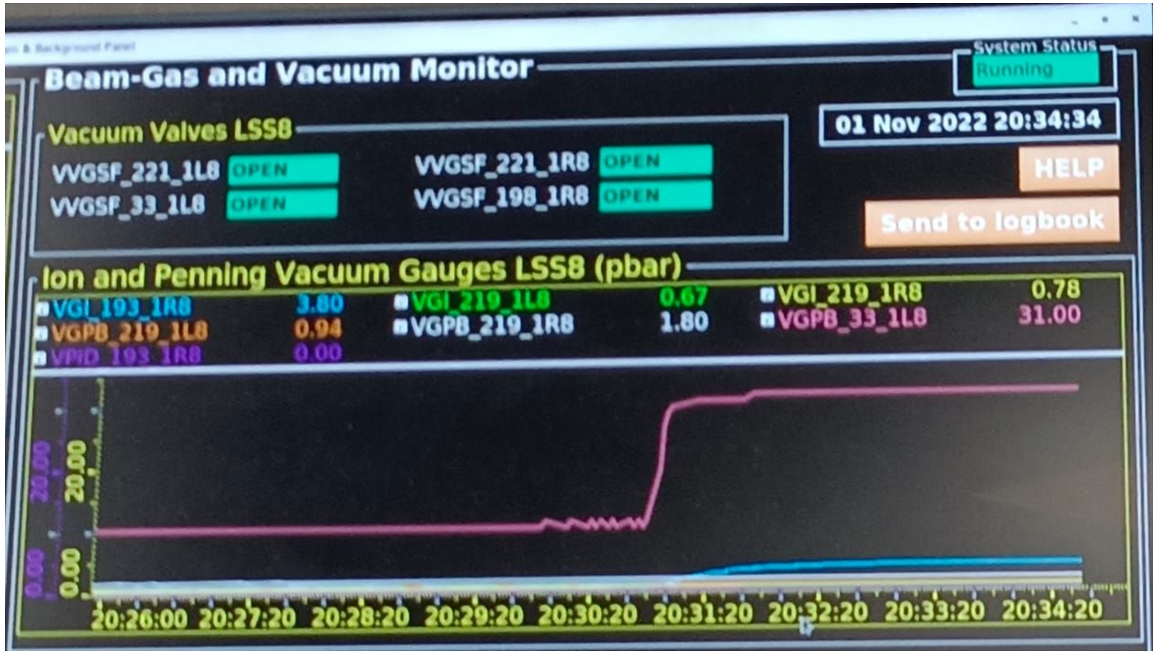

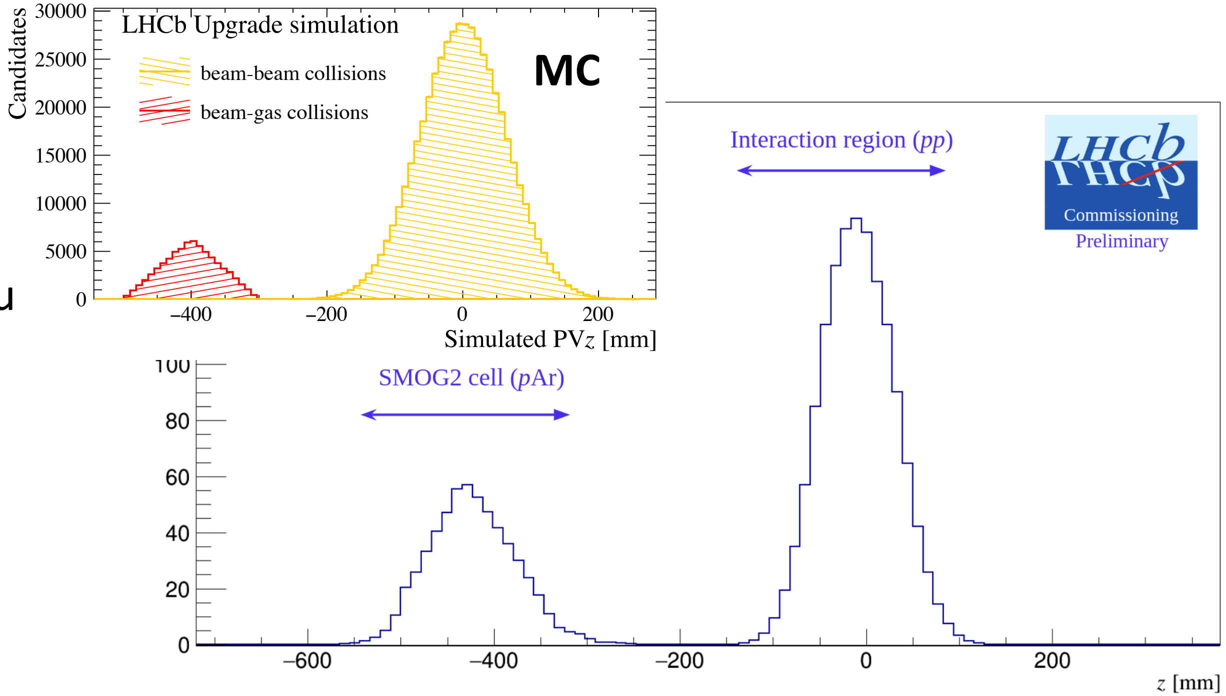

- The two interaction regions are clearly visible and well separated!
- PV distributions consistent with simulations

01/11: first VELO (and SMOG2) closure with circulating beams and injected gas

- Beam stable declared at 19:12
- VELO (and cell) fully closed at 19:34
- Gas injection started at 20:30
- Injected **Ar at $1.6{\times}10^{-8}$ mbar** (a factor 6.5 lower than SMOG, but density x5.5 higher)
- A steep increase of pressure followed by a stable plateau
- **Simultaneous beam-beam and beam-gas data taking with full LHCb detector ON and running**

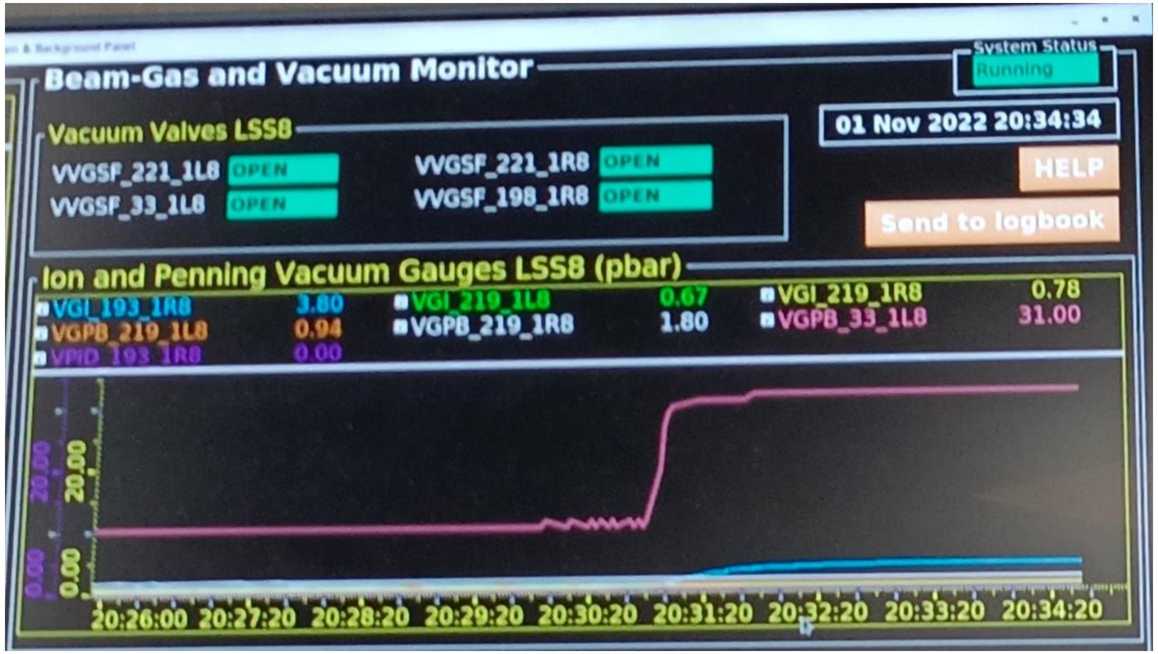

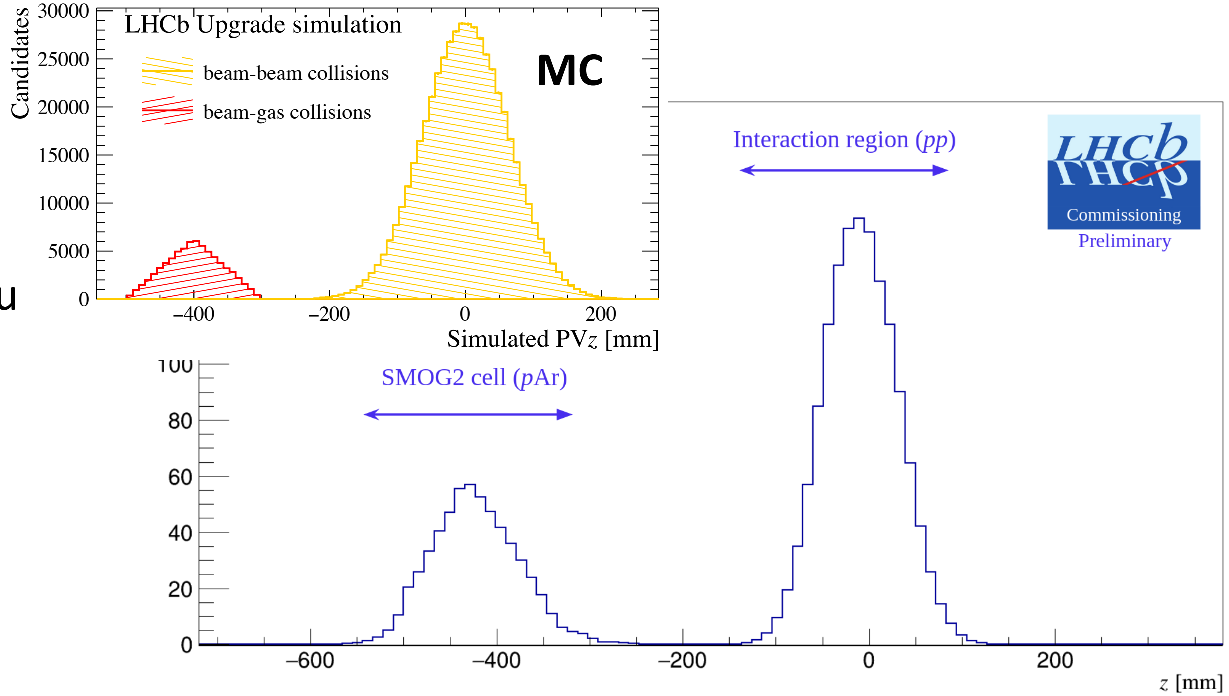

- The two interaction regions are clearly visible and well separated!
- PV distributions consistent with simulations
- **LHCb is now the first (unique) LHC experiment with two simultaneous interaction regions!**

01/11: first VELO (and SMOG2) closure with circulating beams and injected gas

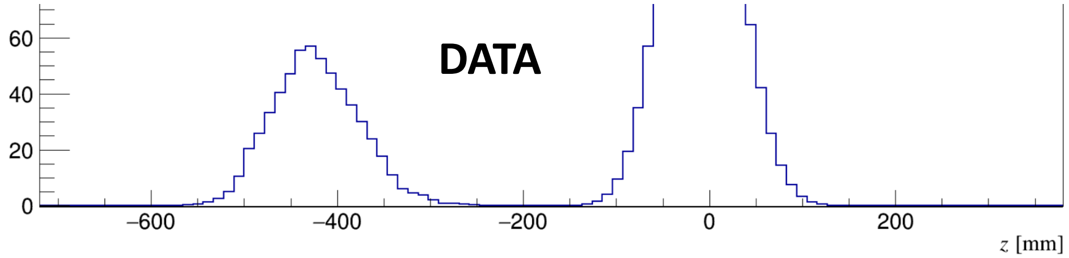

- The shape of the beam-gas PVZ distribution, reflects the triangular density profile inside the cell

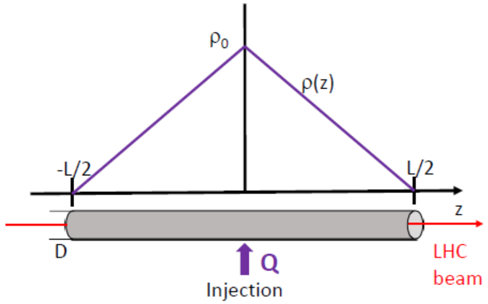

01/11: first VELO (and SMOG2) closure with circulating beams and injected gas

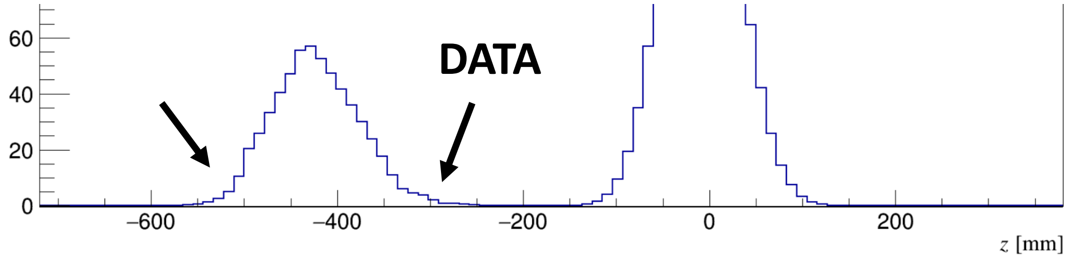

- The shape of the beam-gas PVZ distribution, reflects the triangular density profile inside the cell

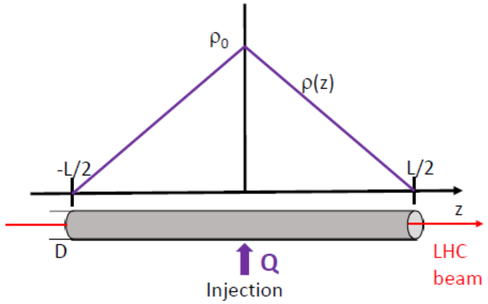

- Deviations observed in the tails reflect the different conductance at the two sides of the cell: small conical aperture on the left, VELO RF foil on the right

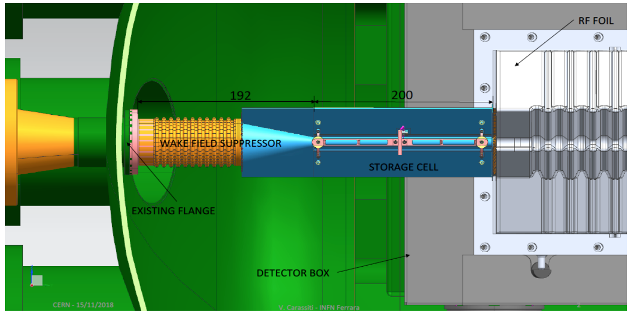

01/11: first VELO (and SMOG2) closure with circulating beams and injected gas

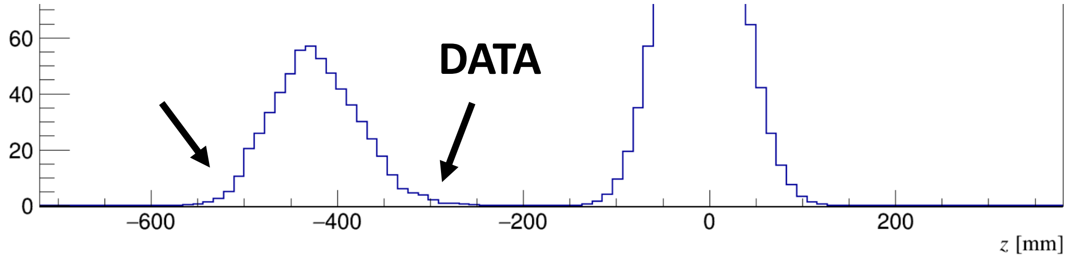

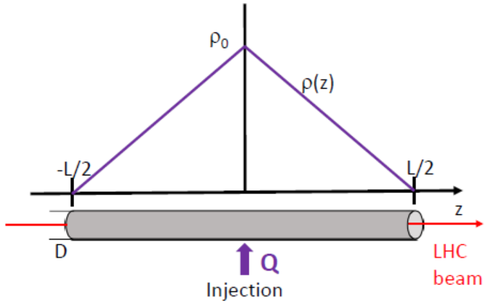

- The shape of the beam-gas PVZ distribution, reflects the triangular density profile inside the cell

- Deviations observed in the tails reflect the different conductance at the two sides of the cell: small conical aperture on the left, VELO RF foil on the right

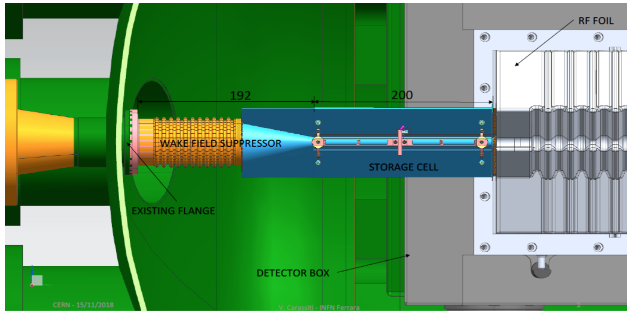

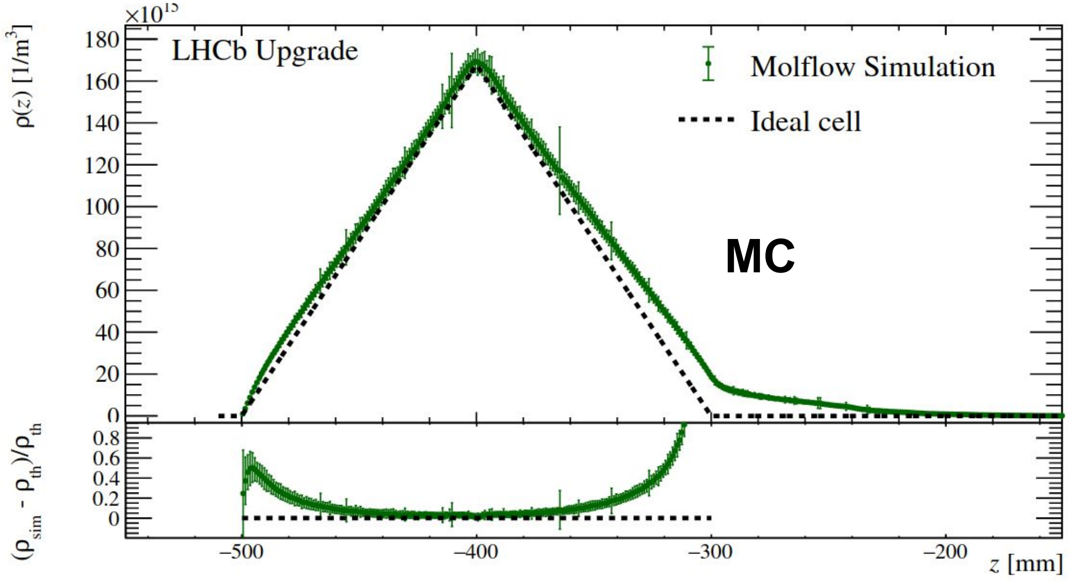

- These distortions are in qualitative agreement with the Molflow simulation

- A detailed study with offline reconstruction will follow closely

SMOG2 commissioning: next phases

- ✓ Low pressure gas injection with OPEN cell (and VELO) and no beam
  → **test new gas injection system**

- ✓ Low pressure gas injection with OPEN cell (and VELO) and beam (first SMOG-like beam-gas collisions)
  → **check luminosity profile vs. gas pressure and first LHCb detector responses**

- ✓ Beam on with OPEN cell (and VELO) and no gas
  → **check temperature profiles (beam-induced cell heating)**

- ✓ Beam on with CLOSED cell (and VELO) and gas
  → **test mechanical closure, simultaneous collider and fixed-target data-taking**

Next steps:

- Perform new injection at higher pressures
- Inject different gas species
- Validate Molflow simulations and trigger/reconstruction algorithms
- Get ready for data taking for physics (also with heavy-ion beams)

A brief update on LHCspin

The LHCspin project

SMOG2 is not only a unique project by itself, but also a fantastic playground for the development of a future polarized gas target for LHCb (**LHCspin project**)

Run 2: **SMOG** → Run 3: **SMOG2** → Run 4 (proposed): **LHCspin**

LHCspin is an R&D project aimed to implement a **new-generation HERMES-like polarized gaseous fixed target** in the **LHCb** spectrometer.

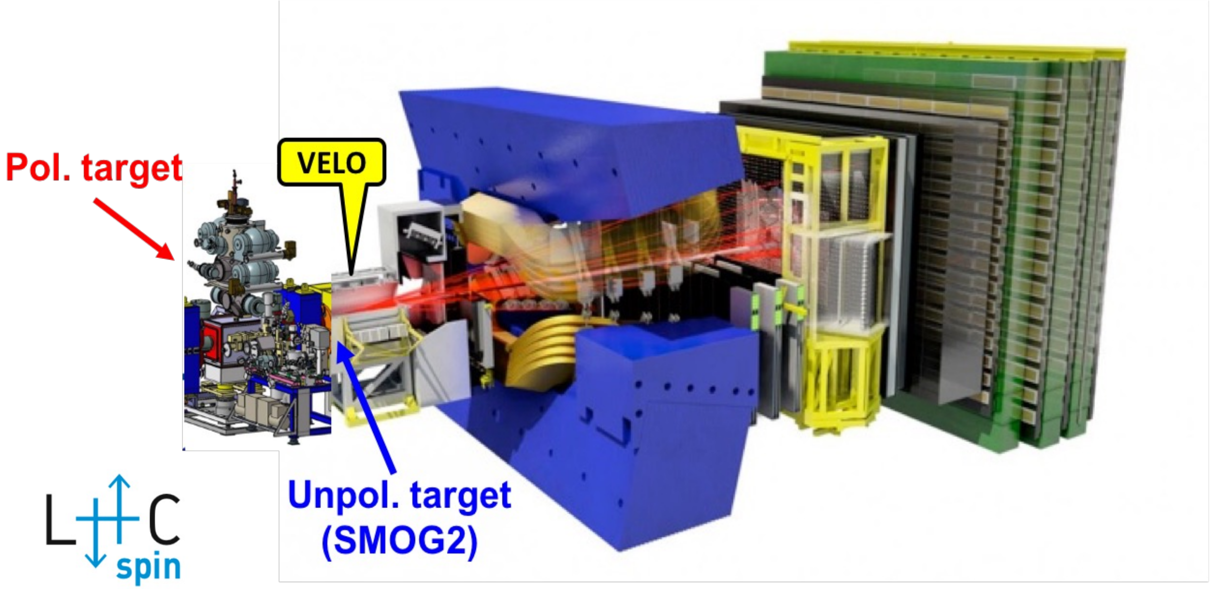

The LHCspin project

SMOG2 is not only a unique project by itself, but also a fantastic playground for the development of a future polarized gas target for LHCb (**LHCspin project**)

Run 2	Run 3	Run 4 (proposed)
SMOG	**SMOG2**	**LHCspin**

LHCspin is an R&D project aimed to implement a **new-generation HERMES-like polarized gaseous fixed target** in the **LHCb** spectrometer.

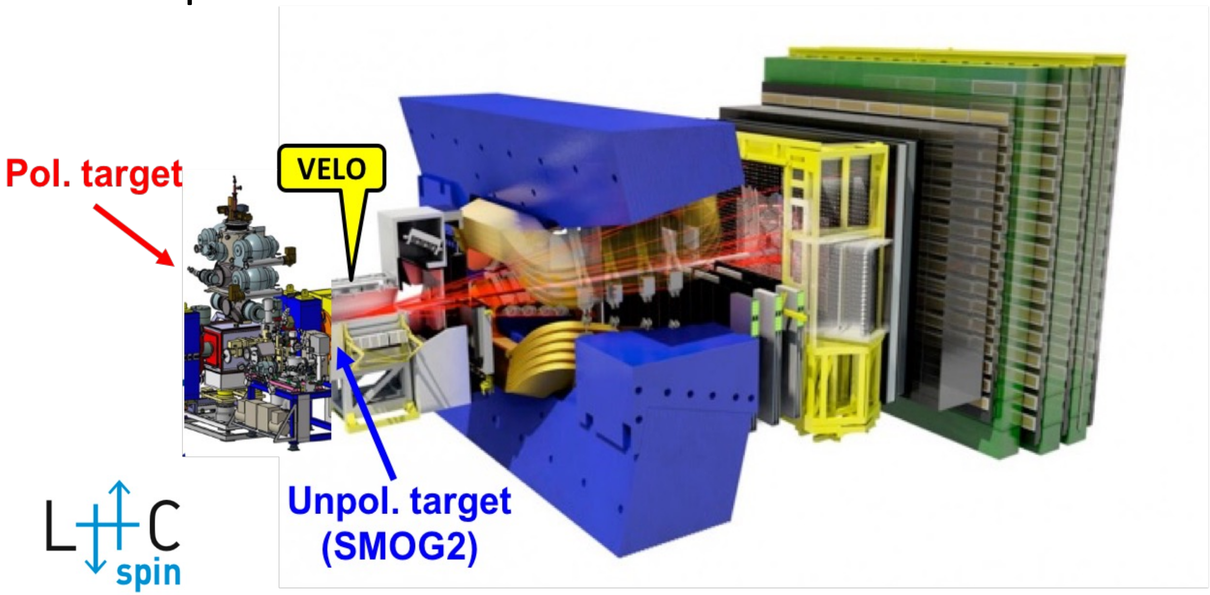

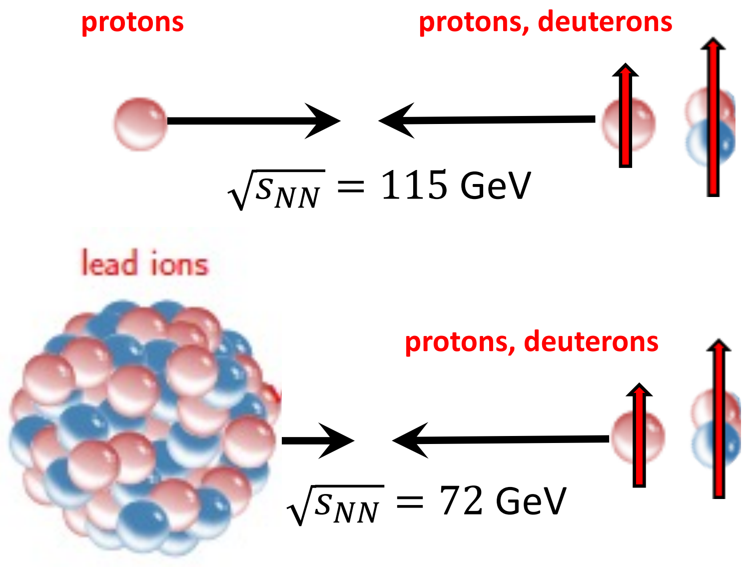

The LHCspin apparatus

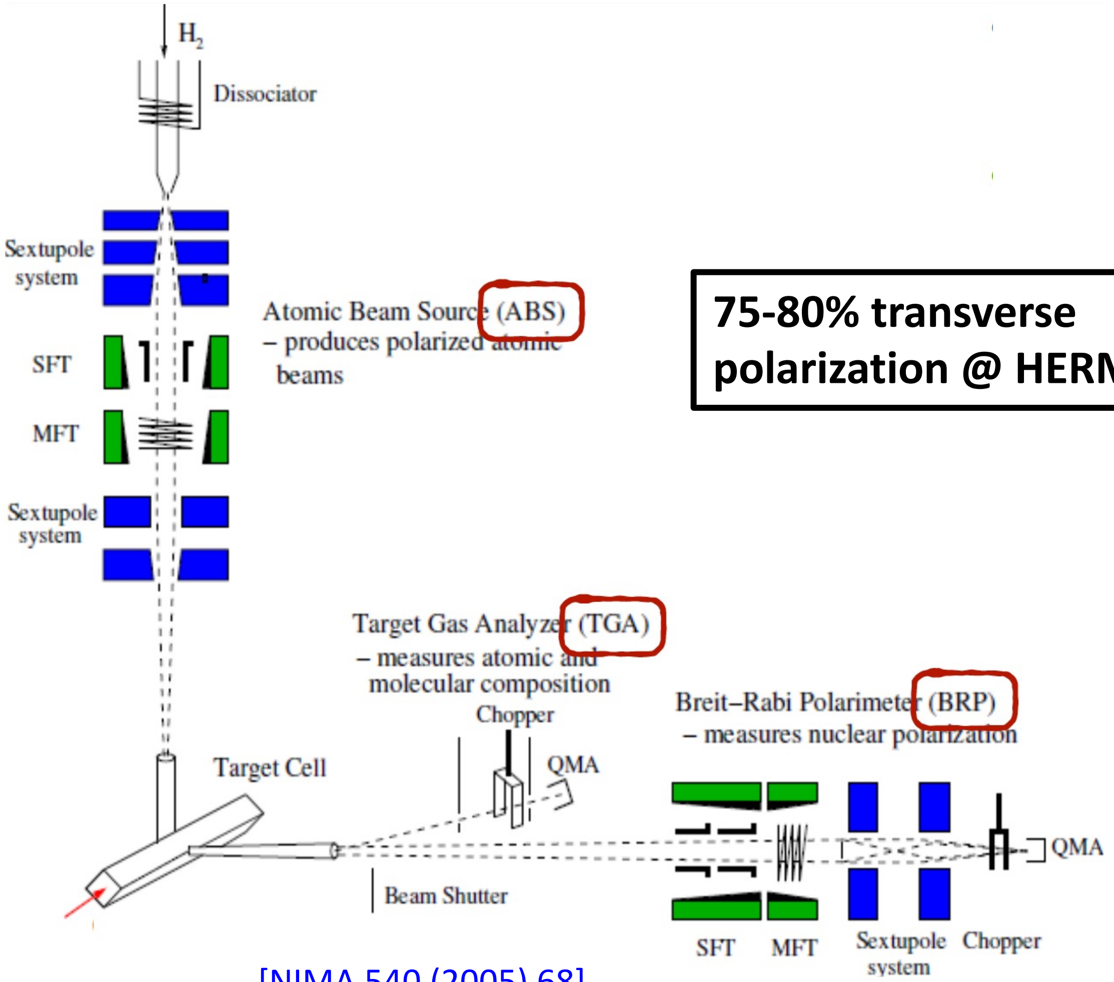

[NIMA 540 (2005) 68]

75-80% transverse polarization @ HERMES

The LHCspin apparatus

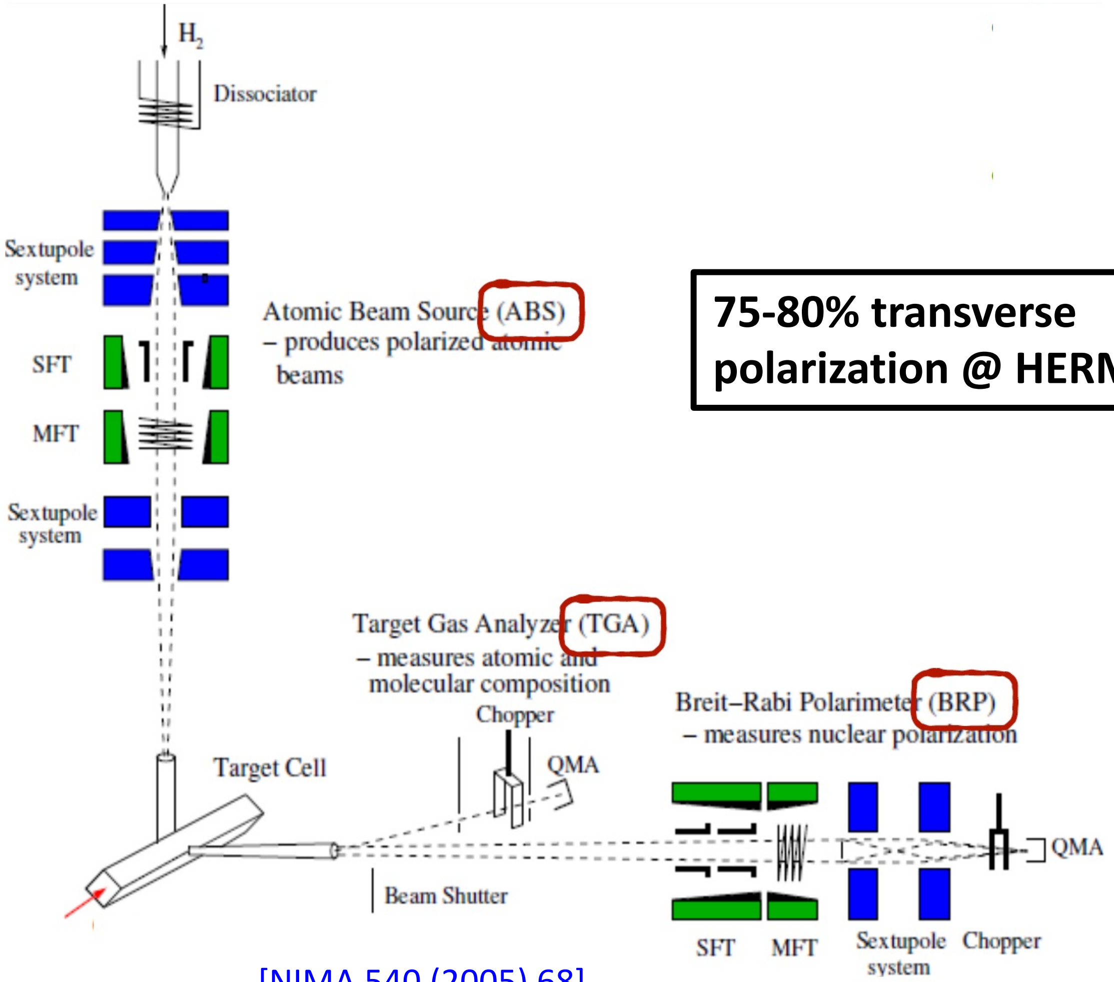

[NIMA 540 (2005) 68]

75-80% transverse polarization @ HERMES

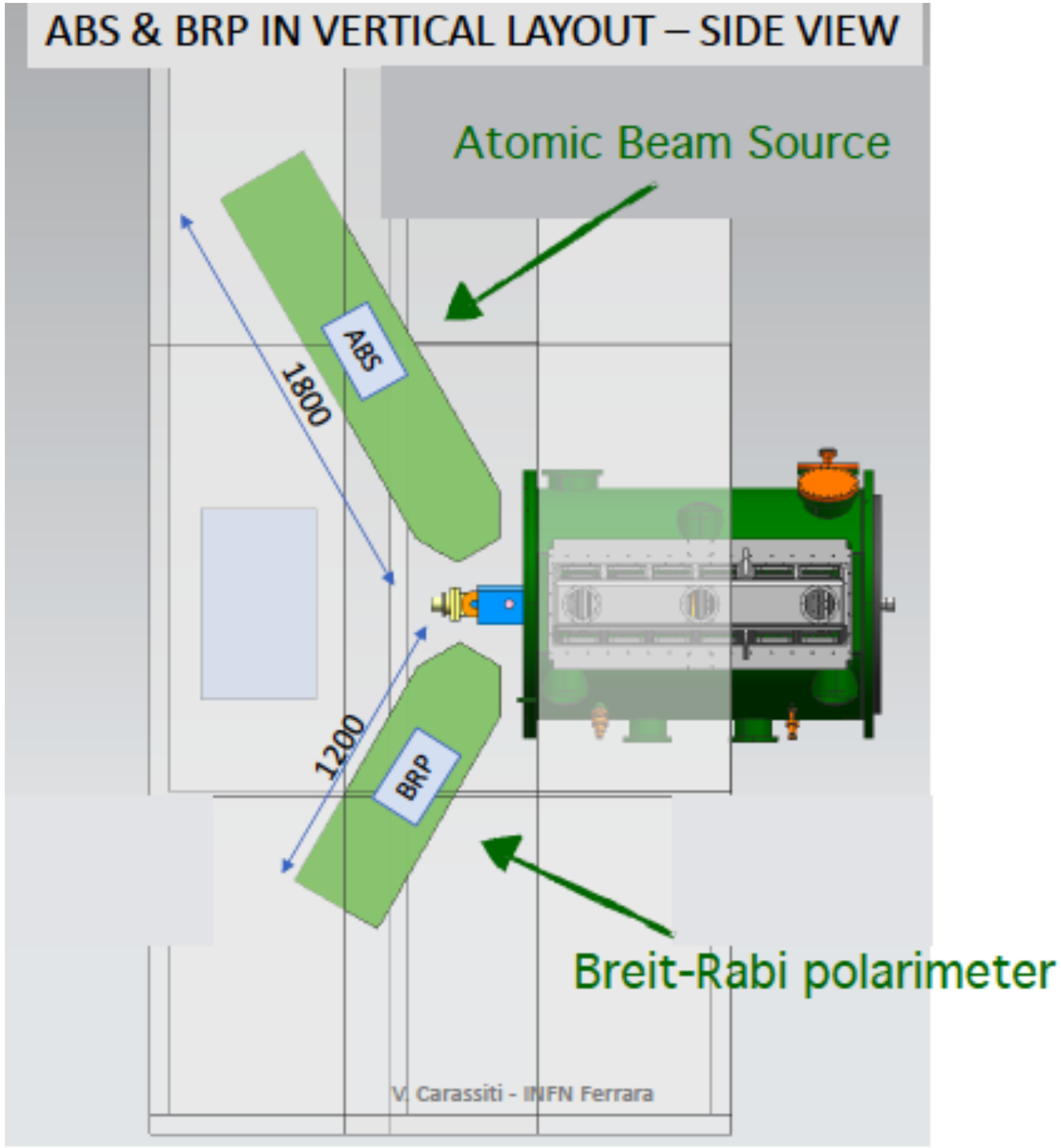

The LHCspin apparatus [PoS (SPIN2018)]

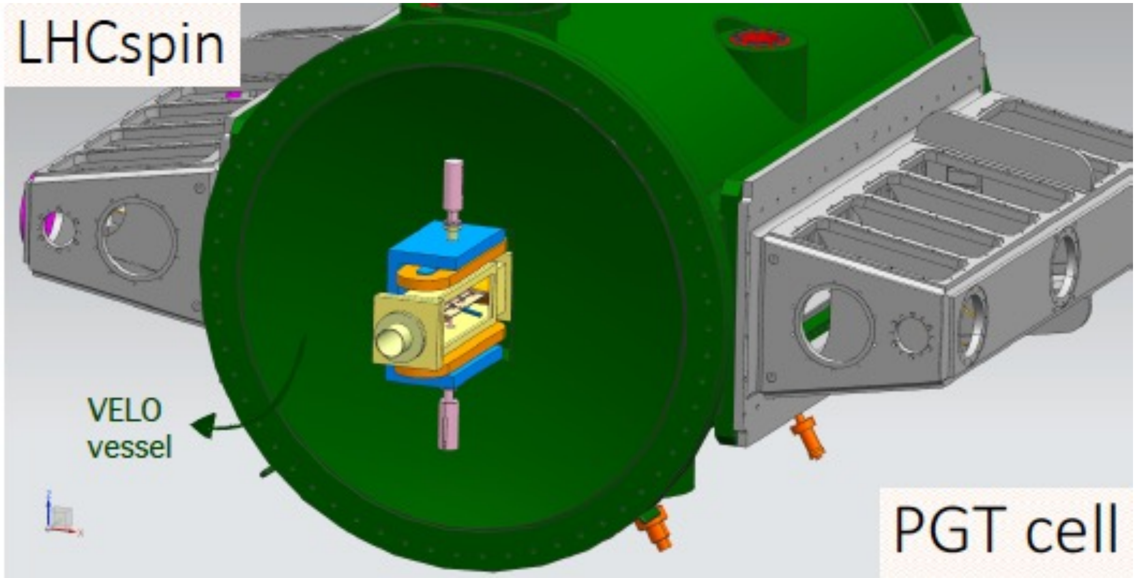

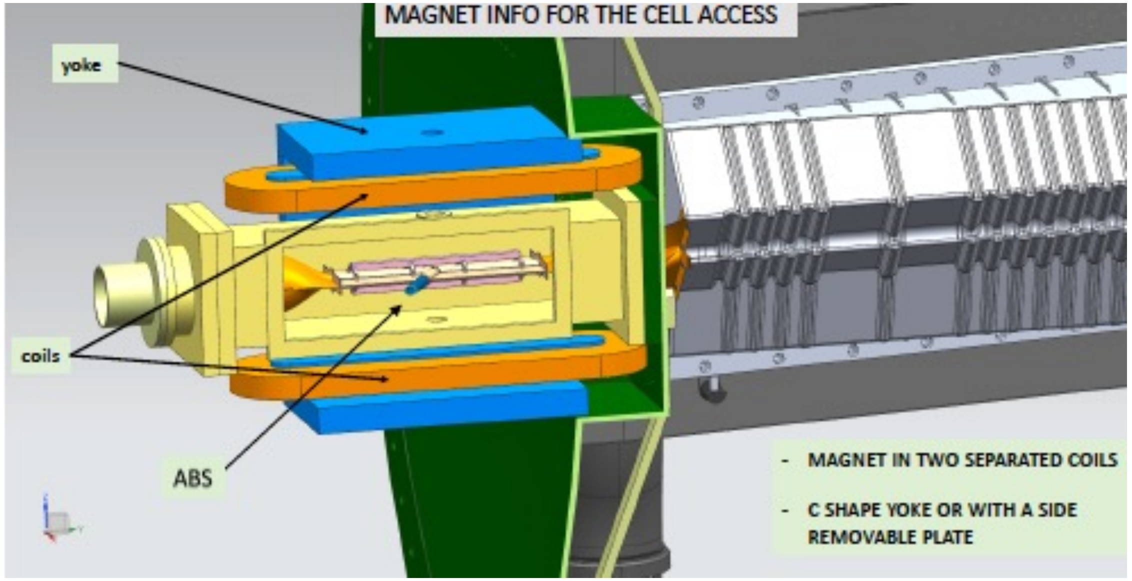

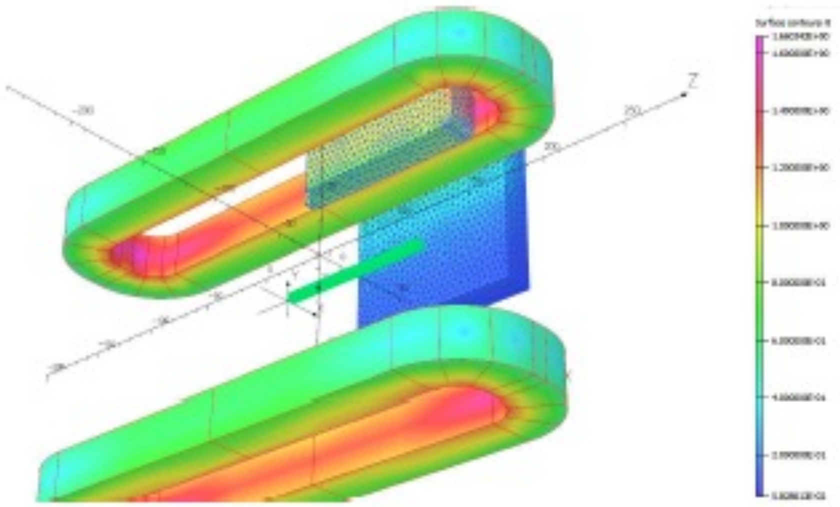

- **Compact superconductive dipole magnet for static transverse field to maintain polarization inside the cell and avoid beam-induced depolarization**
- **Required $B = 300\ mT$ with $\Delta B/B \sim 10\%$**
- **Need to modify main flange of VELO vessel (inward)**
- **No need for additional detectors**
- **Possibility to switch from dipole magnet to solenoid to realize a Longitudinal polarized target in Run5**

The jet target option

Alternative solution with **jet target** also under evaluation:

- lower density ($\sim 10^{12}$ atoms$/cm^2$) → about a factor of 40 smaller
- higher polarization (up to 90%)
- lower systematics in P measurement (virtually close to 0)

The jet target option

Alternative solution with **jet target** also under evaluation:

- lower density ($\sim 10^{12}\ \text{atoms}/cm^2$) → about a factor of 40 smaller
- higher polarization (up to 90%)
- lower systematics in P measurement (virtually close to 0)

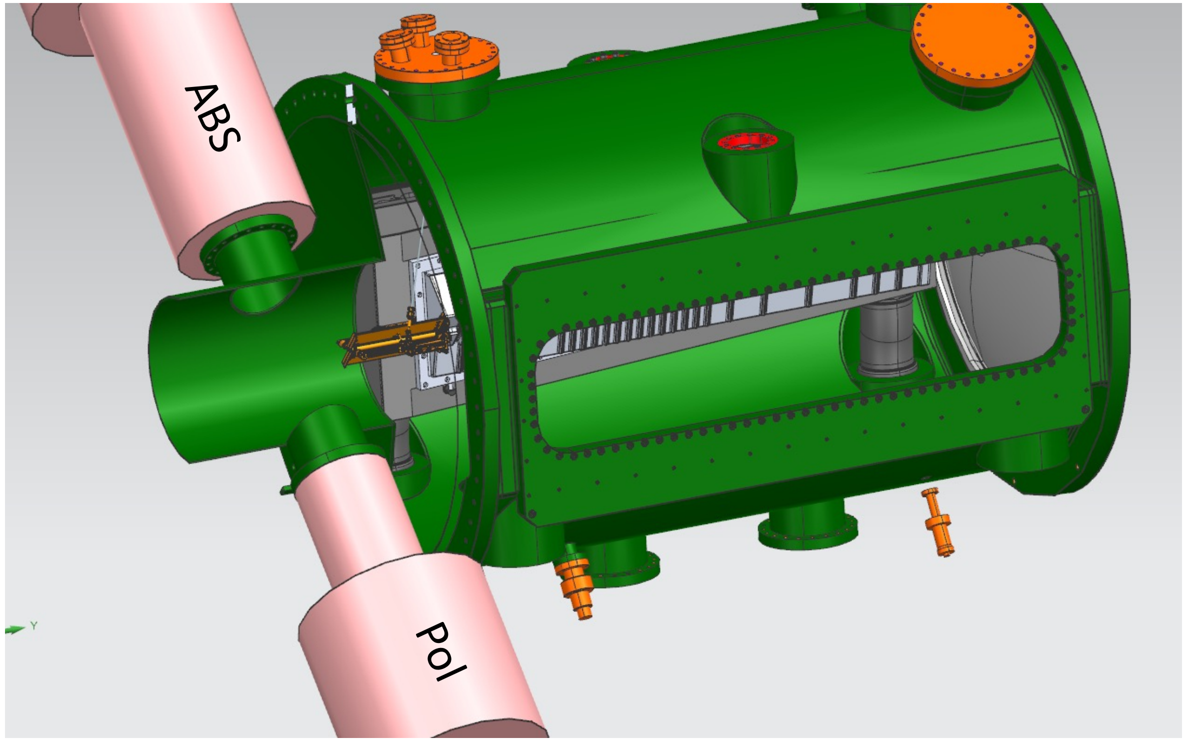

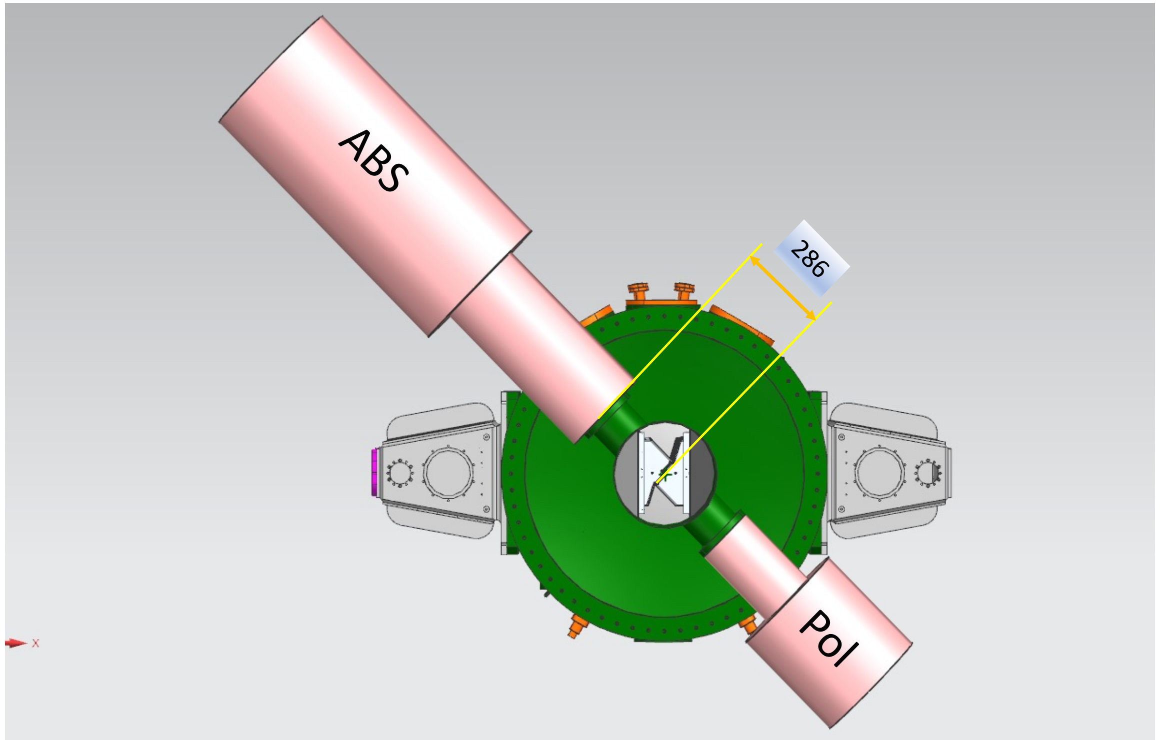

Conclusions

- SMOG2 setup (cell + GFS) installation fully accomplished during LS2
- The SMOG2 commissioning is ongoing
- Many successful tests have been accomplished in the past months/weeks
- Further studies are planned to test higher-pressure injections and use of other gas species as well as to validate the Molflow simulation and the reconstruction algorithms

Conclusions

- SMOG2 setup (cell + GFS) installation fully accomplished during LS2
- The SMOG2 commissioning is ongoing
- Many successful tests have been accomplished in the past months/weeks
- Further studies are planned to test higher-pressure injections and use of other gas species as well as to validate the Molflow simulation and the reconstruction algorithms

First tests confirm the possibility to run simultaneously SMOG2 with the collider mode: a world-wide unique experimental opportunity!

Conclusions

- SMOG2 setup (cell + GFS) installation fully accomplished during LS2
- The SMOG2 commissioning is ongoing
- Many successful tests have been accomplished in the past months/weeks
- Further studies are planned to test higher-pressure injections and use of other gas species as well as to validate the Molflow simulation and the reconstruction algorithms

First tests confirm the possibility to run simultaneously SMOG2 with the collider mode: a world-wide unique experimental opportunity!

- The **LHCspin** R&D is progressing
- Two alternative configurations are being explored: storage cell vs. jet target
- Simulation studies are ongoing to asses the physics performance

Backup

Backup 1: Physics cases for SMOG2

Kinematic conditions for fixed-target collisions at LHC

Assuming pA collisions with $E_p \approx 7\ TeV \implies \sqrt{s_{NN}} \approx \mathbf{115\ GeV}$

$$\boxed{x_2 \approx \frac{Q}{\sqrt{s_{NN}}} e^{-y_{CM}}}$$

$$\boxed{\gamma = \frac{\sqrt{s_{NN}}}{2m_p} \approx 60} \implies$$

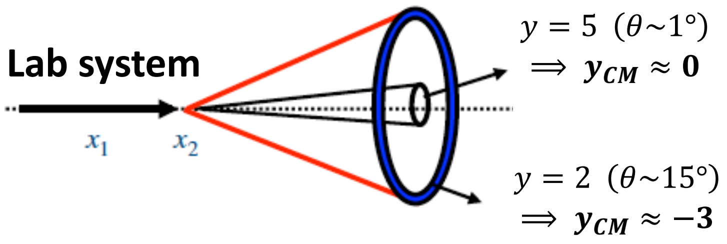

$$\boxed{x_F = \frac{p_L^*}{|max(p_L^*)|} \sim x_1 - x_2 < 0}$$

$$2 \leq y_{LHCb} \leq 5 \implies -3 \leq y_{CM} \leq 0$$

In the fixed-target configuration LHCb allows to cover **mid-to-large x at intermediate Q^2 and negative x_F.**

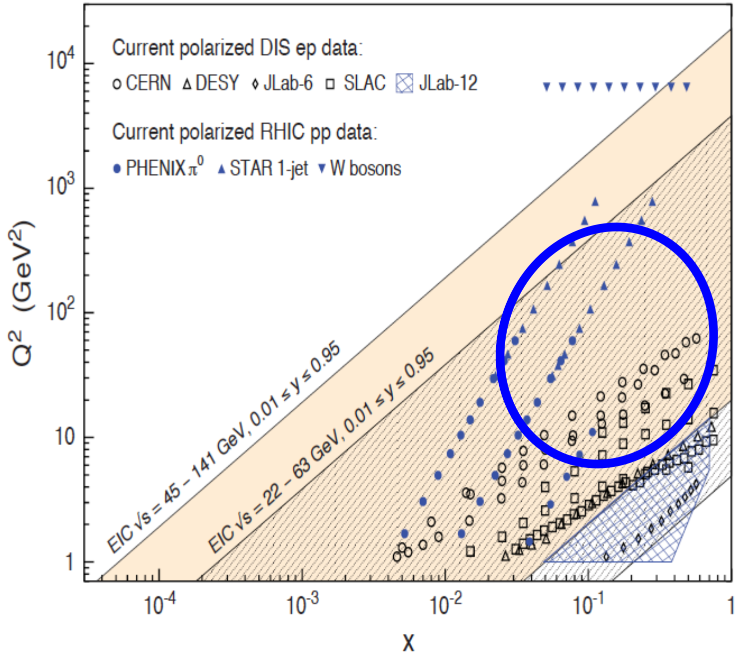

Complementarity is the key!

- Partial overlap with RHIC kinematics
- 12 GeV Jlab probes large-x at small Q^2
- EIC will mainly focus at small-x and large Q^2

SMOG2 projected performances for LHC Run3

LHCb-PUB-2018-015

System	$\sqrt{s_{NN}}$ (GeV)	< pressure> (10^{-5} mbar)	ρ_S (cm^{-2})	$\mathcal{L}$ ($cm^{-2}s^{-1}$)	Rate (MHz)	Time (s)	$\int \mathcal{L}$ (pb^{-1})
pH_2	115	4.0	2.0×10^{13}	6×10^{31}	4.6	2.5×10^6	150
pD_2	115	2.0	1.0×10^{13}	3×10^{31}	4.3	0.3×10^6	9
pAr	115	1.2	0.6×10^{13}	1.8×10^{31}	11	2.5×10^6	45
pKr	115	0.8	0.4×10^{13}	1.2×10^{31}	12	2.5×10^6	30
pXe	115	0.6	0.3×10^{13}	0.9×10^{31}	12	2.5×10^6	22

	SMOG published result pHe@87 GeV	SMOG largest sample pNe@69 GeV	SMOG2 example pAr@115 GeV
Integrated luminosity	7.6 nb^{-1}	$\sim$ 100 nb^{-1}	$\sim$ 45 pb^{-1}
syst. error on J/ψ x-sec.	7%	6 - 7%	2 - 3 %
J/ψ yield	400	15k	15M
D^0 yield	2000	100k	150M
Λ_c^+ yield	20	1k	1.5M
$\psi(2S)$ yield	negl.	150	150k
$\Upsilon(1S)$ yield	negl.	4	7k
Low-mass Drell-Yan yield	negl.	5	9k

A rich and diverse physics program

- ➢ Cold Nuclear Matter effects (nPDFs, absorption, …)
- ➢ Heavy-ion physics with PbA collisions
- ➢ Strangeness production
- ➢ Nucleon structure (quark and gluon TMDs)
- ➢ Ultra-Periferal Collisions and gluon GPDs
- ➢ Intrinsic charm
- ➢ Cosmic-rays and DM
- ➢ …

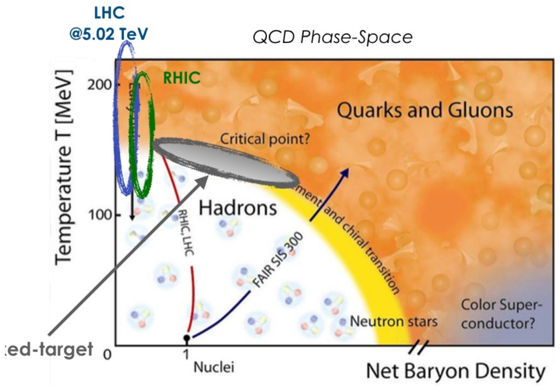

quark pol.

nucleon pol.	U	L	T
U	f_1		$h_1^{\perp}$
L		g_{1L}	$h_{1L}^{\perp}$
T	$f_{1T}^{\perp}$	g_{1T}	$h_1,\ h_{1T}^{\perp}$

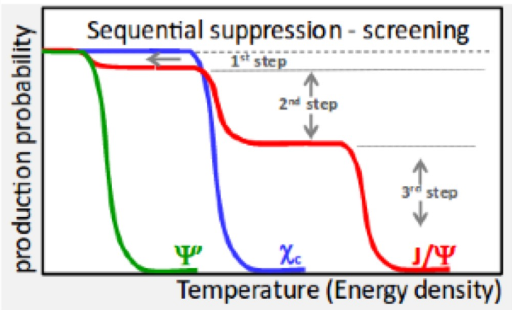

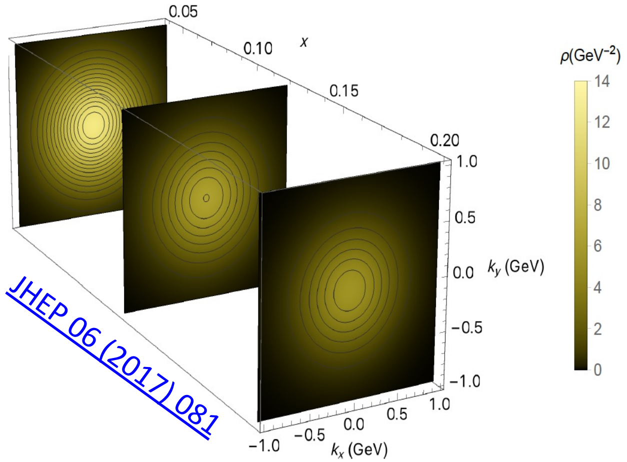

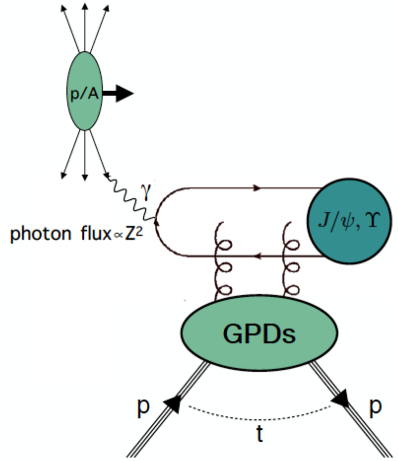

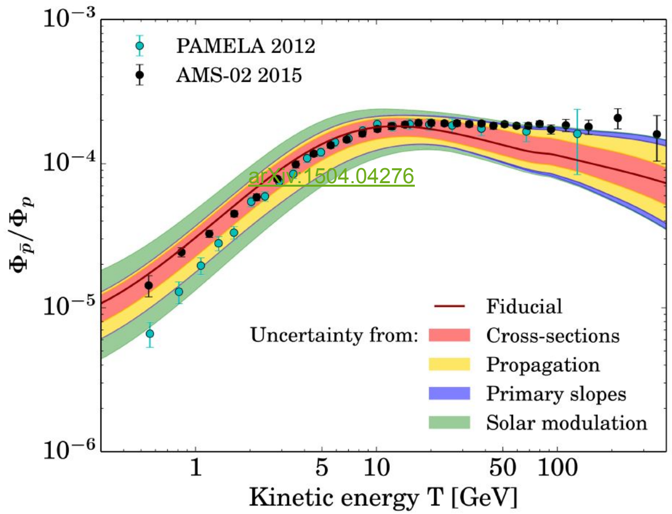

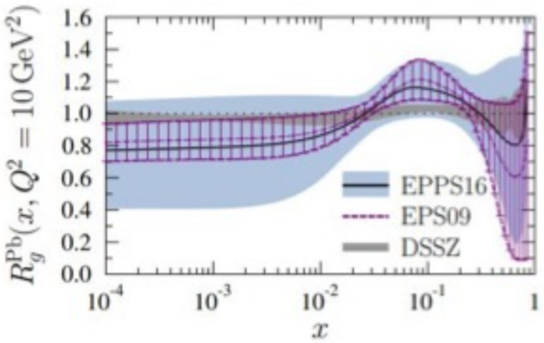

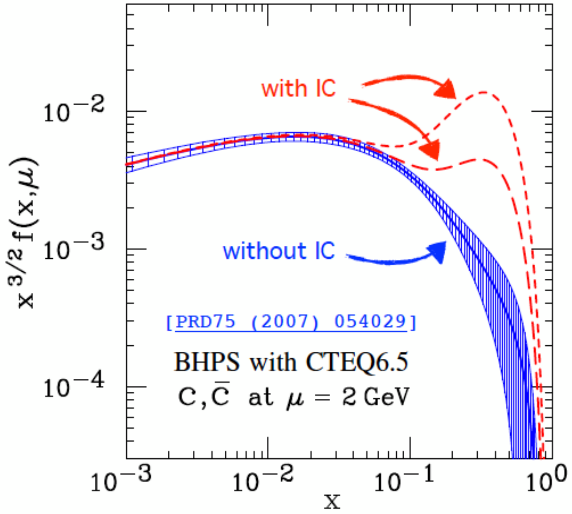

Opportunities with SMOG2: heavy-ion physics

- New measurements of prompt charm production with a significantly increased statistical power. New measurements can also include **charmed baryons** (e.g. Λ_c^+).

- Measurements can be extended to charmonium excited states. Relevant for studying the **sequential charmonia suppression**

arXiv:hep-ph/0512217

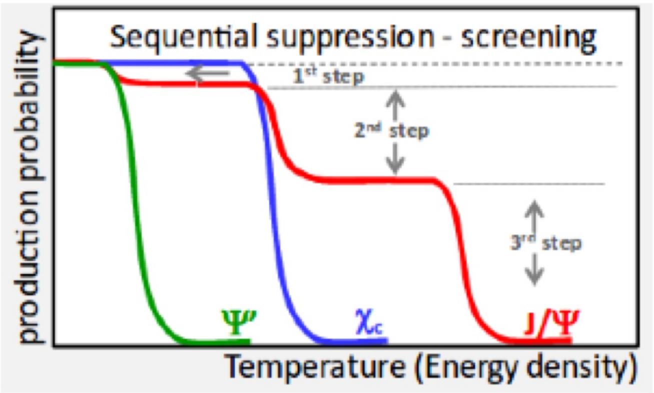

(different binding energies lead to different dissociation temperatures)

- Possibility to measure **prompt beauty production** (7k reconstructed $\Upsilon(1S) \rightarrow \mu^+\mu^-$ events are foreseen with $\mathcal{L} \sim 45\,pb^{-1}$ in pAr collisions)

- Measurement of QGP-related flow observables and correlations in Pb-A collisions at $\sqrt{s_{NN}} \sim 70$ GeV

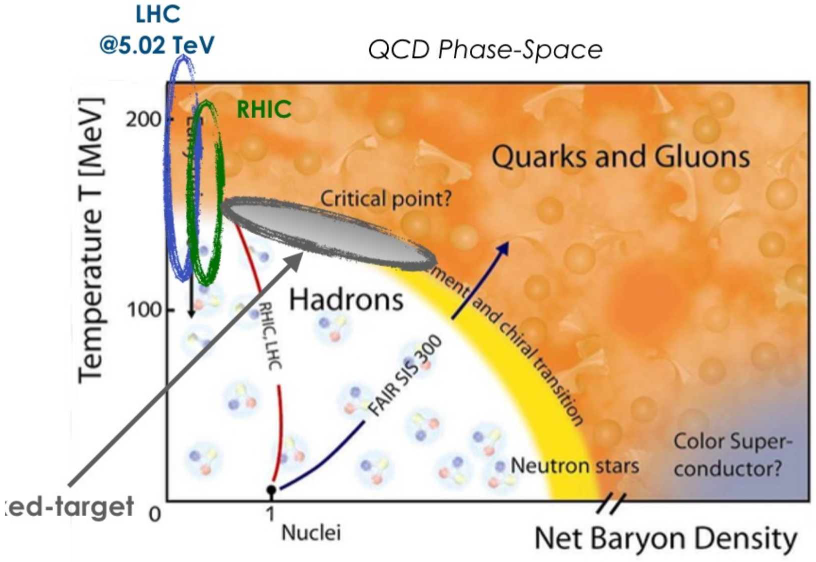

Opportunities with SMOG2: cold nuclear matter effects

Heavy Ions studies and Cold Nuclear Matter Effects

Study and disentangle effects arising from the structure of the initial state of the collision and medium-induced effects

- *Modification of the nucleon PDFs in nuclear matter*
- *High-x parton PDFs*
- *antishadowing, EMC effects*
- *Cronin effect*
- *nuclear absorption*

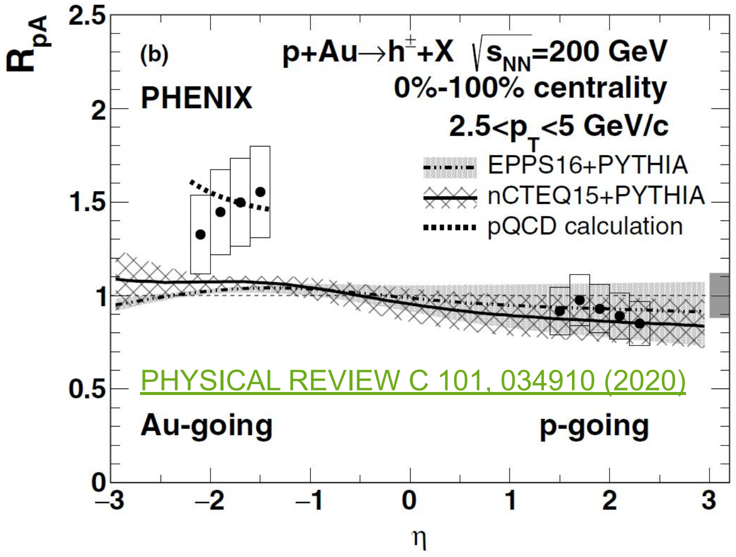

$$R_{pA} = \frac{dY^{pA}/dp_T d\eta}{dY^{pp}/dp_T d\eta} \cdot \frac{1}{\langle N_{coll} \rangle}$$

$$R_i^A(x, Q^2) = \frac{f_i^{p/A}(x, Q^2)}{f_i^{p}(x, Q^2)}$$

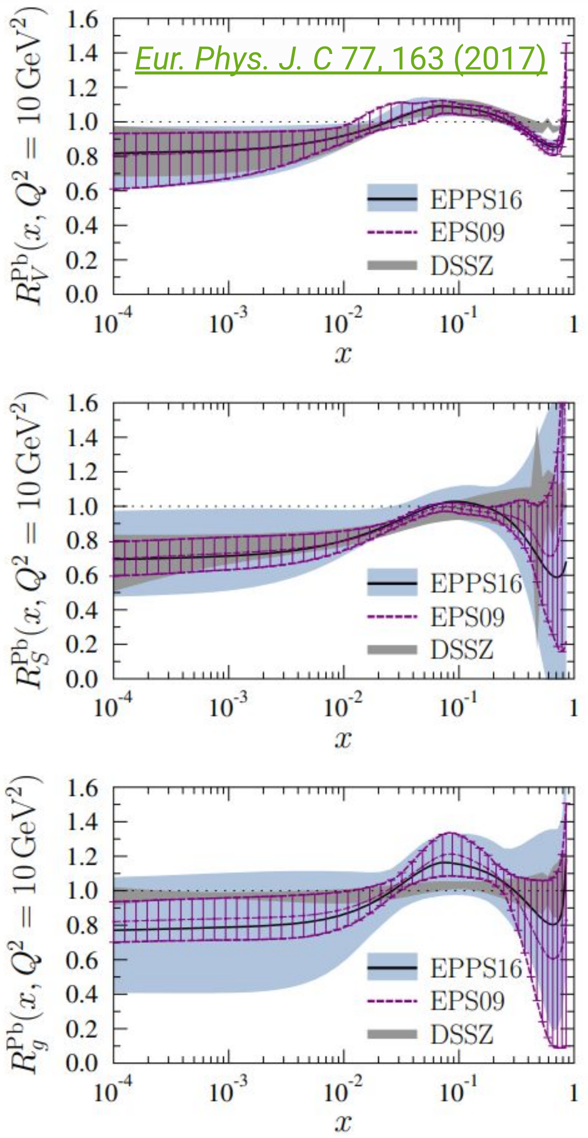

Opportunities with SMOG2: strangeness production in PbA vs. pA

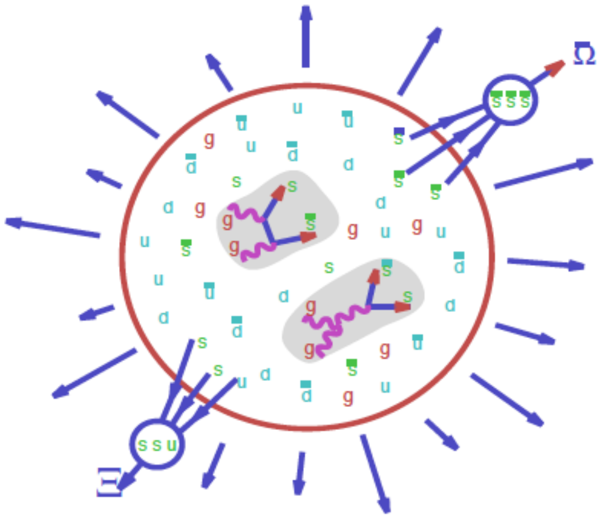

Strangeness enhancement is expected due to:

- high gluon density in the QGP
- dominance of the gluonic production channel for strangeness in the QGP ($gg \to s\bar{s}$)
- mass of the s quark being similar to the critical temperature T for the QCD phase transition ($\sim 150\ MeV$)
- strangeness formation time similar to the expected lifetime of the QGP. Therefore strangeness chemical equilibration in QGP is possible, leading to abundant strange quark density in QGP

Strange/non-strange hadron ratios vs. event multiplicity $\boldsymbol{p_T}$ and $\boldsymbol{\eta}$

- $(K^+ + K^-)/(\pi^+ + \pi^-)$
- $K_S^0/(\pi^+ + \pi^-)$
- $(\Lambda + \bar{\Lambda})/(\pi^+ + \pi^-)$
- $(\Xi^- + \bar{\Xi}^+)/(\pi^+ + \pi^-)$
- $(\Omega^- + \bar{\Omega}^+)/(\pi^+ + \pi^-)$

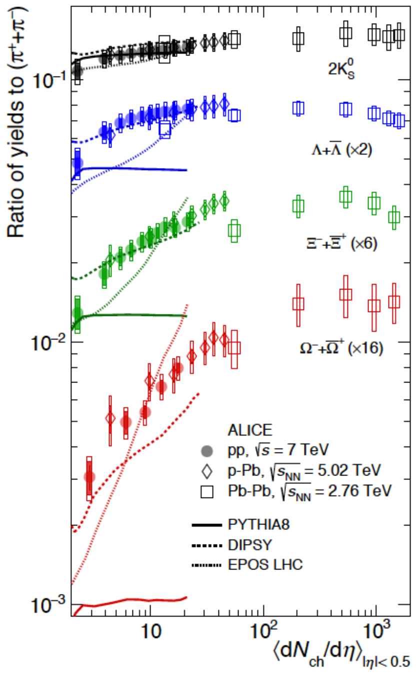

Baryon/meson ratios: $\boldsymbol{p/\pi, \Lambda/K, \Lambda/\phi, \Omega/\phi}$,…

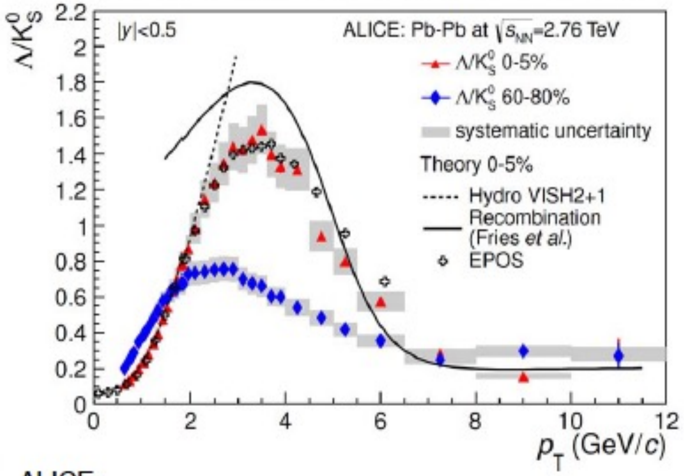

ALICE
PRL111, 222301 (2013)

Opportunities with SMOG2: nucleon structure

- SMOG2 operated with H_2 and D_2 targets offers unique conditions to probe quark and gluon PDFs in nucleons and nuclei, especially at high-x and moderately-high Q^2, where present experimental data are largely insufficient to constraint the theoretical distributions.

- Measurements of **quark and gluon transverse-momentum-dependent (TMD) PDFs**, respectively in Drell-Yan and inclusive production of quarkonia (J/ψ, ψ', Υ, etc.), will significantly improve our understanding of the 3D structure of the nucleon in the non-perturbative regime of QCD.

Unpolarized Drell-Yan

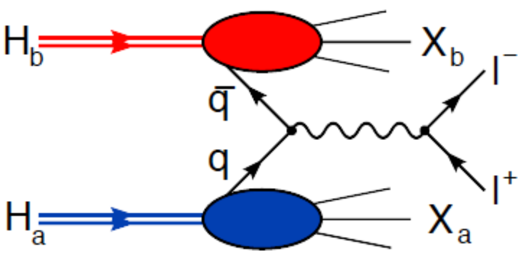

nucleon pol. \ quark pol.	U	L	T
U	f_1		$h_1^\perp$
L		g_{1L}	$h_{1L}^\perp$
T	$f_{1T}^\perp$	g_{1T}	h_1, $h_{1T}^\perp$

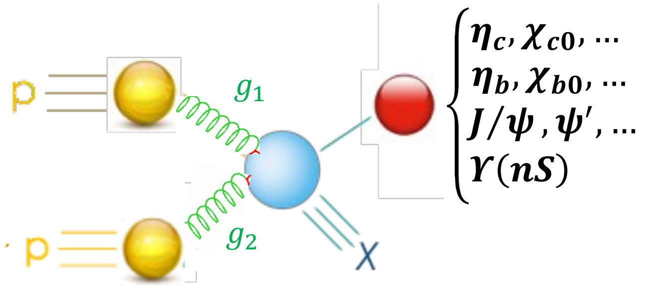

nucleon pol. \ gluon pol.	U	Circularly	Linearly
U	f_1^g		$h_1^{\perp g}$
L		g_{1L}^g	$h_{1L}^{\perp g}$
T	$f_{1T}^{\perp g}$	g_{1T}^g	h_1^g, $h_{1T}^{\perp g}$

Opportunities with SMOG2: quark TMDs

	quark pol. U	L	T
nucleon pol. U	f_1		$h_1^\perp$
L		g_{1L}	$h_{1L}^\perp$
T	$f_{1T}^\perp$	g_{1T}	$h_1,\ h_{1T}^\perp$

Unpolarized Drell-Yan

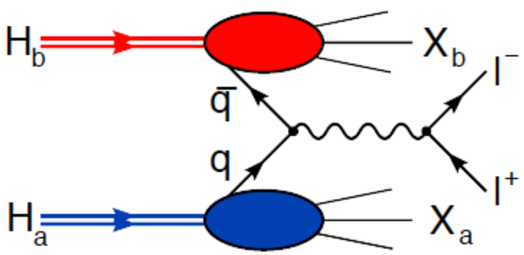

- Theoretically cleanest hard h-h scattering process
- LHCb has excellent μ-ID & reconstruction for $\mu^+\mu^-$
- **dominant**: $\bar{q}(x_{beam}) + q(x_{target}) \rightarrow \mu^+\mu^-$
- suppressed: $q(x_{beam}) + \bar{q}(x_{target}) \rightarrow \mu^+\mu^-$
- beam sea quarks probed at small x
- target valence quarks probed at large x

Sensitive to unpol. and BM TMDs for $q_T \ll M_{ll}$

(violation of Lam-Tung relation)

$$d\sigma_{UU}^{DY} \propto f_1^{\bar{q}} \otimes f_1^{q} + \cos 2\phi \ h_1^{\perp,\bar{q}} \otimes h_1^{\perp,q}$$

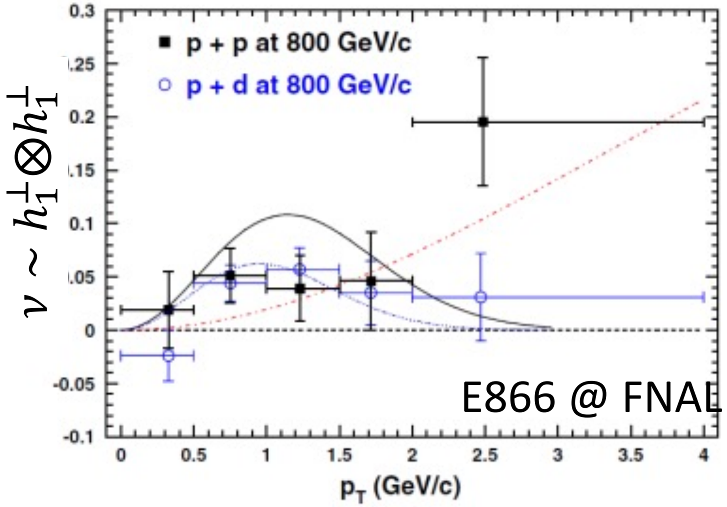

[PRL 102 2009 182001]

[Nature 590, 561 (2021)]

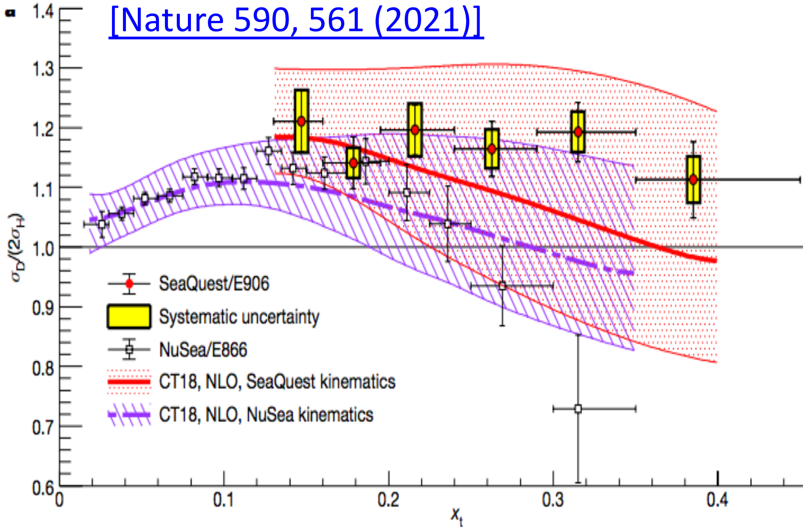

- Lattice QCD: $\bar{s}(x) \neq s(x)$ [arXiv:1809.04975]
- **proton sea more complex than originally thought!**
- **intrinsic heavy quarks**?
- Still a lot to be understood

- H & D targets allow to study the **antiquark content of the nucleon**
- SeaQuest (E906): $\bar{d}(x) > \bar{u}(x) \implies$ **sea is not flavour symmetric!**

Opportunities with SMOG2: gluon TMDs

In high-energy hadron collisions, heavy quarks are dominantly produced through gg fusion:

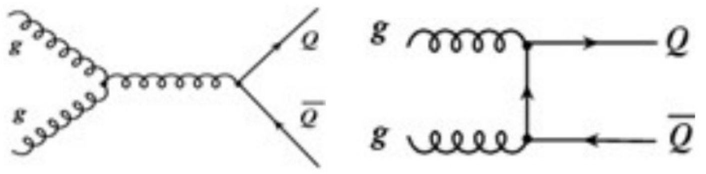

The most efficient way to access the gluon dynamics inside the proton at LHC is to **measure heavy-quark observables**

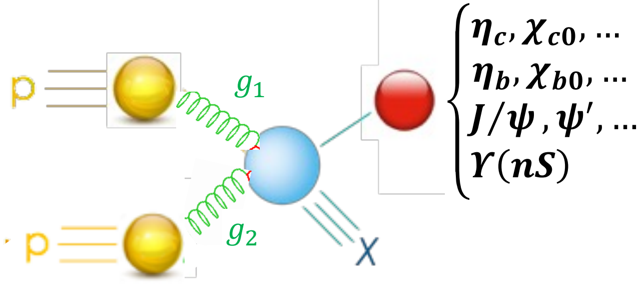

- **Inclusive quarkonia production in (un)polarized pp interaction** $(pp^{(\uparrow)} \to [Q\bar{Q}]X)$ turns out to be an ideal observable to access gTMDs (assuming TMD factorization)

- TMD factorization requires $q_T(Q) \ll M_Q$. Can look at **associate quarkonia production**, where only the relative q_T needs to be small:

  E.g.: $pp^{(\uparrow)} \to J/\psi + J/\psi + X$

- Due the larger masses this condition is more easily matched in the case of **bottomonium**, where TMD factorization can hold at larger q_T (although very challenging for experiments!)

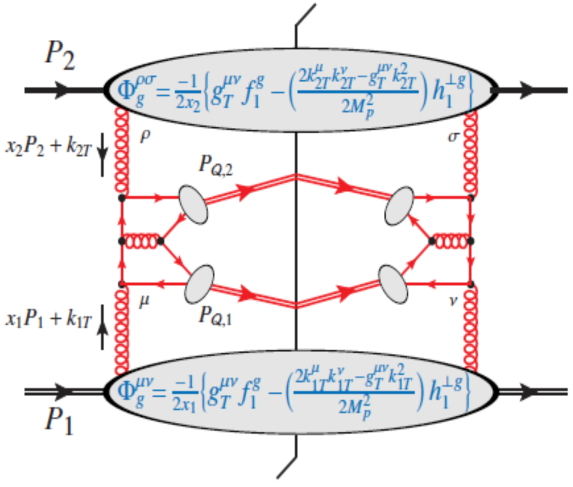

$pp \to J/\psi\, J/\psi\, X$

Opportunities with SMOG2: gluon TMDs

$$\frac{d\sigma}{dM_{QQ}dY_{QQ}d^2\boldsymbol{P}_{QQ_T}d\Omega} = \frac{\sqrt{M_{QQ}^2 - 4M_Q^2}}{(2\pi)^2 8s\, M_{QQ}^2}$$

$$\Big\{ F_1(M_{QQ},\theta_{CS})\, \mathcal{C}\left[f_1^g f_1^g\right](x_{1,2},\boldsymbol{P}_{QQ_T})$$

$$+F_2(M_{QQ},\theta_{CS})\, \mathcal{C}\left[w_2 h_1^{\perp g} h_1^{\perp g}\right](x_{1,2},\boldsymbol{P}_{QQ_T})$$

$$+\left(\boxed{F_3(M_{QQ},\theta_{CS})\, \mathcal{C}\left[w_3 f_1^g h_1^{\perp g}\right](x_{1,2},\boldsymbol{P}_{QQ_T}) + F_3'(M_{QQ},\theta_{CS})\, \mathcal{C}\left[w_3' h_1^{\perp g} f_1^g\right](x_{1,2},\boldsymbol{P}_{QQ_T})\Big) \cos 2\phi_{CS}} \boxed{+F_4(M_{QQ},\theta_{CS})\, \mathcal{C}\left[w_4 h_1^{\perp g} h_1^{\perp g}\right](x_{1,2},\boldsymbol{P}_{QQ_T}) \cos 4\phi_{CS}\Big\}}$$

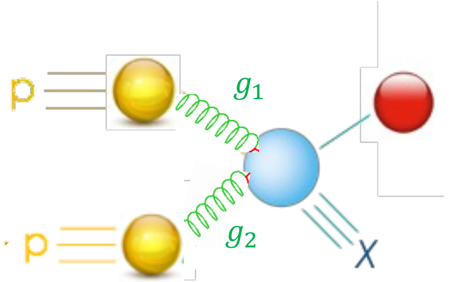

$\begin{cases} J/\psi + J/\psi \\ \Upsilon + \Upsilon \\ \ldots \end{cases}$

gluon pol.

nucleon pol.	U	Circularly	Linearly
U	f_1^g		$h_1^{\perp g}$
L		g_{1L}^g	$h_{1L}^{\perp g}$
T	$f_{1T}^{\perp g}$	g_{1T}^g	$h_1^g,\ h_{1T}^{\perp g}$

Predictions based on CSM + TMD evolution for $x_1 \sim x_2 \sim 10^{-3}$ at forward rapidity [EPJ C 80, 87 (2020)]

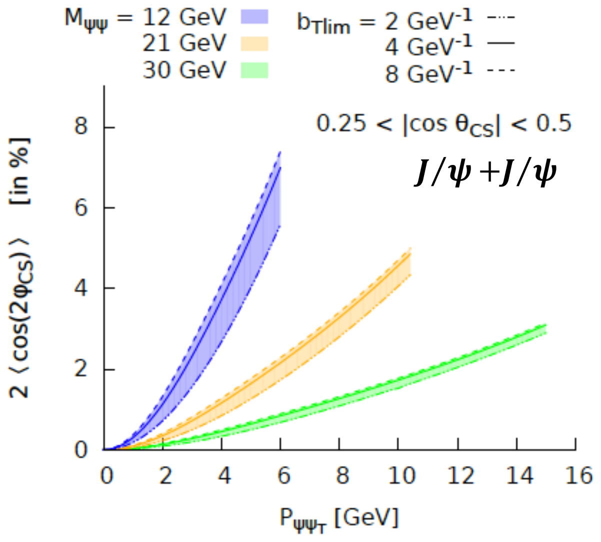

Azimuthal amplitudes $\sim 5\%$!

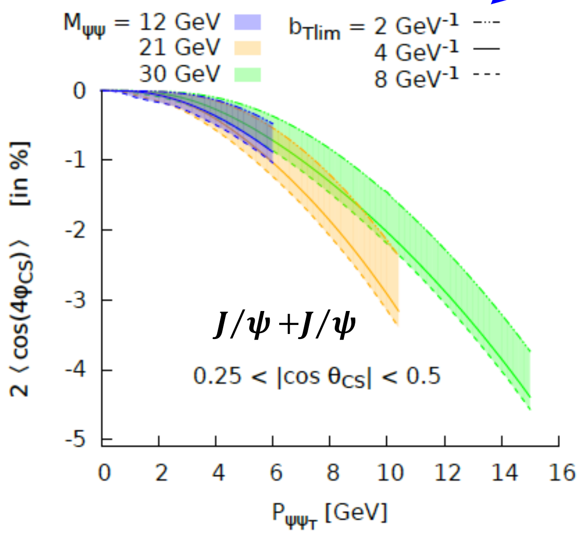

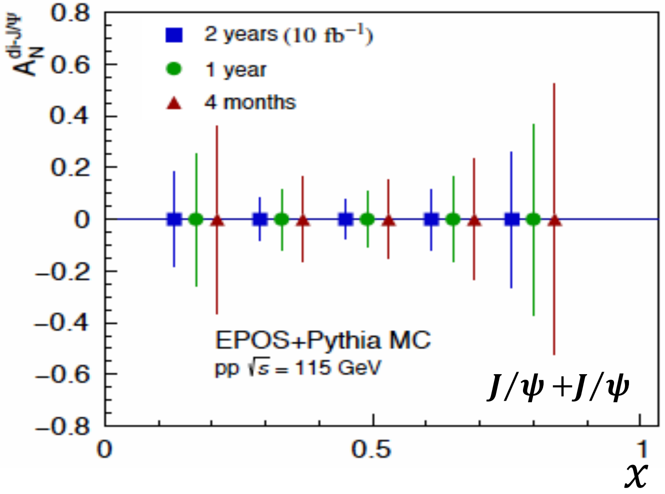

Opportunities with SMOG2: gluon TMDs

GPD	U	L	T
U	H		$\mathcal{E}_T$
L		$\tilde{H}$	$\tilde{E}_T$
T	E	$\tilde{E}$	$H_T,\ \tilde{H}_T$

Gluon GPDs can be accessed at LHC in **Ultra-Peripheral collisions (UPC)**

- Impact parameter larger than sum of radii
- Process dominated by EM interaction
- Gluon distributions probed by pomeron exchange
- Exlcusive quarkonia prod. sensitive to gluon GPDs [PRD 85 (2012), 051502]

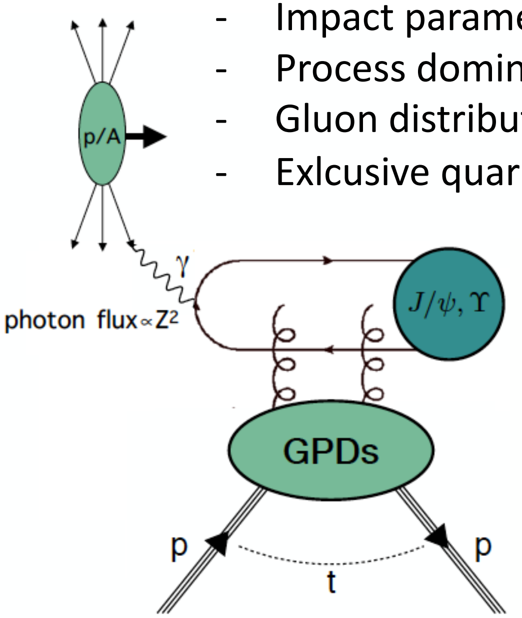

3D maps of parton densities in coordinate space

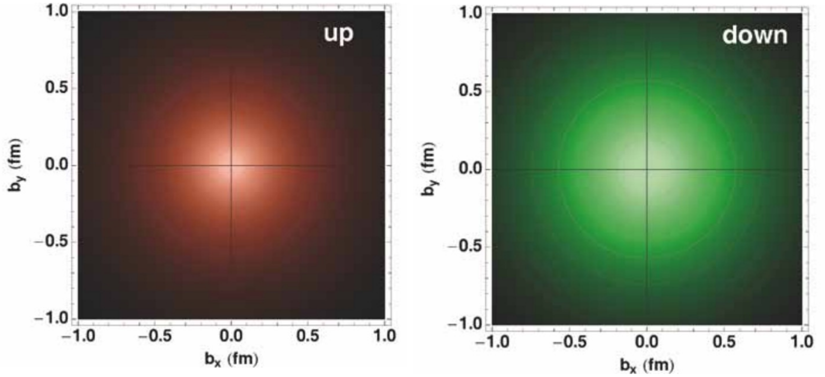

[NS 28 (2012), 1]

First results from LHCb in PbPb UPC

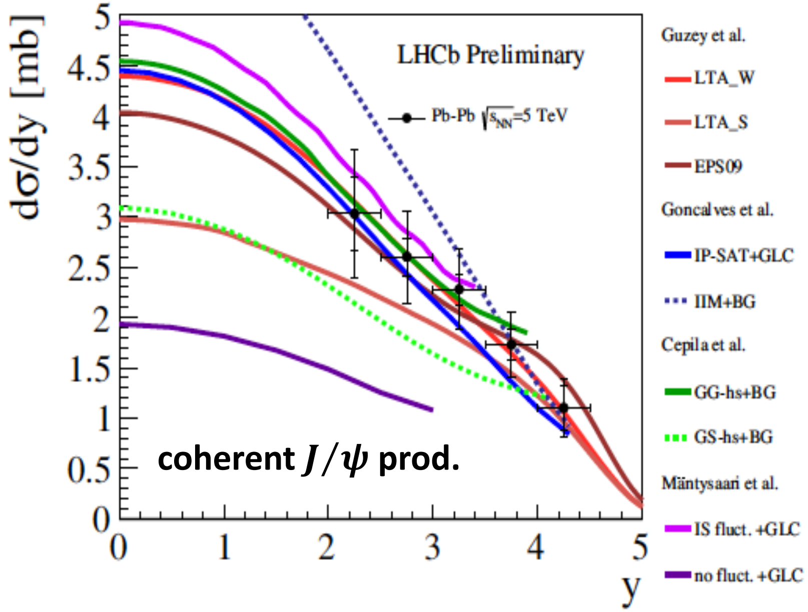

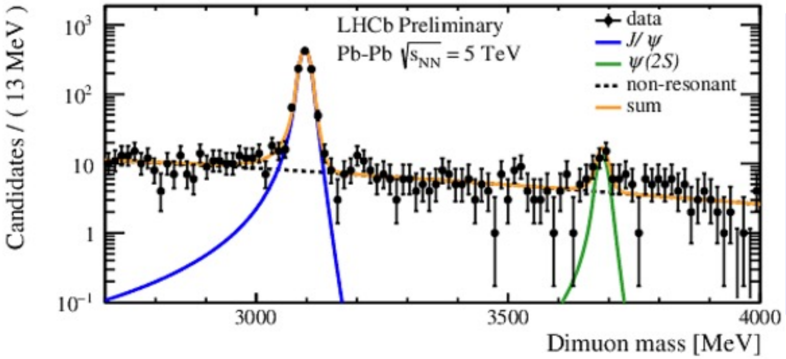

[NPA 982 (2019) 247]

Opportunities with SMOG2: intrinsic charm

Intrinsic heavy-quark

- 5-quark Fock state of the proton may contribute at high x!
- **charm PDFs** at large x could be larger than obtained from conventional fits

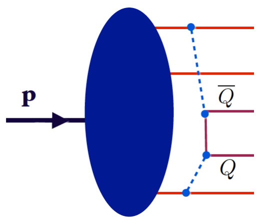

[PRD 75 (2007) 054029]

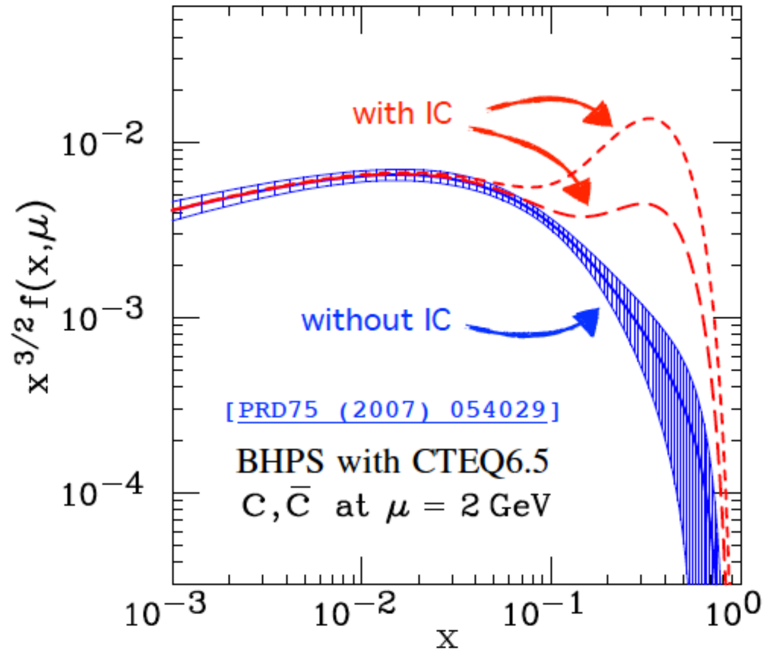

- **Significant contributions of IC expected at large x**

- First search performed with SMOG [PRL 122 (2019)]
- New intriguing LHCb results with pp collisions at large rapidity [arXiv:2109.08084]
- Still to be investigated!

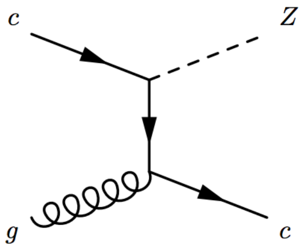

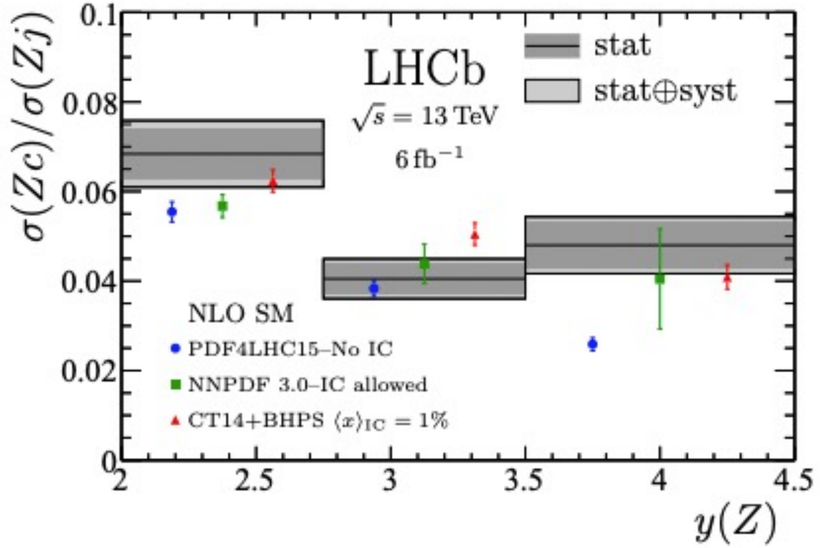

Opportunities with SMOG2: cosmic rays and DM

- Thanks to the possibility to use also a H_2 target, it will be possible to precisely measure the ratio:

$$\frac{\sigma(pHe \to \bar{p}X)}{\sigma(pH \to \bar{p}X)}$$

where many systematic uncertainties cancel

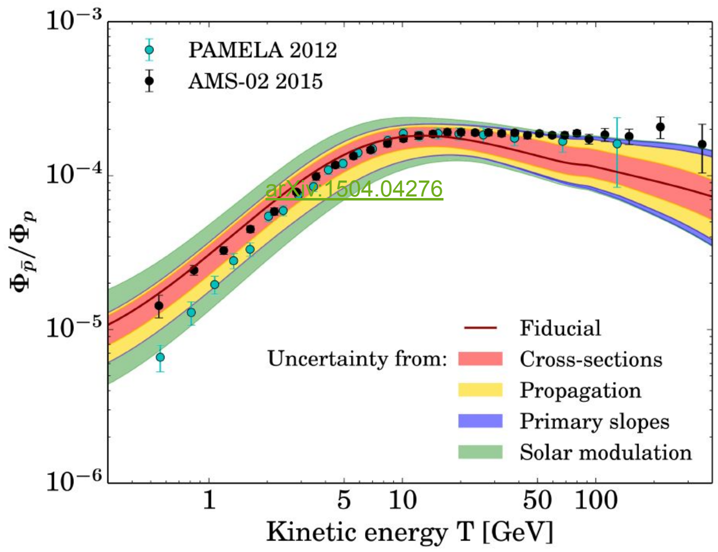

- By injecting H_2 and D_2 it will be possible to test isospin symmetry in the ratio:

$$\frac{\sigma(pD \to \bar{p}X)}{\sigma(pH \to \bar{p}X)}$$

which can allow to put constraints on the unknown production ratio

$$\frac{\sigma(pH \to \bar{n}X)}{\sigma(pH \to \bar{p}X)}$$

- Light anti-nuclei production: $pp,\ pHe \ \to\ \bar{d}\,,\ \overline{H_e}$

- $pp,\ pHe \ \to\ \pi, K$ to model positron source term

SMOG2 commissioning phases

1. Low pressure gas injection with OPEN cell (and VELO) and no beam
   → **test new gas injection system**

2. Low pressure gas injection with OPEN cell (and VELO) and beam (first SMOG-like beam-gas collisions)
   → **check luminosity profile vs. gas pressure and first responses of upgraded LHCb detector**

3. Circulating beam with OPEN cell (and VELO) and no gas
   → **check temperature profiles (beam-induced heating of the cell)**

4. Circulating beam with CLOSED cell (and VELO) and low-pressure gas
   → **test mechanical closure, simultaneous collider and fixed-target data-taking**

Backup 2: H2 injection studies for SMOG2

SMOG2: H_2 injection studies

- NEG (non-evaporable getter) coating is used is some sections of the LHC beam-pipe and in the VELO RF foil to ensure low SEY (Secondary Electron Yield)
- Due to their small mass and high reactivity, hydrogen atoms are easily absorbed by the NEG coated surface and can cause embrittlement of the coating and peel-off in the beam pipe.

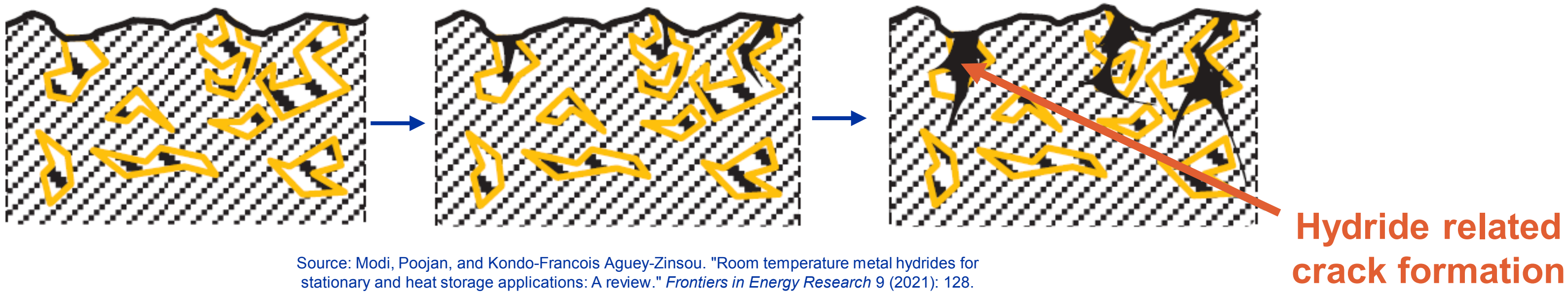

Source: Modi, Poojan, and Kondo-Francois Aguey-Zinsou. "Room temperature metal hydrides for stationary and heat storage applications: A review." *Frontiers in Energy Research* 9 (2021): 128.

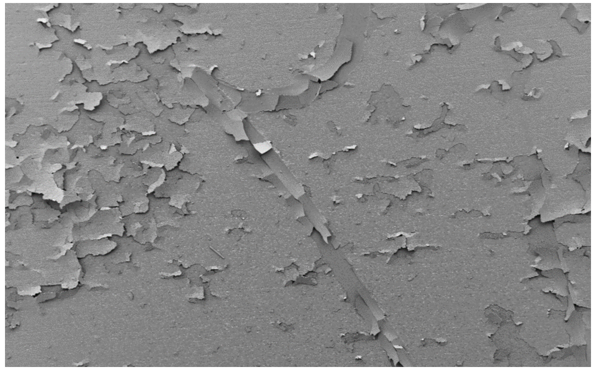

- An extensive H_2 load can result in a partial saturation of the NEG coating, which would prevent further hydrogen absorption
- **Simulations and laboratory studies are needed to quantify the extent of the saturation induced by H_2 injection and the consequent enhancement of the SEY, as well as possible effects of embrittlement and peel-off**

A crucial parameter is the **sticking coefficient:** ratio of atoms/molecules that "stick" to a surface to the total number of atoms/molecules that impinge upon that surface in the same time. A small sticking coeff. (saturation) implies reduced pumping capabilities of the NEG coating.

SMOG2: H_2 injection studies

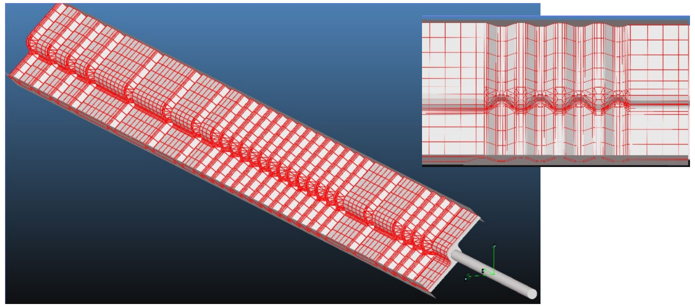

- **Molflow studies of H_2 and N_2 adsorption on NEG-coated surfaces in the LHCb environment (C. Lucarelli)**
- Simulations based on actual geometry of SMOG2 cell and VELO RF foil

H_2 (preliminary) results:

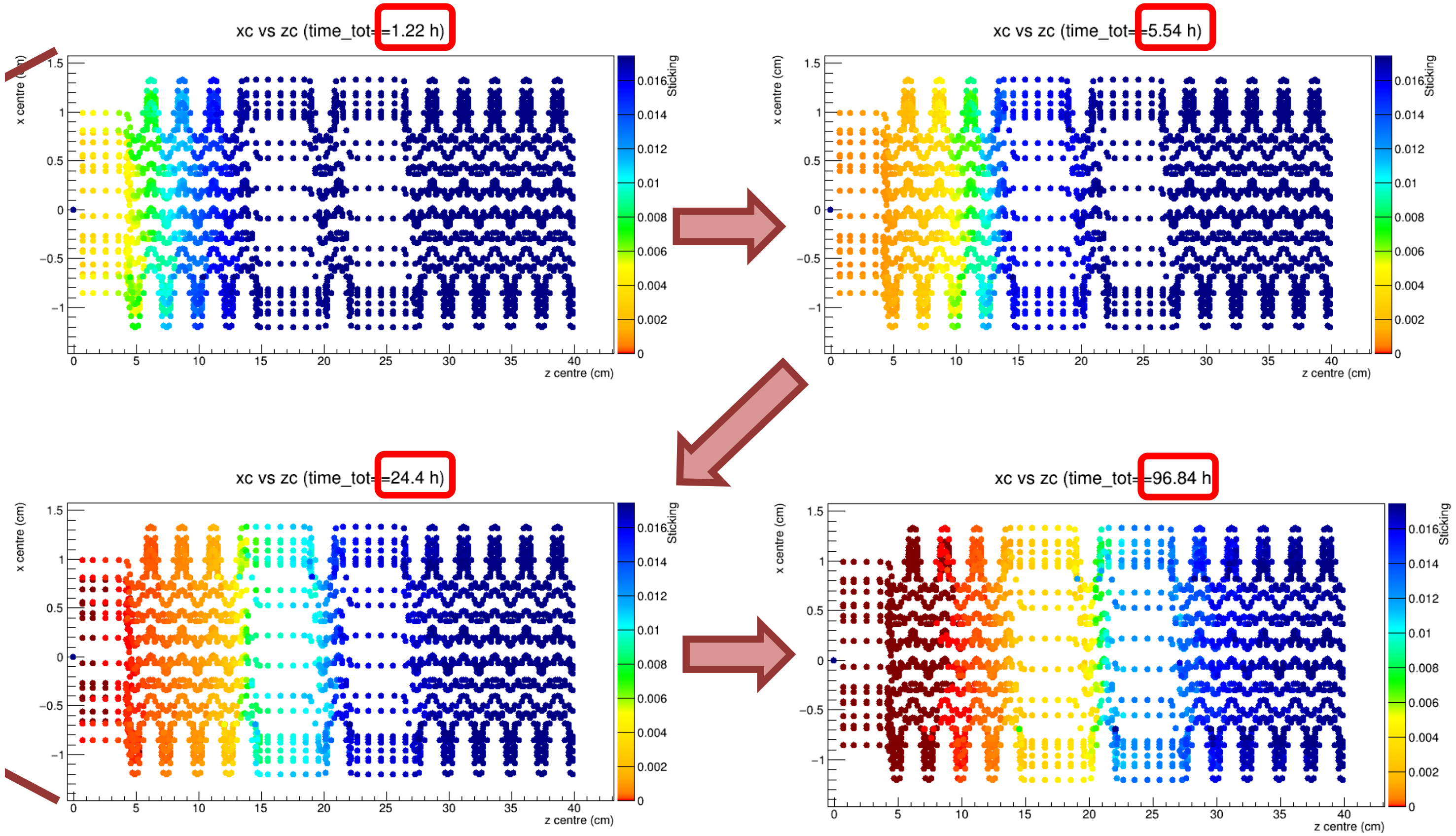

- After 96 h of continuous injection, only a small fraction of RF foil is saturated (first 7-8 cm)
- The propagation of saturation through the RF foil slows down progressively with time
- Vacuum experts ensure that these results suggest possibility to safely inject hydrogen for short runs
- Experimental studies of NEG coating embrittlement/delamination, saturation and SEY with high and low pressure H_2 injections interleaved with reactivation cycles are being performed by the vacuum group (see backup slides)

SMOG2: H_2 injection studies

- **Saturation measurement performed by the vacuum group (Dávid Máté Parragh) with dedicated experimental setup**

Witness samples placed at the entrance of the pipe

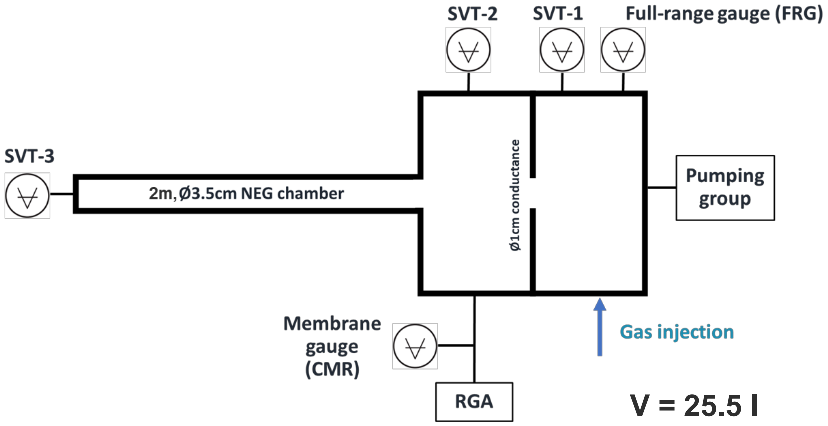

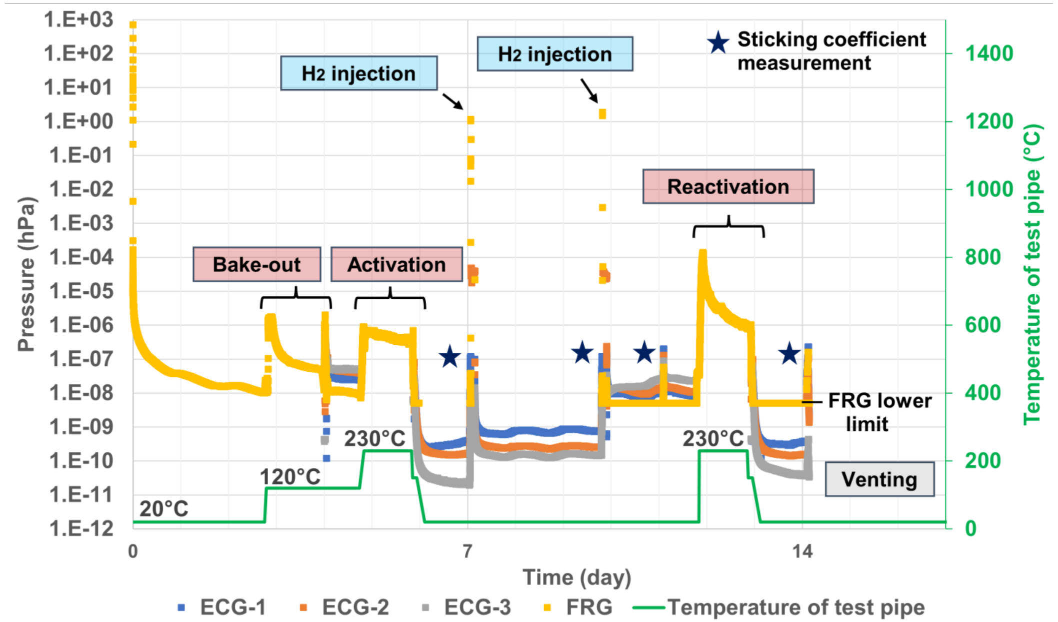

2m long NEG coated DN40 304L stainless steel pipe:

- 1.2144g (0.0223mol) NEG coating
- 2200cm² surface area

Experimental procedure:

1. Bake-out and activation (230°C for 24 h)
2. H_2 sticking coefficient measurement
3. High pressure H_2 injection (1 mbar)
   – afterwards: static vacuum (2 h) + 24 h pumping
4. H_2 sticking coefficient measurement
5. High pressure H_2 injection (1 mbar)
   – afterwards: static vacuum (2 h) + 24 h pumping
6. (H_2 sticking coefficient measurement)
7. Reactivation (230°C for 24 h)
8. H_2 sticking coefficient measurement
9. Venting, witness sample retrieval, and visual inspection

Repeated 6 times

SMOG2: H_2 injection studies

- **Saturation measurement performed by the vacuum group (Dávid Máté Parragh) with dedicated experimental setup**

1. Bake-out and activation (230°C for 24 h)
2. **Sticking coefficient measurement**
3. High pressure injection (1 mbar)
   – afterwards: static vacuum (2 h) + 24 h pumping
4. **Sticking coefficient measurement**
5. High pressure injection (1 mbar)
   – afterwards: static vacuum (2 h) + 24 h pumping
6. (Sticking coefficient measurement)
7. Reactivation (230°C for 24 h)
8. **Sticking coefficient measurement**
9. Venting, witness sample retrieval, and visual inspection

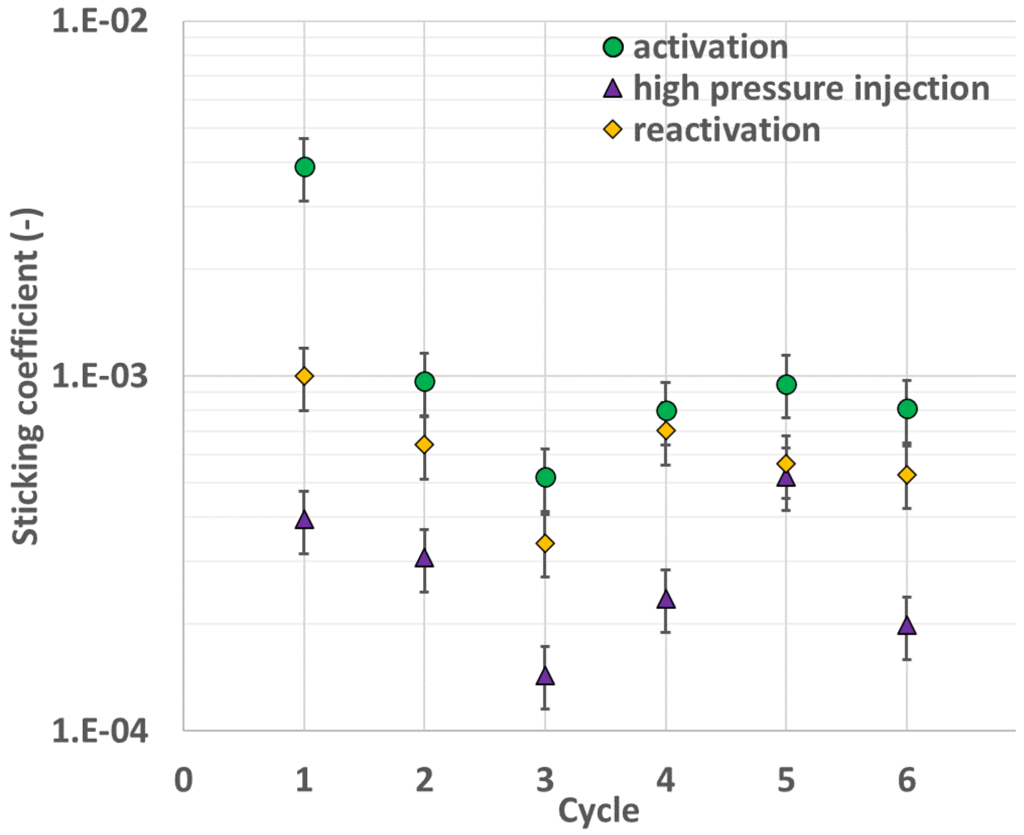

- Sticking coefficient decreases with increased quantity of absorbed hydrogen
- only partially recoverable with 24 h reactivation at 230 °C

SMOG2: H_2 injection studies

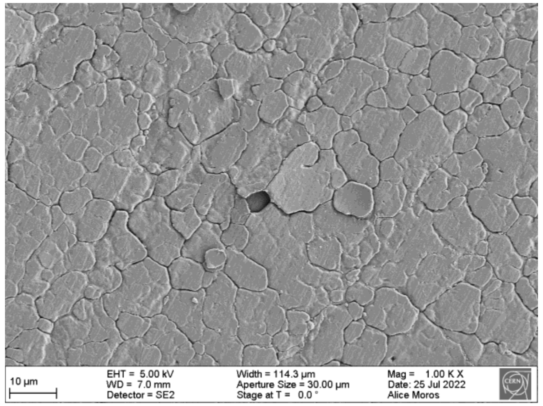

Top SEM image of HP-6 witness sample

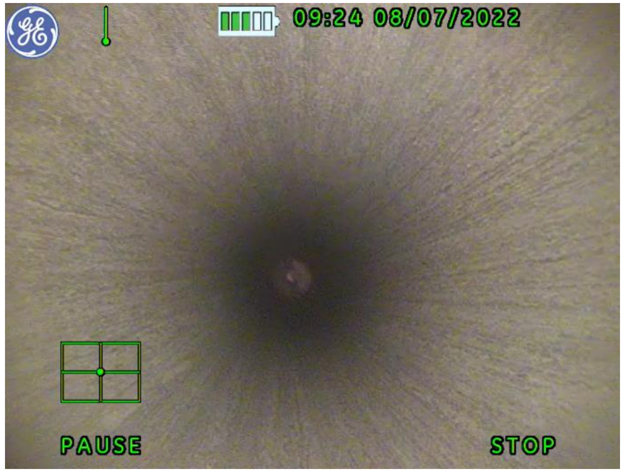

Endoscopic view of the TiZrV coated test pipe after the 6th cycle

- No visible sign of peel-off in the beam-pipe at 1 mbar injection pressure
- Coating delamination needs further studies with flat samples

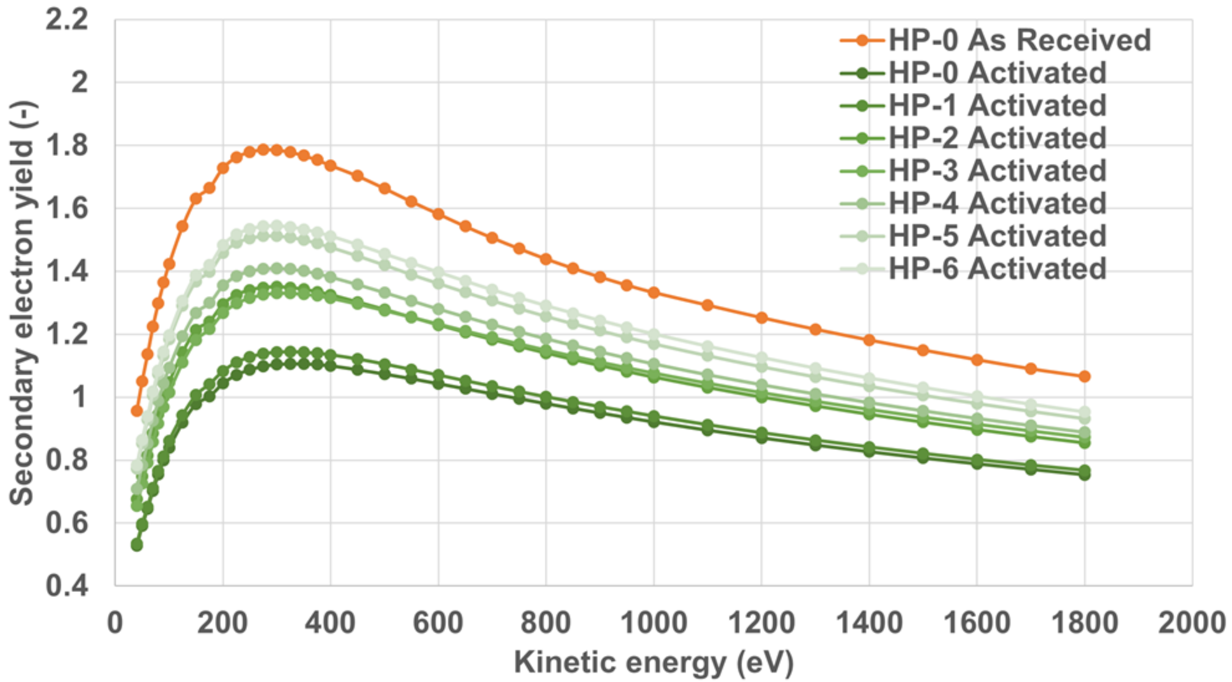

Secondary electron yield of witness samples after 1h 250°C in-situ activation

- An increase of the SEY is observed after each cicle

Backup 3: LHCspin performace

Expected performance

Target

- $I_0 = 6.5 \cdot 10^{16} s^{-1}$ (HERMES)
- C_{tot} = 17.4 l/s (20 cm cell)
- **θ= 3.7 ·10^{13} atoms/cm^2**

Beam

- $1.2 \cdot 10^{11}$ p/bunch (RUN3)
- 2808 bunches
- $\boldsymbol{I_{beam} = 3.8 \cdot 10^{18}\ p/s}$

$$\boldsymbol{\mathcal{L}_{pH}(300\ K) \approx 1.4 \cdot 10^{32}\ \mathrm{cm}^{-2}\mathrm{s}^{-1}}$$

$$\boldsymbol{L_{pH}(Run\ 4) \approx 5\ fb^{-1}}$$

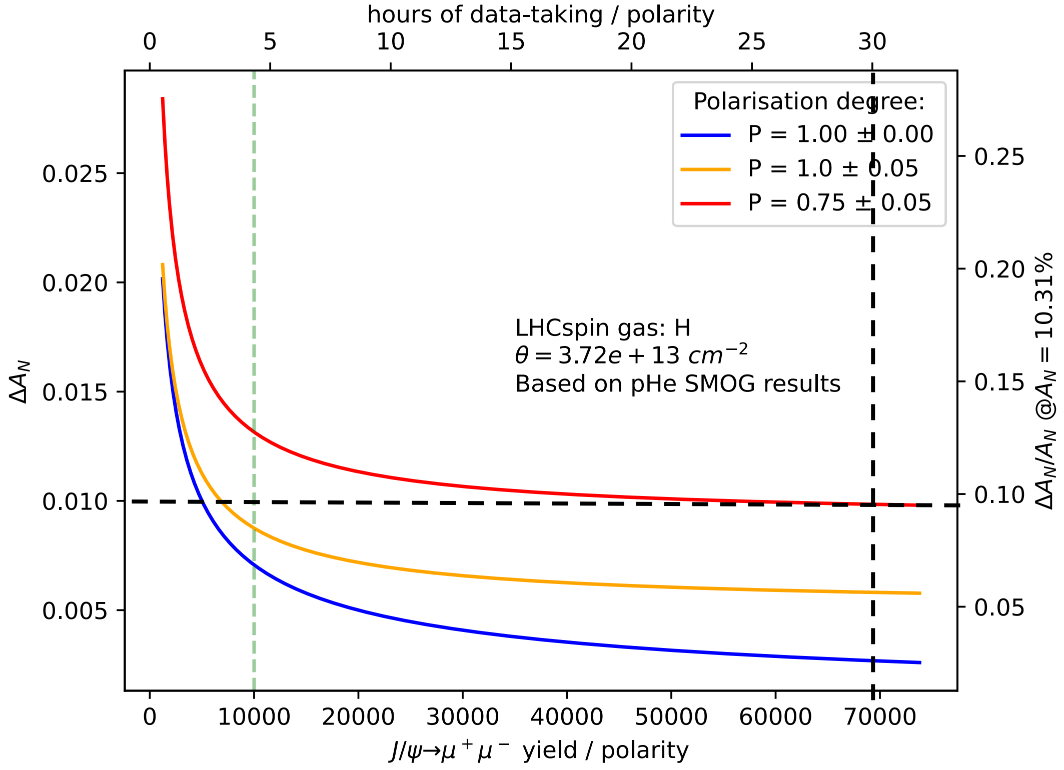

Expected yields for Run4 (Run4+Run5):

Channel	Events / week	Total events
$J/\psi \to \mu^+\mu^-$	194k (434k)	23M (75M)
$\psi(2S) \to \mu^+\mu^-$	3.5k (7.7k)	414k (1.3M)
$D^0 \to K^-\pi^+$	976k (2.2M)	117M (380M)
$J/\psi J/\psi \to \mu^+\mu^-\mu^+\mu^-$	77 (170)	930 (3000)
Drell Yan ($5 < M_{\mu\mu} < 9$ GeV)	110 (250)	13k (43k)
$\Upsilon \to \mu^+\mu^-$	83 (187)	10k (32k)
$\Lambda_c^+ \to pK^-\pi^+$	19k (43k)	2.3M (7.5M)

assumptions:

- 120 weeks/RUN
- 84h/week
- $Stat(Run5) \sim \sqrt{5}\, Stat(Run4)$

Reconstruction efficiencies

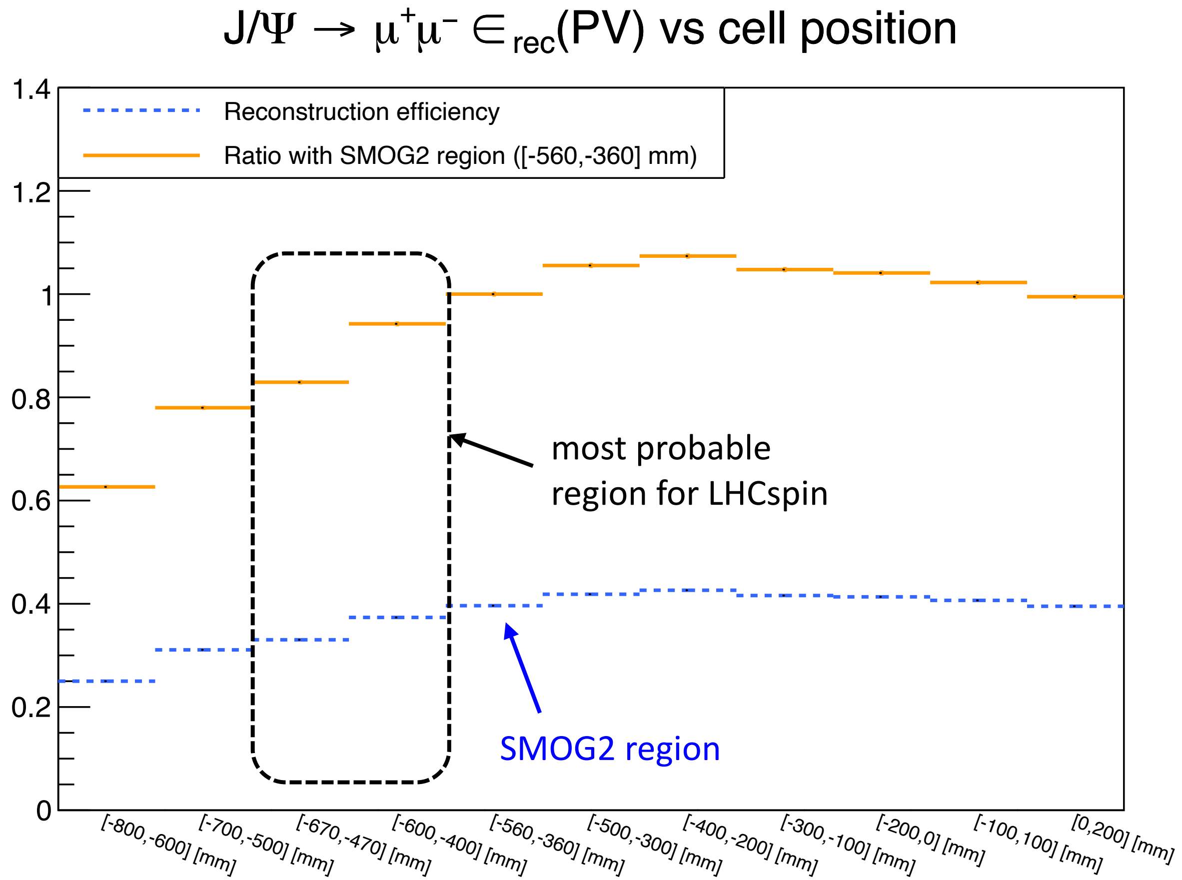

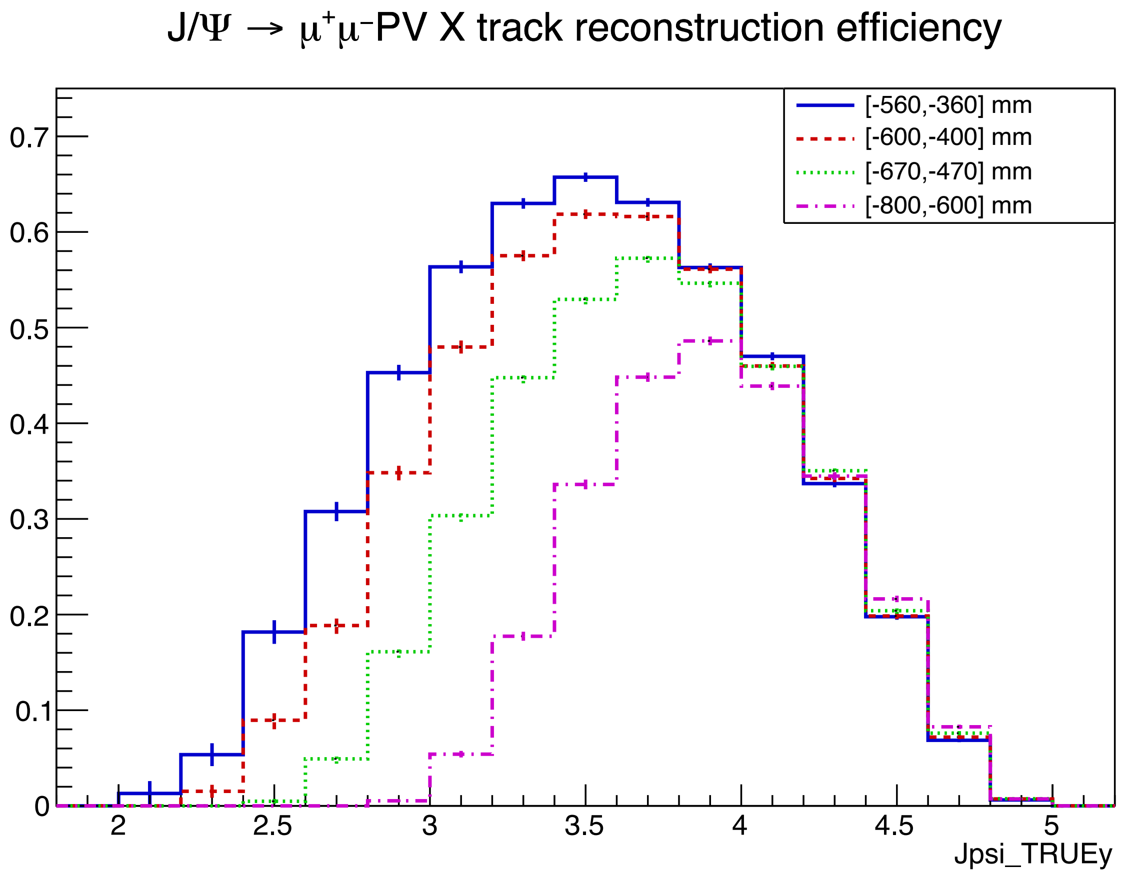

Kinematic coverage

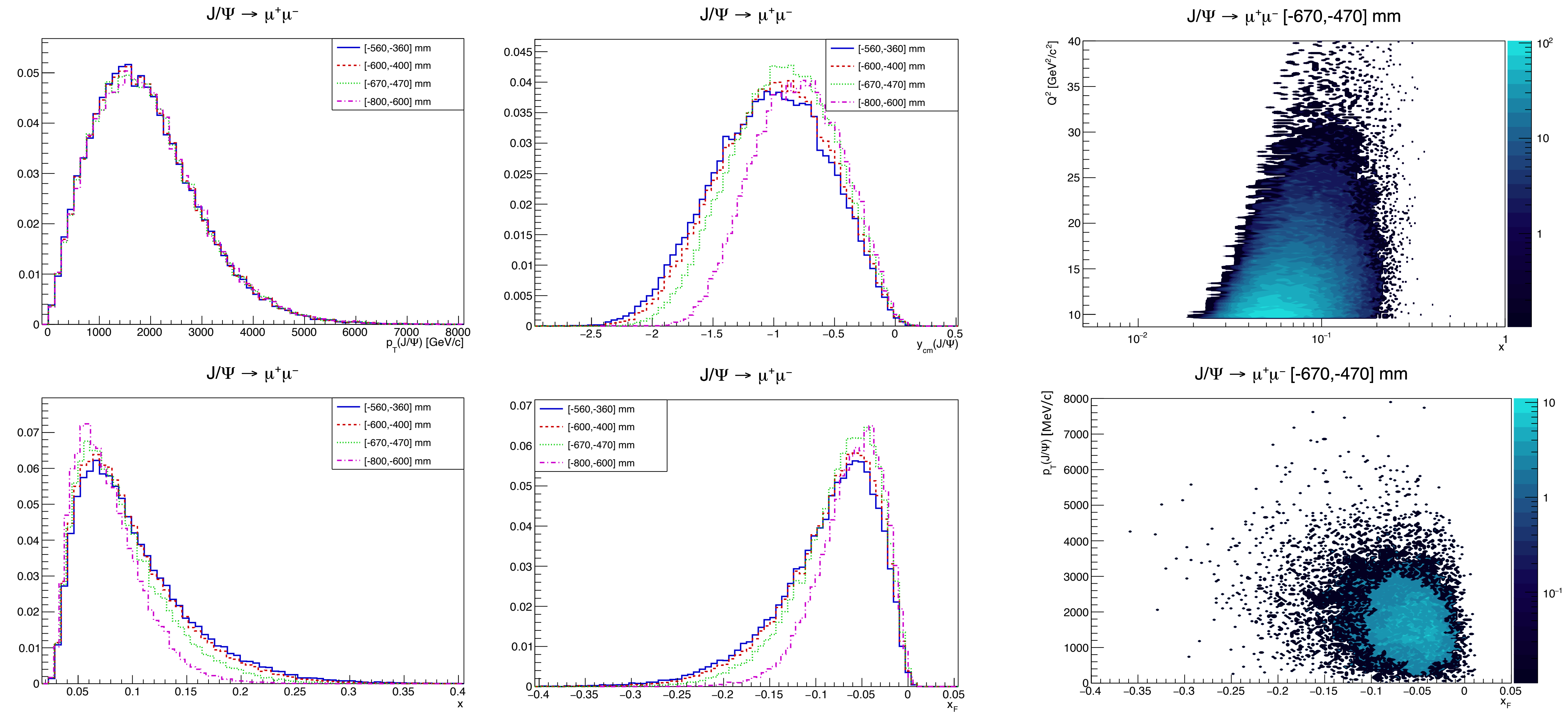

A preliminary analysis tool for pseudo-data

A pseudo-data set based on a transversely Pol. H target has been generated to study the interplay between statistical and systematic (due solely to the measurement of the polarization) uncertainties.

Similar approach used at HERMES (Appendix C of [JHEP, 12:010, 2020]):

- Use official LHCb MC data for inclusive production of $J/\psi \to \mu^+\mu^-$ in fixed-target configuration (PYTHIA8 + EPOS)
- Assign to each simulated event a target polarization state (↑ or ↓) using a random extraction modulated with a model for the cross section (in this way we **introduce a spin-dependence in the simulation**)
- The model assumes a dominant $\sin\phi$ modulation (e.g. sensitive to the gluon Sivers) plus a suppressed $\sin 2\phi$ modulation (to account e.g. for possible higher-twist contributions). Both terms depend mildly on the kinematics (x, p_T):

$$\rho = \frac{1}{2}\left[1 + \left(a_1 + a_2\frac{x-\overline{x}}{x_{max}} + a_3\frac{p_T-\overline{p_T}}{p_{T\ max}}\right)\sin\phi + \left(b_1 + b_2\frac{x-\overline{x}}{x_{max}} + b_3\frac{p_T-\overline{p_T}}{p_{T\ max}}\right)\sin 2\phi\right]$$

- Using these pseudo-data the TSSA is computed in the usual way:

$$A_N = \frac{1}{P}\frac{N^{\uparrow} - N^{\downarrow}}{N^{\uparrow} + N^{\downarrow}}$$

and the uncertainties on $N^{\uparrow(\downarrow)}$ (Poisson) and P (systematic) propagated accordingly.

A preliminary analysis tool for pseudo-data

- The data points are binned in x_F and p_T (2D binning), represented vs. ϕ and fitted with $f = a_1 \sin\phi + a_2 \sin 2\phi$ where the free parameters a_1 and a_2 represent the amplitude of the corresponding azimuthal modulation

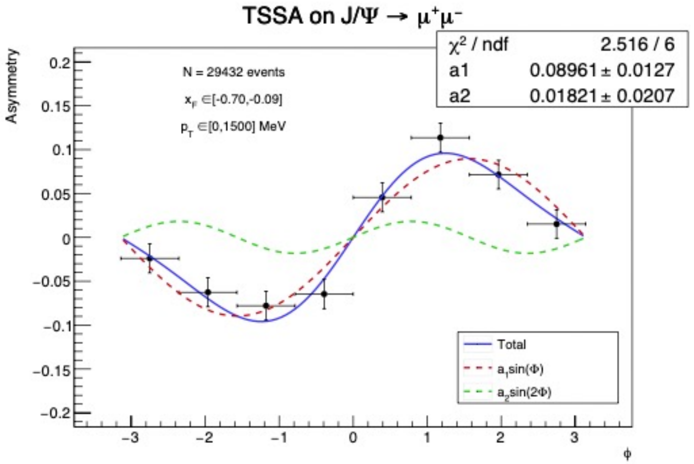

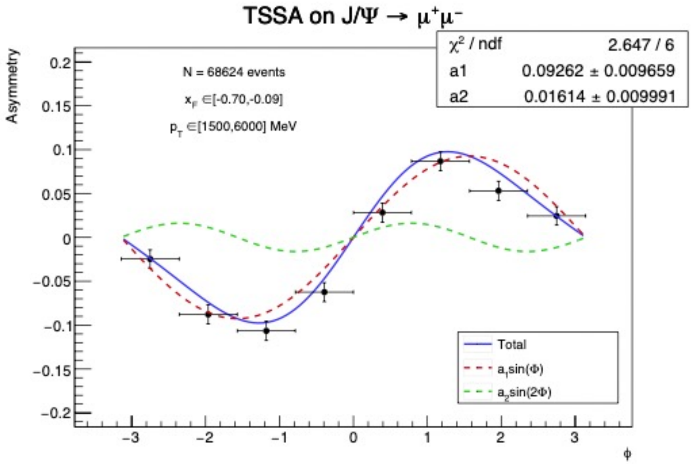

- The extracted parameters a_1 and a_2 are consistent with those used to generate the model (no bias is observed)
- With the available MC statistics (corresponding to 2 weeks of data-taking) there is no sensitivity for the $\sin 2\phi$ term

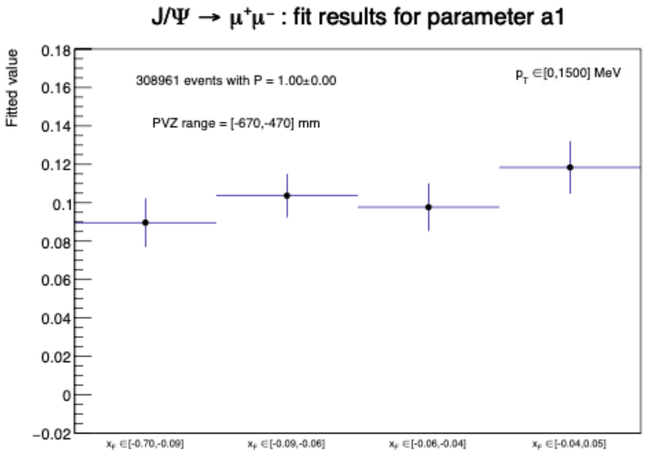

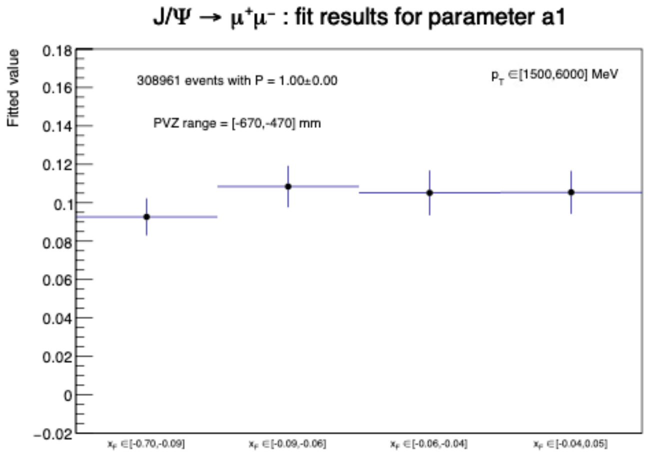

- The amplitudes a_1 are the reported vs. x_F in bins of p_T (and vice-versa)
- A mild kinematic dependence is observed consistent with the model

Statistical vs Systematics uncertainties

- This analysis tool allows to study the interplay between statistical uncertainties and systematic uncertainties (due to the measurement of the polarization) under different data-taking scenarios

p_T (MeV)	x_F	a_1 ($\Delta P = 0\%$)	a_1 ($\Delta P = 5\%$)	a_1 ($\Delta P = 20\%$)	a_1 ($\Delta P = 50\%$)
[0,1500]	[-0.70,-0.09]	0.090 ± 0.013	0.089 ± 0.013	0.087 ± 0.014	0.087 ± 0.022
[0,1500]	[-0.09,-0.06]	0.104 ± 0.011	0.104 ± 0.012	0.103 ± 0.016	0.100 ± 0.027
[0,1500]	[-0.06,-0.04]	0.098 ± 0.012	0.098 ± 0.013	0.097 ± 0.016	0.094 ± 0.027
[0,1500]	[-0.04,0.05]	0.118 ± 0.014	0.117 ± 0.014	0.114 ± 0.017	0.113 ± 0.030
[1500,6000]	[-0.70,-0.09]	0.093 ± 0.010	0.092 ± 0.010	0.090 ± 0.013	0.089 ± 0.023
[1500,6000]	[-0.09,-0.06]	0.108 ± 0.011	0.108 ± 0.011	0.108 ± 0.015	0.107 ± 0.027
[1500,6000]	[-0.06,-0.04]	0.105 ± 0.012	0.105 ± 0.012	0.104 ± 0.015	0.103 ± 0.026
[1500,6000]	[-0.04,0.05]	0.105 ± 0.011	0.105 ± 0.012	0.102 ± 0.015	0.102 ± 0.026

- A 5% systematic uncertainty on P has no impact on the total uncertainty on a_1
- For $\Delta P = 20\%$ the systematic uncertainty amounts to 30-40% of the statistical uncertainty
- For $\Delta P = 50\%$ the systematic uncertainty approximately equals the statistical uncertainty
- **We expect $\boldsymbol{\Delta P \approx 10 - 15\%}$ for the storage cell hypothesis**

Backup 4: The LHCspin physics case

Quark TMDs

		quark pol.	
nucleon pol.	U	L	T
U	f_1		$h_1^\perp$
L		g_{1L}	$h_{1L}^\perp$
T	$f_{1T}^\perp$	g_{1T}	$h_1,\ h_{1T}^\perp$

Unpolarized Drell-Yan

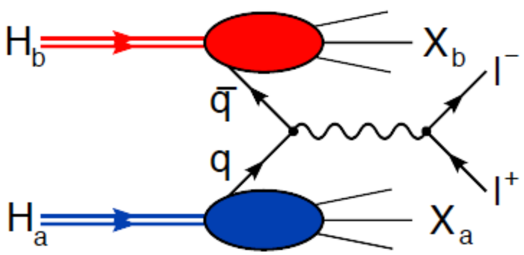

- Theoretically cleanest hard h-h scattering process
- LHCb has excellent μ-ID & reconstruction for $\mu^+\mu^-$
- **dominant**: $\bar{q}(x_{beam}) + q(x_{target}) \rightarrow \mu^+\mu^-$
- beam sea quarks probed at small x
- target valence quarks probed at large x

Sensitive to unpol. and BM TMDs for $q_T \ll M_{ll}$

$$d\sigma_{UU}^{DY} \propto f_1^{\bar{q}} \otimes f_1^{q} + \cos 2\phi \; h_1^{\perp,\bar{q}} \otimes h_1^{\perp,q}$$

violation of Lam-Tung relation

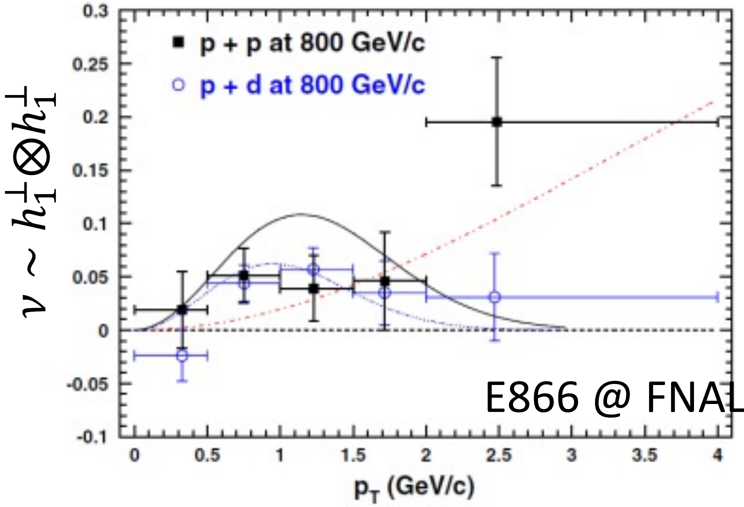

[PRL 102 2009 182001]

[Nature 590, 561 (2021)]

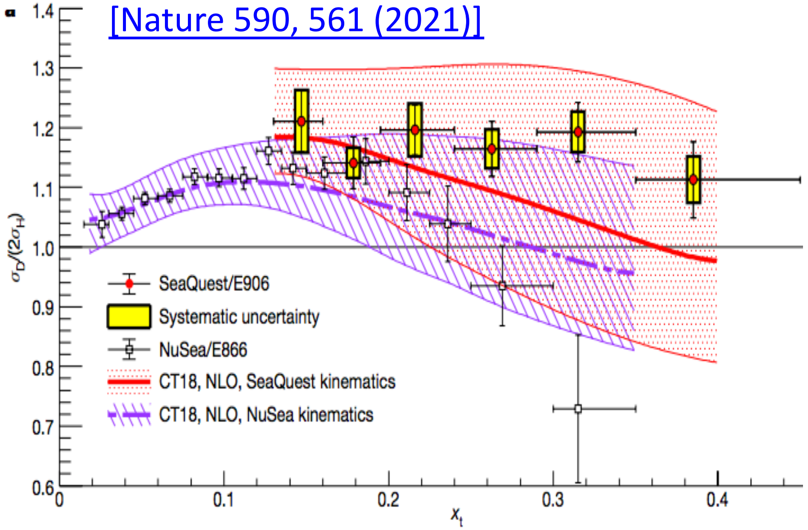

- Lattice QCD: $\bar{s}(x) \neq s\,(x)$ [arXiv:1809.04975]
- **proton sea more complex than originally thought!**
- **intrinsic heavy quarks**?
- Still a lot to be understood

- H & D targets allow to study the **antiquark content of the nucleon**
- SeaQuest (E906): $\bar{d}(x) > \bar{u}(x) \implies$ **sea is not flavour symmetric!**

Quark TMDs

nucleon pol. \ quark pol.	U	L	T
U	f_1		$h_1^{\perp}$
L		g_{1L}	$h_{1L}^{\perp}$
T	$f_{1T}^{\perp}$	g_{1T}	$h_1,\ h_{1T}^{\perp}$

Transv. polarized Drell-Yan

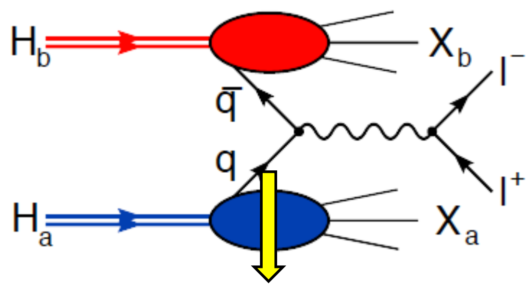

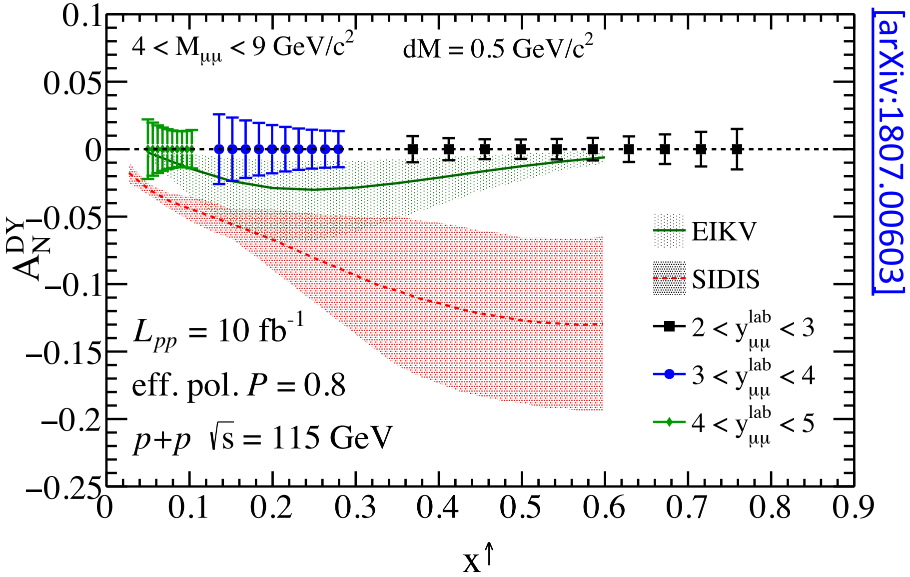

- **Sensitive to quark TMDs through TSSAs**

$$A_N^{DY} = \frac{1}{P}\frac{\sigma_{DY}^{\uparrow} - \sigma_{DY}^{\downarrow}}{\sigma_{DY}^{\uparrow} + \sigma_{DY}^{\downarrow}} \Longrightarrow \quad A_{UT}^{sin\phi_S} \sim \frac{f_1^q \otimes f_{1T}^{\perp q}}{f_1^q \otimes f_1^q}, \quad A_{UT}^{sin(2\phi-\phi_S)} \sim \frac{h_1^{\perp q} \otimes h_1^q}{f_1^q \otimes f_1^q}, \ \ldots$$

(ϕ: azimuthal orientation of lepton pair in dilepton CM)

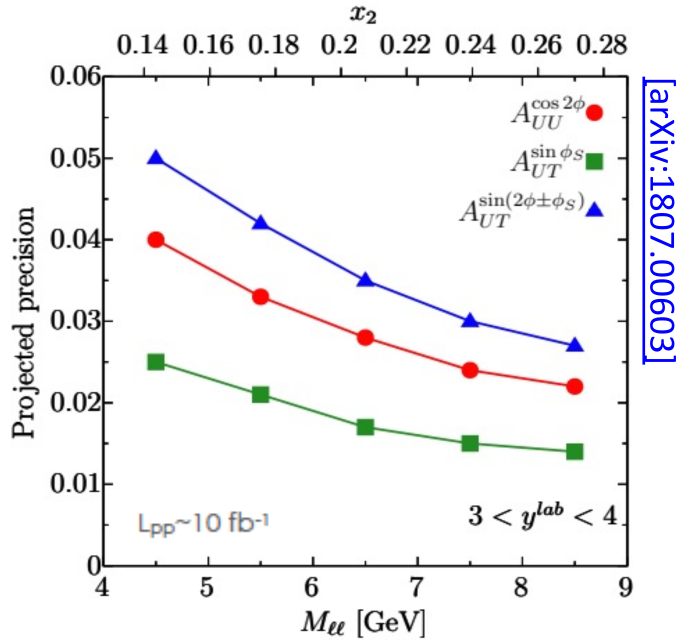

- Extraction of qTMDs does not require knowledge of FF
- Verify sign change of Sivers function wrt SIDIS

$$f_{1T}^{\perp}\big|_{DY} = -f_{1T}^{\perp}\big|_{SIDIS}$$

- Test flavour sensitivity using both H and D targets

Gluon TMDs

nucleon pol. \ gluon pol.	U	Circularly	Linearly
U	f_1^g		$h_1^{\perp g}$
L		g_{1L}^g	$h_{1L}^{\perp g}$
T	$f_{1T}^{\perp g}$	g_{1T}^g	h_1^g, $h_{1T}^{\perp g}$

Theory framework well consolidated **…but experimental access still extremely limited!**

Similar naming/notation of quark TMDs, but there are important differences!

- the **linearity gTMD** (h_1^g) is completely unrelated to the quark transversity (h_1^q), and has no collinear counterpart
- **different naïve-time-reversal properties**

	T-even	T-odd
q	$\mathbf{h_1^q}$	$\mathbf{h_1^{\perp q}}$
g	$\mathbf{h_1^{\perp g}}$	$\mathbf{h_1^g}$

- Also the gTMD phenomenology is enriched by the **process dependence** originating by ISI/FSI encoded in the **gauge links**.
- **The gluon correlator depends on 2 path-dependent gauge links**, resulting in a more complex process dependence

"Future pointing" Wilson line ("+")

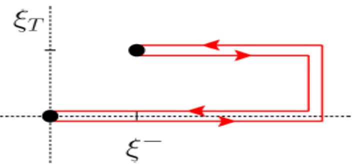

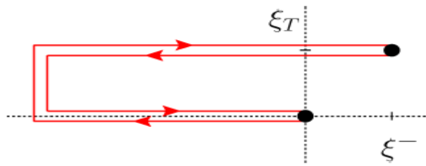

"Past pointing" Wilson line ("−")

- Depending on their combinations, **there are 2 independent versions of each gTMD** that can probed in different processes and can have different magnitude and width and different x and k_T dependencies!
- E.g. there are 2 types of f_1^g and $h_1^{\perp g}$: $[+\,+] = [-\,-]$ Weizsacker-Williams (WW) ; $[+\,-] = [-\,+]$ DiPole (DP)
- 2 indep. GSF: $f_{1T}^{\perp g[+,+]}$ **"f-type"** → antisymm. colour structure ; $f_{1T}^{\perp g[+,-]}$ **"d-type"** → symm. colour structure

Probing the gTMDs

In high-energy hadron collisions, heavy quarks are dominantly produced through gg fusion:

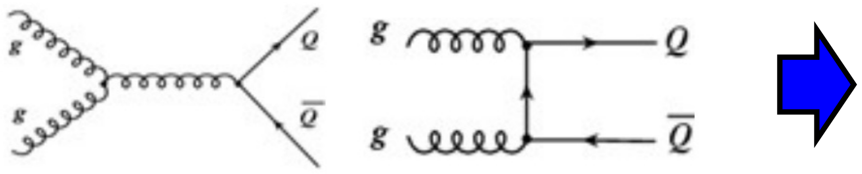

The most efficient way to access the gluon dynamics inside the proton at LHC is to **measure heavy-quark observables**

- **Inclusive quarkonia production in (un)polarized pp interaction** $(pp^{(\uparrow)} \to [Q\bar{Q}]X)$ turns out to be an ideal observable to access gTMDs (assuming TMD factorization)

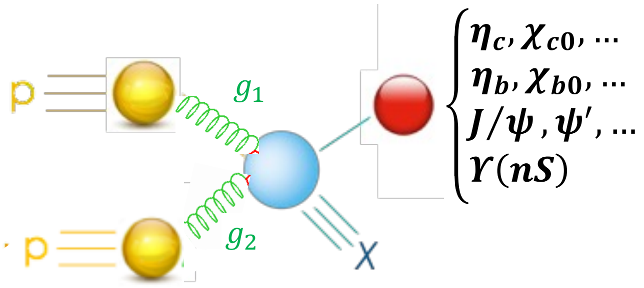

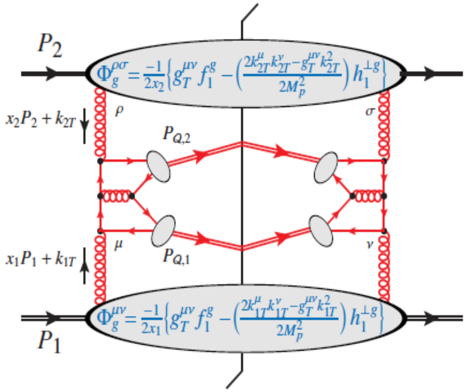

- TMD factorization requires $q_T(Q) \ll M_Q$. Can look at **associate quarkonia production**, where only the relative q_T needs to be small:

  E.g.: $pp^{(\uparrow)} \to J/\psi + J/\psi + X$ (→ **Alice**)

- Due the larger masses this condition is more easily matched in the case of **bottomonium**, where TMD factorization can hold at larger q_T (although very challenging for experiments!)

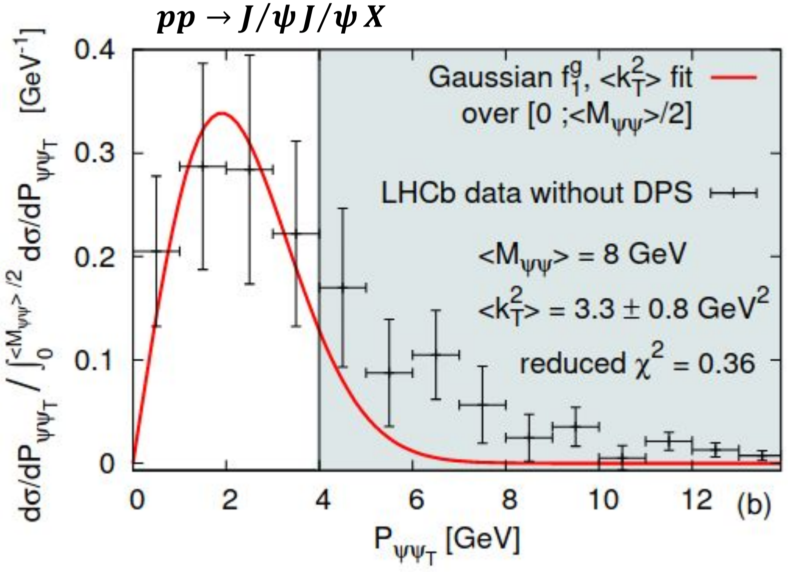

First extraction of f_1^g from LHCb di-J/ψ production data at collider energies [Lansberg et. al.]

Probing the gTMDs

$$\frac{d\sigma}{dM_{QQ}dY_{QQ}d^2\boldsymbol{P}_{QQ_T}d\Omega} = \frac{\sqrt{M_{QQ}^2 - 4M_Q^2}}{(2\pi)^2 8s\, M_{QQ}^2}$$
$$\Big\{F_1(M_{QQ},\theta_{CS})\,\mathcal{C}\left[f_1^g f_1^g\right](x_{1,2},\boldsymbol{P}_{QQ_T})$$
$$+F_2(M_{QQ},\theta_{CS})\,\mathcal{C}\left[w_2 h_1^{\perp g} h_1^{\perp g}\right](x_{1,2},\boldsymbol{P}_{QQ_T})$$
$$+\boxed{\left(F_3(M_{QQ},\theta_{CS})\,\mathcal{C}\left[w_3 f_1^g h_1^{\perp g}\right](x_{1,2},\boldsymbol{P}_{QQ_T}) + F_3'(M_{QQ},\theta_{CS})\,\mathcal{C}\left[w_3' h_1^{\perp g} f_1^g\right](x_{1,2},\boldsymbol{P}_{QQ_T})\right)\cos 2\phi_{CS}}\ \boxed{+F_4(M_{QQ},\theta_{CS})\,\mathcal{C}\left[w_4 h_1^{\perp g} h_1^{\perp g}\right](x_{1,2},\boldsymbol{P}_{QQ_T})\cos 4\phi_{CS}\Big\}}$$

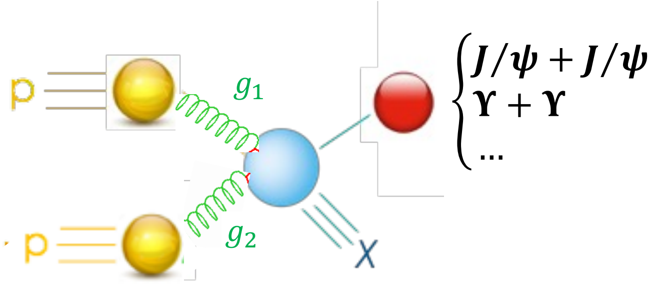

gluon pol.

nucleon pol.	U	Circularly	Linearly
U	f_1^g		$h_1^{\perp g}$
L		g_{1L}^g	$h_{1L}^{\perp g}$
T	$f_{1T}^{\perp g}$	g_{1T}^g	$h_1^g,\ h_{1T}^{\perp g}$

Predictions based on CSM + TMD evolution for $x_1 \sim x_2 \sim 10^{-3}$ at forward rapidity [EPJ C 80, 87 (2020)]

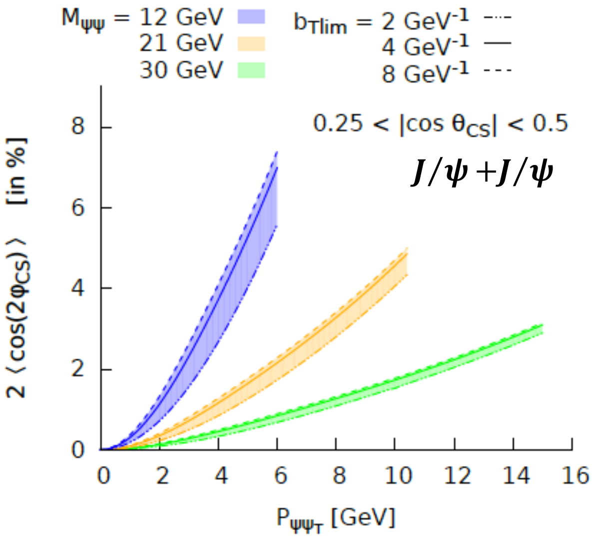

Azimuthal amplitudes ~5%!

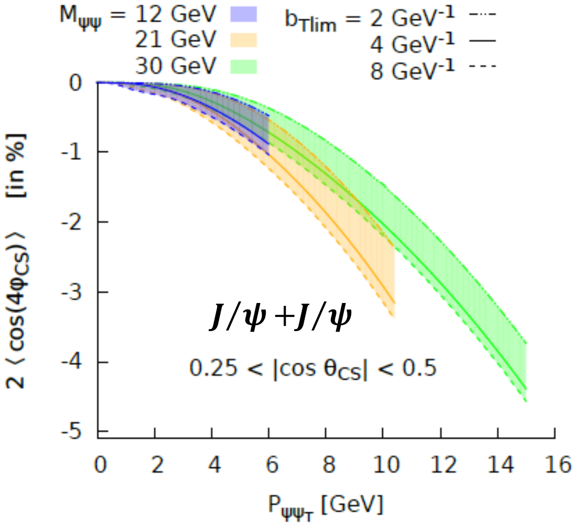

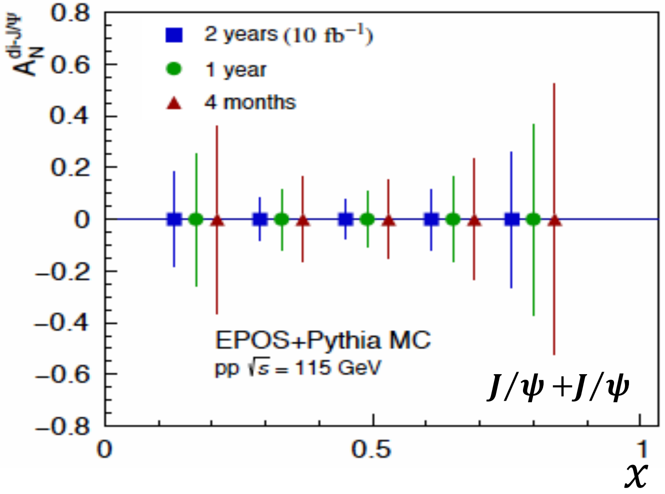

Probing the gluon Sivers funct.

$$\Gamma_T^{\mu\nu}(x,\boldsymbol{p}_T)=\frac{x}{2}\left\{g_T^{\mu\nu}\frac{\epsilon_T^{\rho\sigma}p_{T\rho}S_{T\sigma}}{M_p}f_{1T}^{\perp g}(x,\boldsymbol{p}_T^2)+\dots\right\}$$

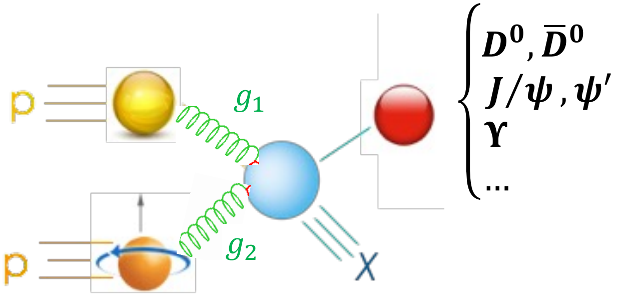

nucleon pol. \ gluon pol.	U	Circularly	Linearly
U	f_1^g		$h_1^{\perp g}$
L		g_{1L}^g	$h_{1L}^{\perp g}$
T	$f_{1T}^{\perp g}$	g_{1T}^g	$h_1^g,\ h_{1T}^{\perp g}$

- Sheds light on spin-orbit correlations of unpol. gluons inside a transv. pol. proton
- sensitive to color exchange among IS and FS and to gluon OAM
- expected to be quite small (quasi-saturation of Burkardt sum rule by $f_{1T}^{\perp q}$ and QCD predictions in large-N_c limit)
- can be accessed through the measurement of the TSSAs in **inclusive heavy meson production**

$$A_N=\frac{1}{P}\frac{\sigma^{\uparrow}-\sigma^{\downarrow}}{\sigma^{\uparrow}+\sigma^{\downarrow}}\propto\left[f_{1T}^{\perp g}(x_a,k_{\perp a})\otimes f_g(x_b,k_{\perp b})\otimes d\sigma_{gg\to QQg}\right]\sin\phi_S+\cdots$$

Predictions for pol. FT meas. at LHC (LHCspin-like) [Phys. Rev. D 102, 094011 (2020)]

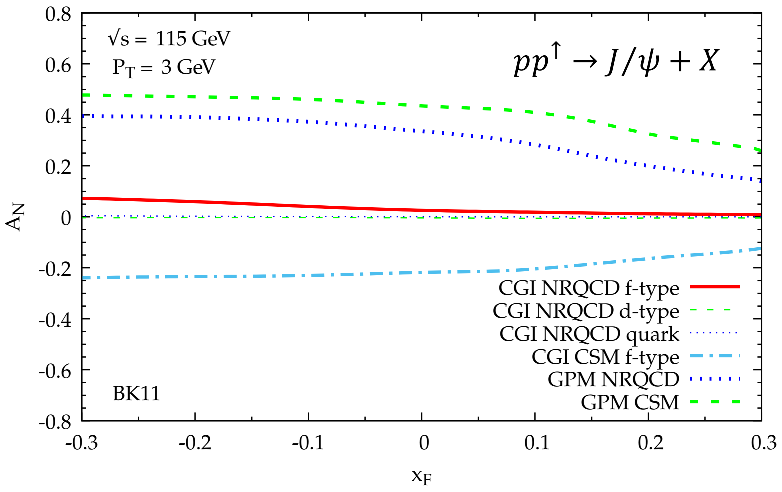

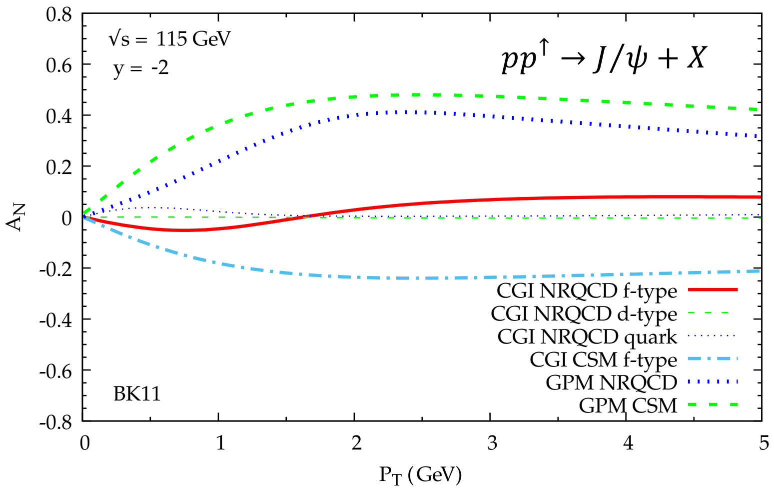

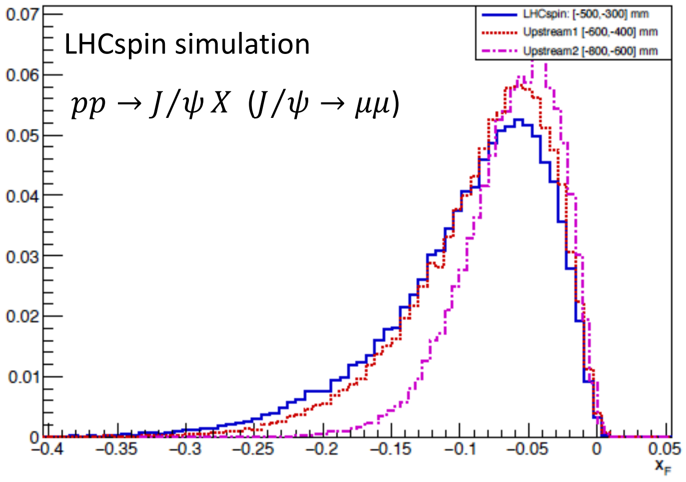

Merging spin physics with heavy-ion physics

- probe collective phenomena in heavy-light systems through **ultra-relativistic collisions of heavy nuclei with trasv. pol. deuterons**
- polarized light target nuclei offer a unique opportunity to control the orientation of the formed fireball by measuring the **elliptic flow** relative to the polarization axis (**ellipticity**).

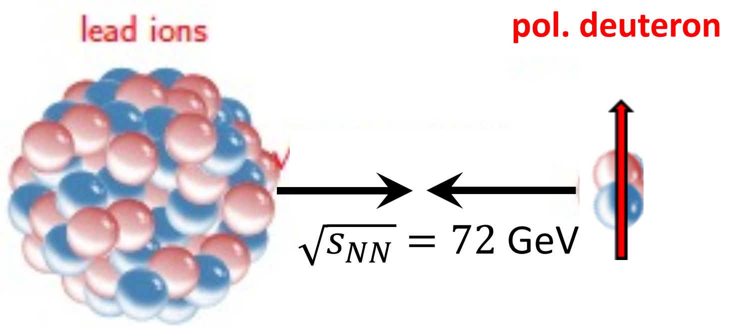

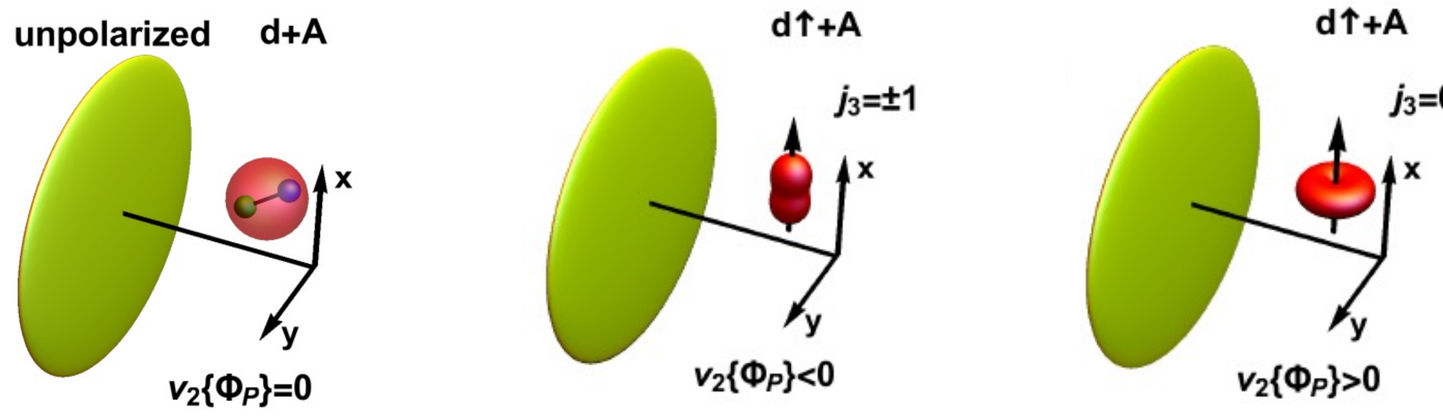

Unpol. deuterons: the **fireball is azimuthally symmetric** and $v_2 \approx 0$.

$j_3 = \pm 1$ → **prolate fireball** stretched along the pol. axis, corresponds to $v_2 < 0$

$j_3 = 0$ → **oblate fireball** corresponds to $v_2 > 0$

Predictions for LHC FT kinematics

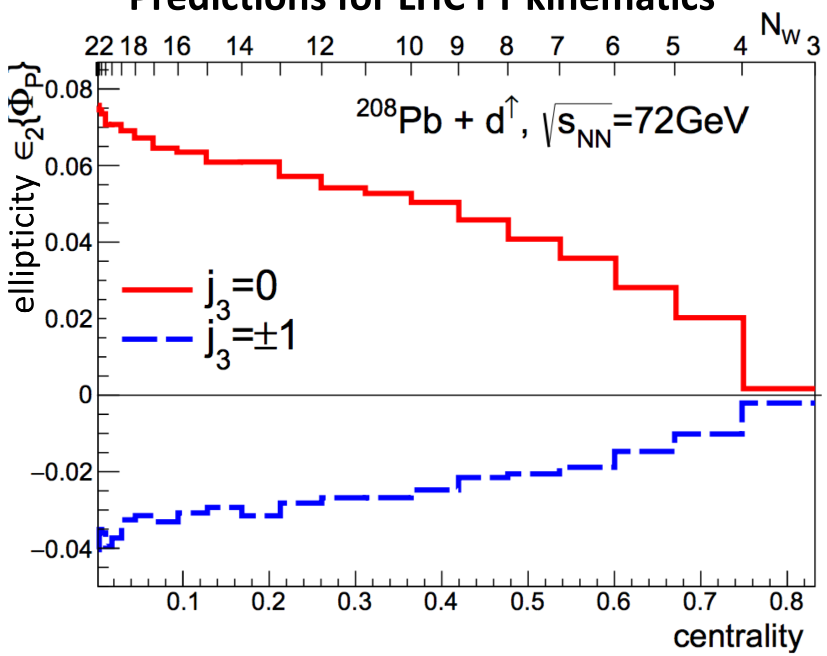

[PRC 101 (2020) 024901]

UPC and gGPDs

GPD	U	L	T
U	H		$\mathcal{E}_T$
L		$\tilde{H}$	$\tilde{E}_T$
T	E	$\tilde{E}$	$H_T,\ \tilde{H}_T$

Can be accessed at LHC in **Ultra-Peripheral collisions (UPC)**

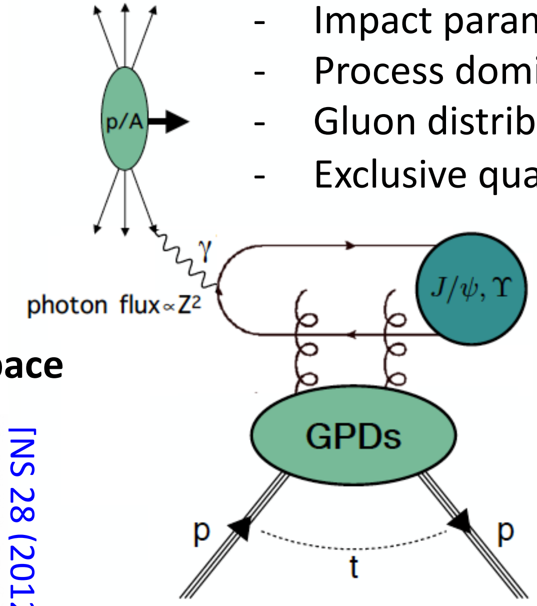

- Impact parameter larger than sum of radii
- Process dominated by EM interaction
- Gluon distributions probed by pomeron exchange
- Exclusive quarkonia prod. sensitive to gluon GPDs [PRD 85 (2012), 051502]

3D maps of parton densities in coordinate space

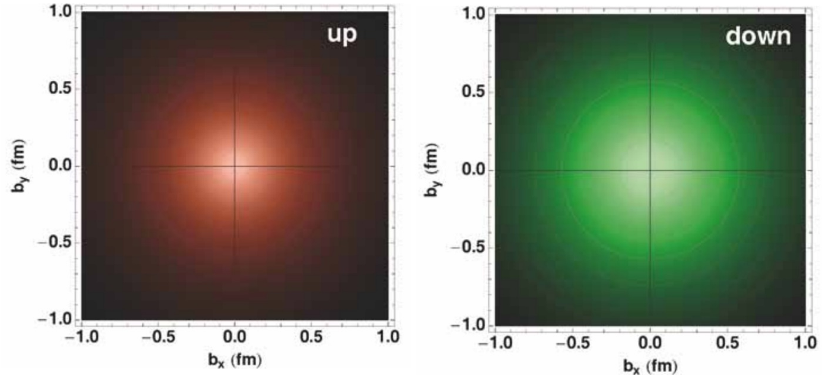

[NS 28 (2012), 1]

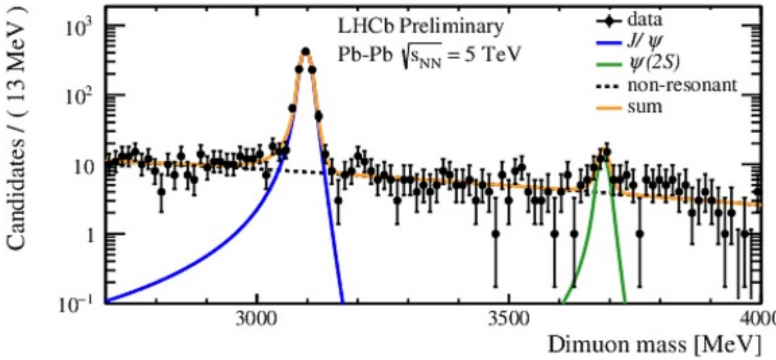

[NPA 982 (2019) 247]

First results from LHCb in PbPb UPC

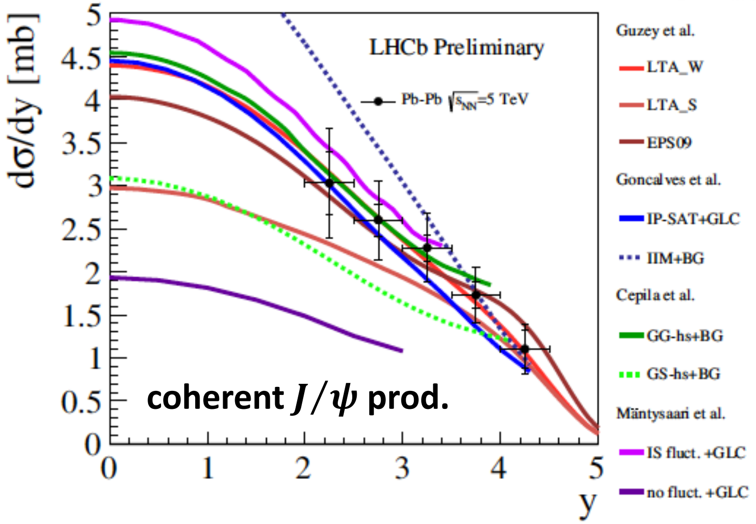

LHCspin could allow to access the GPD E^g (a key ingredient of the Ji sum rule)

$$J^g = \frac{1}{2}\int_0^1 dx\Big(H^g(x,\xi,0) + E^g(x,\xi,0)\Big)$$